University of Groningen

Master Thesis

Leptoquarks in an $SO(10)$ Grand Unified Theory

Jetze J. Keuning

S3719049

Supervisor:
prof. dr. Daniël Boer

July 5, 2024

Abstract

The Standard Model (SM) of particle physics is an experimentally successful theory describing the strong, weak and electromagnetic forces. These forces are described by distinct interactions in the SM. Grand Unified Theories (GUTs) attempt to unify these forces into a single interaction. The hypothesis is that at high energies, the coupling constants associated with each group in the SM, $SU(3)_C \times SU(2)_L \times U(1)_Y$, will unify into a single coupling constant. The three forces will then be combined into a single gauge group. In this work we treat a GUT based on $SO(10)$ with three intermediate symmetry scales between the GUT-scale and the SM. This model accommodates all fermions in a single representation, including a right-handed neutrino, which is absent from the SM. The coupling constants are shown to unify in such a scenario, for a range of intermediate energy scales. The most relevant of these intermediate symmetries is the Pati-Salam model, based on $SU(4)_C \times SU(2)_L \times SU(2)_R$. This model unifies leptons and quarks into a single representation, therefore giving rise to leptoquarks. Leptoquarks are particles that have a coupling with both a quark and a lepton. The model we discuss contains three leptoquarks below the GUT scale, a vector leptoquark U_1, with SM representation $(3, 1, 2/3)$ and two scalar leptoquarks R_2 and $\tilde{R}_2$, with representations $(3, 2, 7/6)$ and $(3, 2, 1/6)$, respectively. The vector leptoquarks are experimentally restricted to lie at energies greater than 2 PeV. We describe a scenario with TeV-scale scalar leptoquarks. These leptoquarks mainly interact with the heaviest fermions (the third generation) and could potentially be observed at pp colliders through final states such as $q\overline{q} + \tau\overline{\tau}$, $q + \tau\overline{\tau}$ and $\tau\overline{\tau}$, with the quark being either a top or a bottom.

Contents

Chapter 1

Introduction

The Standard Model of Particle Physics (SM) is a highly successful description of particle physics. In the 1960s, Sheldon Glashow proposed a unified theory of the electromagnetic and weak interactions in order to explain parity violation [1]. This theory was based on the $SU(2)_L \times U(1)_Y$ gauge group. Unfortunately, the result was not renormalisable. Steven Weinberg and Abdus Salam combined the Higgs mechanism and electroweak theory into the Glashow-Weinberg-Salam theory of electroweak interactions [2, 3]. This theory featured spontaneous symmetry breaking of the gauge group through the Higgs field, the existence of which was not proven until the famous discovery at the Large Hadron Collider (LHC) in 2012 [4]. Gerard 't Hooft and Martinus Veltman showed that this theory of electroweak interactions was in fact renormalisable [5].

The 1970s would see the development of Quantum Chromodynamics (QCD) based on $SU(3)_C$ by physicists Harald Fritzsch, Murray Gell-Mann and Heinrich Leutwyler [6], to explain the strong interaction. Together, QCD and the electroweak theory form the SM, based on the gauge group $SU(3)_C \times SU(2)_L \times U(1)_Y$. Since then this theory has been hugely experimentally successful, with the discovery of the $W^\pm$ and Z^0 bosons, the gluons and additional quarks. We will further expand upon the SM in chapter 2.

The success of the SM, a theory with its origins in unifying the weak and electromagnetic interactions, begs the question: can we accomplish any further unification? Specifically, can we unify all three interactions into a single force at higher energies? The answer to this question is a resounding, but strictly theoretical, yes. Grand Unified Theories (GUTs) were quickly theorized in the early days of the SM. Many of the physicists involved in developing the SM would contribute to the development of GUTs. In the 1970s Glashow would develop the Georgi-Glashow theory based on $SU(5)$, together with Howard Georgi [7]. Abdus Salam and Jogesh Pati developed Pati-Salam theory [8], based on $SU(4)_C \times SU(2)_L \times SU(2)_R$, although this is strictly speaking not a GUT, as the couplings are not unified. Furthermore, Harald Fritzsch and Peter Minkowski formulated a model based on $SO(10)$ [9]. Clearly, the development of the SM sparked a great interest in creating GUTs.

An appealing quality of GUTs is their ability to resolve some shortcomings of the SM. The charges of particles in the SM are seemingly arbitrary, yet an electron and a proton have exactly equal and opposite charge. A GUT could explain this by putting quarks and leptons in the same representations, causing their charges to be inherently connected. Furthermore, the strength with which the three interactions couple is not equal in the SM. There is no clear reason for this hierarchy between the forces. A GUT would feature a single coupling, which then breaks up into several couplings, one for each group. The running of these couplings down to the SM could provide an origin for the couplings we observe.

Clearly, it is theoretically possible to formulate GUTs, unlike the SM though, it has been difficult to test their predictions. GUTs are inherently hard to verify, as their effects are generally only noticeable at energies far beyond the scale of experiment. The scale associated with a GUT is generally on the order of 10^{16} GeV, due to the constraints from proton decay [10]. However, we do not have to assume that there is a 'particle desert' between the SM and a potential GUT-scale, in which there is no new physics. In fact, many GUTs allow for, or even require, intermediate scales with different gauge groups [11, 12]. These GUTs can therefore predict BSM physics at energies much lower than the GUT-scale. A common class of new particles in GUTs are leptoquarks, which carry both lepton number and baryon number. This quality allows these particles to couple to leptons and quarks simultaneously. The fact that these particles are so prevalent in these theories is inherent. GUTs rely on larger symmetries with larger representations for the fermions. Naturally, this unification can lead to mixing of leptons and quarks. This new type of mixed lepton-quark coupling allows for a wide range of new phenomenology. Observing these new processes would hint at the existence of a GUT, although leptoquarks can exist outside the context of GUT as well.

Leptoquarks can be found in both the gauge and scalar sectors of several GUTs. A search for low energy leptoquarks in GUTs was performed in [12]. The conclusions of this work, along with an introduction to leptoquarks, will be given in chapter 3. This chapter will lead us to continue examining a model based on $SO(10)$ with three intermediate scales. The gauge group of one of these intermediate scales is in fact the aforementioned Pati-Salam theory. This theory contains a vector leptoquark that has the theoretical potential to have a mass as low as 5 TeV, putting it in range of collider experiment. However, this option will turn out to be ruled out.

The main purpose of this work is to review and expand on the $SO(10)$ GUT with TeV-scale leptoquarks found in [12]. This means that we will dive deeper into the model, making sure that it is consistent and realistic. Furthermore, we need to perform a broader review of the experimental constraints on this model. All of this will be done in order to answer the question: is there a consistent GUT scenario with TeV-scale leptoquarks that could be observed at collider experiments?

In chapter 4 we will treat all necessary group theory for building a GUT based on $SO(10)$. This includes a classification of many scalar representations, which will lead us to identify additional (with respect to [12]) leptoquarks in $SO(10)$. The mathematical tools from this chapter will then be used to formulate a model in chapter 5. In that chapter we will also delve deeper into the more complicated aspects of symmetry breaking in this GUT. Furthermore, we will show the running and unification of the couplings from the SM up to the GUT-scale. These two chapters together intend to establish a clear case for a GUT with leptoquarks at the TeV-scale.

With a scenario for low energy leptoquarks in hand, we move on to the phenomenology of the vector leptoquarks (U_1) in chapter 6 and of the scalar leptoquarks (R_2 and $\tilde{R}_2$) in chapter 7. The mediation of rare meson decays due to vector leptoquarks will lead to their exclusion at the TeV-scale. However, these constraints are not as strong for the scalar leptoquarks, as their couplings to first and second generation matter can be small. This will lead us to examine processes of the scalar leptoquarks involving third generation fermions. We will identify several final states that are relevant for observing these particles at pp colliders.

Chapter 2

The Standard Model

Before we engage in building a Grand Unified Theory based on the $SO(10)$ symmetry group, we should examine the experimentally successful Standard Model (SM). This model represents the current state of particle physics, so it is instructive to study it before we try to build something that would contain it. Currently, it is uncertain up to which energy scale the SM is a valid theory for describing particle interactions. All we know is that, on the scale of current-day collider experiments ($\sim$ TeV), it is a good theory for describing the interactions of the strong, weak and electromagnetic forces.

The SM is based on the $SU(3)_C \times SU(2)_L \times U(1)_Y$ symmetry group, which has 12 generators. This makes it significantly smaller than $SO(10)$, which has a 45-dimensional adjoint representation. Regardless, many of the principles in this chapter have a direct analogy to the GUT we intend to build. In an $SO(10)$ model, particles are still in irreducible representations, the Lagrangian is still based on Yang-Mills theory, the adjoint representation still determines the gauge interactions and scalar particles perform spontaneous symmetry breaking. Therefore, we will describe these things in the context of the SM first.

2.1 Particles and Representations

All particles in a theory, be it fermions, gauge bosons or scalar bosons, have to be represented in a certain representation of the gauge group of a theory. As stated before, the SM is based on $SU(3)_C \times SU(2)_L \times U(1)_Y$. Fermions are generally represented in fundamental or trivial representations of a group, indicating how they transform. Gauge bosons are always in the adjoint representation. Lastly, scalars can be in any valid irreducible representation. This section is largely based on [13] and [14].

2.1.1 Representation Theory

In general a group G can be represented by a certain representation D, for which the following holds:

$$D(g_1) \circ D(g_2) = D(g_1 g_2), \quad g_1, g_2 \in G. \tag{2.1}$$

An infinite amount of such representations can be constructed, the most relevant ones are the fundamental and the adjoint representation. For a global $SU(N)$ symmetry we generally have a representation:

$$U = e^{-i\alpha^a T^a}, \tag{2.2}$$

where α^a are real parameters quantifying the transformation, and T^a are the $N^2 - 1$ generators of the group. Take a set of N complex numbers arranged in a vector:

$$\psi^i = \begin{pmatrix} \psi^1 \\ \psi^2 \\ \vdots \\ \psi^N \end{pmatrix}, \quad i = 1, ..., N, \tag{2.3}$$

this vector transforms under $SU(N)$ as follows:

$$\psi^i \to \psi'^i = U^i_j \psi^j = 1 - i\alpha^a (T^a)^i_j \psi^j + \mathcal{O}(\alpha^2), \tag{2.4}$$

where the expansion is only valid for infinitesimal α. Representations that transform in this manner are called the fundamental representation. The fundamental representation of $SU(N)$ always has N dimensions. The generators T^a themselves also transform under the group:

$$(T^a)^i_j \to (T'^a)^i_j = U^i_k (T^a)^k_l (U^\dagger)^l_j = 1 - i[\alpha^a T^a, T^a] + \mathcal{O}(\alpha^2), \tag{2.5}$$

therefore the generators themselves also form an $N^2 - 1$ dimensional representation. The expansion is again only valid for infinitesimal transformations. This is called the adjoint representation. Many more representations can be constructed by taking the product of two representations and decomposing them into irreducible representations. An irreducible representation is a representation that cannot be further decomposed into smaller representations.

These representations are essential in writing down a Lagrangian for a theory. The aim is to formulate a Lagrangian that is invariant under a local $SU(N)$ transformation. A local transformation is slightly different from a global transformation:

$$U = e^{-i\alpha^a(x)T^a}, \tag{2.6}$$

as can be seen we now have a coordinate-dependent $\alpha^a(x)$ instead of a constant α^a. This means that the transformation is dependent on position. If we take the fundamental representation $\Psi = \psi^i$ and place fermions in it, we can attempt to write down an invariant kinetic term in the Lagrangian:

$$\mathcal{L}_{kin} = \overline{\Psi}(\partial_\mu \gamma^\mu)\Psi, \tag{2.7}$$

where γ^μ are defined as in section A.1, and $\overline{\Psi} = \Psi^\dagger \gamma^0$. This does not work however, as we have the following transformation property:

$$\partial_\mu \Psi \to U \partial_\mu \Psi + (\partial_\mu U)\Psi. \tag{2.8}$$

There is an extra term in the transformation due to the fact that we have a local symmetry. With a global symmetry we would have had $\partial_\mu U = 0$, as the transformation would not be position dependent. This extra term in this transformation makes the Lagrangian not invariant under $SU(N)$. Instead, we need a derivative with the following transformation property:

$$D_\mu \Psi \to U D_\mu \Psi, \tag{2.9}$$

this is the so-called covariant derivative. This derivative is defined as:

$$D_\mu = \partial_\mu - igA^a_\mu T^a, \tag{2.10}$$

where A^a_μ is the gauge field and g is the coupling constant. Using this derivative instead gives us the invariant term:

$$\mathcal{L}_{kin} = \overline{\Psi}(\not{D})\Psi, \tag{2.11}$$

where we have used Feynman slash notation $\not{D} = D_\mu \gamma^\mu$. Since the covariant derivative contains the gauge field, the kinetic term contains couplings between the fermions and the gauge bosons. From the transformation of the covariant derivative we can determine the transformation properties of the gauge field:

$$A^a_\mu T^a \rightarrow A^a_\mu T^a + \frac{i}{g}\partial_\mu \alpha^a T^a + i[\alpha^a T^a, A^b_\mu T^b] + \mathcal{O}(\alpha^2), \tag{2.12}$$

which we can recognize as the transformation of the adjoint representation. Simply by requiring the Lagrangian to be $SU(N)$ invariant, the kinetic term automatically provides the couplings between fermions and gauge bosons; the group structure entirely determines the possible interactions.

2.1.2 Fermions

The SM has 15 fermions per generation. These are the three up-type quarks, the three down-type quarks, their respective antiquarks, the electron, the positron and the left-handed neutrino. The right-handed neutrino is generally absent from the SM. These 15 fermions are embedded into SM representations as follows:

$$\begin{aligned}
&Q_L = \begin{pmatrix} u_L \\ d_L \end{pmatrix} \in (3, 2, 1/6), \\
&u_R \in (\overline{3}, 1, -2/3), \\
&d_R \in (\overline{3}, 1, 1/3), \\
&e_L = \begin{pmatrix} \nu_L \\ e_L \end{pmatrix} \in (1, 2, -1/2), \\
&e_R \in (1, 1, 1),
\end{aligned} \tag{2.13}$$

where the first two numbers indicate dimension of the irrep of $SU(3)_C$ and $SU(2)_L$ respectively. The bar on the $\overline{3}$ means that it is a conjugate representation. The last number is the eigenvalue under $U(1)_Y$; the hypercharge. For representations that have more than 1 particle, this number is the average of the electromagnetic charge of all the particles in the representation. These numbers immediately tell us something important about the fermions. A representation that is 3-dimensional under $SU(3)_C$ contains particles that are in the fundamental representation of that group. Therefore, they carry colour charge and can interact with each other through the strong force associated with $SU(3)_C$. Conversely, particles that are 1-dimensional under $SU(3)_C$ do not interact with the strong force, as they transform trivially. The same applies for $SU(2)_L$. For $U(1)_Y$, a nonzero eigenvalue indicates that the particle has interactions with the boson associated with $U(1)_Y$.

2.1.3 Gauge Bosons

The adjoint representations of $SU(3)_C$, $SU(2)_L$ and $U(1)_Y$ contain the gauge bosons. The adjoint representation of $SU(3)_C$ is 8 dimensional, consisting of basis matrices labelled $U_1, U_2, ..., U_8$ (the Gell-Mann matrices). With each basis matrix we associate a field, therefore we have 8 bosons, the gluons, these are labelled G^1_μ through G^8_μ in eq. (2.14). $SU(2)_L$ has 3 bosons, one each for L_1, L_2 and L_3, labelled W^1_μ, W^2_μ and W^3_μ. Lastly, $U(1)_Y$ has 1 gauge boson: B_μ, associated with the generator Y.

$$\begin{aligned}
G^1_\mu, G^2_\mu, ..., G^8_\mu &\in (8, 1, 0), \\
W^1_\mu, W^2_\mu, W^3_\mu &\in (1, 3, 0), \\
B_\mu &\in (1, 1, 1).
\end{aligned} \tag{2.14}$$

These 12 particles mediate the interactions in the SM. We can now write down a corresponding covariant derivative:

$$D_\mu = \partial_\mu - ig_s G^i_\mu U^i - igW^j_\mu L^j - ig' B_\mu Y/2, \tag{2.15}$$

which allows us to determine the specific gauge interactions possible. The kinetic term for the gauge fields themselves is:

$$G^a_{\mu\nu} G^{\mu\nu,a} + W^b_{\mu\nu} W^{\mu\nu,b} + B_{\mu\nu} B^{\mu\nu}, \quad a = 1, 2, ..., 8, \quad b = 1, 2, 3. \tag{2.16}$$

These tensors, called the field strength tensors are defined as follows:

$$G^a_{\mu\nu} = \partial_\mu G^a_\nu - \partial_\nu G^a_\mu - igf^{abc} G^b_\mu G^c_\nu, \tag{2.17}$$

where f^{abc} are the group structure constants. The definitions for $W^b_{\mu\nu}$ and $B_{\mu\nu}$ are similar. The last term is absent for $B_{\mu\nu}$, as it corresponds to an abelian group, which means all structure constants must be zero.

2.1.4 Scalar Particles

The SM also contains scalar particles. Unlike the fermions these do not transform like spinors, since they have spin 0. The SM uses the Higgs boson to give masses to the fermions and to break the SM symmetry. The Higgs boson is placed in the $(1, 2, 1/2)$ representation of the SM. It is an $SU(2)_L$ doublet, hence this representation is often referred to as the Higgs doublet. We have:

$$\phi = \begin{pmatrix} \phi^+ \\ \phi^0 \end{pmatrix} \in (1, 2, 1/2), \tag{2.18}$$

where ϕ^0 and ϕ^+ are complex fields, with the superscripts indicating their charge. We can further parameterize these fields into their real and imaginary components:

$$\phi = \begin{pmatrix} \phi_1 + i\phi_2 \\ \phi_3 + i\phi_4 \end{pmatrix}, \tag{2.19}$$

giving us four real fields. In this work we will make extensive use of much larger representations for the Higgs sector of the $SO(10)$ model we discuss.

2.2 The Higgs Mechanism

When trying to formulate the SM, one quickly runs into a problem. The gauge bosons, $W^\pm_\mu$ and Z^0 are known to be massive, yet it is not possible to write a mass term for them without breaking the symmetry of the SM. A simple mass term (e.g. $m^2 B_\mu B^\mu$) would immediately break the symmetry, as the transformation for gauge bosons in eq. (2.12) does not leave such a term invariant. Furthermore, the $W^\pm$ and Z^0 bosons do not have the same mass, that difference cannot be created with mass terms in an $SU(2)_L$ invariant way.

The fermions suffer from a similar problem. Fermions cannot have Majorana masses, as a term of the form $m^2 e^- e^-$ would result in a vertex that does not respect charge conservation, e.g. a positron could spontaneously turn into an electron. Then we are left with Dirac mass terms, of the form $m\overline{\Psi}\Psi$. This raises another problem, the conjugated field does not transform in the same way as Ψ. If one is left-handed, the conjugate is right-handed. The SM is clearly not left-right symmetric, so these do not transform in the same way. Take for example e_L and e_R from eq. (2.13), the former is an $SU(2)_L$ doublet, the latter is a singlet. Clearly a term of the form $me_L e_R$ is not $SU(2)_L$ invariant.

The solution to both of these problems is the Higgs mechanism. The Higgs mechanism breaks the Electroweak (EW) $SU(2)_L \times U(1)_Y$ symmetry to $U(1)_Q$, the electromagnetic gauge group. In this process it gives mass to the $W^\pm$ and Z^0 bosons. The mechanism can be summarized as follows: at high enough energies the Higgs potential is perfectly symmetric, but at low energies it has a ground state that is not symmetric. In this ground state the Higgs field acquires a vacuum expectation value (vev), this vev then goes on to provide all the necessary mass terms. Essentially, the mechanism provides a way to write an invariant Lagrangian that *spontaneously* breaks the symmetry at a lower energy.

In this section we discuss the mechanism behind spontaneous symmetry breaking (SSB) and how it provides gauge bosons and fermions with masses. Parts of this section are based on [11, 12, 15]

2.2.1 Spontaneous Symmetry Breaking

How does the Higgs mechanism actually perform this spontaneous symmetry breaking? To see that we need to look at the potential. A general potential for a Higgs field, including a quartic self-coupling, could be:

$$V_{Higgs} = -\mu^2(\phi^\dagger\phi) + \lambda(\phi^\dagger\phi)^2, \tag{2.20}$$

which is clearly $SU(2) \times U(1)$ invariant. Note the negative mass term, this is an integral part of the mechanism. The Higgs fields are massless so far, as the square root of $-\mu^2$ is not a real positive mass. Due to this negative term the potential has a minimum that is not at $\phi = 0$. This means that the ground state is shifted away from the centre of the potential; the field develops a vacuum expectation value at low energies. The vev can be found by taking the derivative of the potential with respect to the square of the field:

$$\frac{\partial V_{Higgs}}{\partial(\phi^\dagger\phi)} = 0, \quad \langle\phi^\dagger\phi\rangle = \langle\phi_1^2\rangle + \langle\phi_2^2\rangle + \langle\phi_3^2\rangle + \langle\phi_4^2\rangle = \sqrt{\frac{\mu^2}{2\lambda}} \equiv \frac{v^2}{2}. \tag{2.21}$$

We are free to assign this value to any of the four real fields in eq. (2.19), or a linear combination thereof, as long as the condition above is satisfied. The choice of field will determine the residual symmetry. The SM Higgs doublet decomposes as follows to $SU(3)_C \times U(1)_Q$:

$$(1, 2, 1) \to (1, 1) + (1, 0), \tag{2.22}$$

obviously we want to give the chargeless component a vev, as the other one would also break the $U(1)_Q$ symmetry. When a field obtains a vev, the largest symmetry group (contained in the original group) under which that field is a singlet, will be the residual symmetry of the theory. In assigning a vev to ϕ^0 we are free to decide on a complex phase. For now, we assign a vev to ϕ_3, we get:

$$\phi_{vac} = \frac{1}{\sqrt{2}}\begin{pmatrix} 0 \\ v \end{pmatrix}. \tag{2.23}$$

The branching rule in eq. (2.22) already gave away what the remaining symmetry should be, but we should verify it regardless. A general $SU(2)_L \times U(1)_Y$ transformation can be parameterized as follows: $U = e^{i\alpha^a(x)L_a + i\beta(x)Y/2}$. We can apply it to ϕ_{vac} and keep terms up to first order in α^a and β [11]:

$$U\phi_{vac} = \phi_{vac} + \frac{i}{2}\begin{pmatrix} \alpha^3 + \beta & \alpha^1 + i\alpha^2 \\ \alpha^1 - i\alpha^2 & \alpha^3 - \beta \end{pmatrix}\phi_{vac} = \phi_{vac} + \frac{iv}{2\sqrt{2}}\begin{pmatrix} \alpha^1 + i\alpha^2 \\ \alpha^3 - \beta \end{pmatrix}. \tag{2.24}$$

For ϕ_{vac} to be invariant we require the second term to be zero, therefore we have $\alpha^1 = -i\alpha^2 = 0$, and $\alpha^3 = \beta$. So only a transformation associated with the linear combination of generators:

$$Q = L_3 + \frac{Y}{2}, \tag{2.25}$$

leaves this potential invariant (aside from $SU(3)_C$ invariance). Q is precisely the operator for the electric charge, associated with $U(1)_Q$, the symmetry of quantum electrodynamics. We have now performed the following SSB of the SM:

$$SU(3)_C \times SU(2)_L \times U(1)_Y \to SU(3)_C \times U(1)_Q. \tag{2.26}$$

The Lagrangian no longer being invariant under the SM group symmetry is not the only consequence. This mechanism has given masses to several gauge bosons, the Higgs boson and, by adding the right terms, to the fermions.

2.2.2 Scalar Masses

The Higgs mechanism provides a mass to some of the scalar fields contained in the Higgs representation $(1, 2, 1/2)$. The masses of the scalar sector can be identified easily, we expand the Higgs potential as a power series around the vev, then the second derivatives with respect to the fields correspond to the mass terms such that [16]:

$$\frac{\partial^2 V}{\partial\phi_i \partial\phi_j}\Big|_{\phi_{vac}} \equiv M_{ij}^2. \tag{2.27}$$

In general this matrix does not have to be diagonal, especially if multiple Higgs representations are used. When it is not diagonal, the mass eigenstates are combinations of scalar fields. For the potential of the SM Higgs doublet we get the following mass matrix:

$$M_{ij}^2 = \begin{pmatrix} 0 & & & \\ & 0 & & \\ & & 2\mu^2 & \\ & & & 0 \end{pmatrix}, \tag{2.28}$$

which is quite straightforward. The fields ϕ_1, ϕ_2 and ϕ_4 are massless, these are the so-called Goldstone bosons. In the relativistic case, every broken generator should have one Goldstone boson associated with it. Since we have broken three generators, this is in agreement. The ϕ_3 field, often called h after symmetry breaking, has acquired a mass of $\sqrt{2}\mu$.

There remains a problem however, these massless Goldstone bosons are never actually seen. There is a solution, by applying the right gauge transformation to the broken generators we can remove any terms involving the Goldstone bosons. In this manner, the Goldstone bosons are absorbed by the massive gauge bosons. This gives the massive bosons a third polarization degree of freedom, whereas massless particles only have two.

2.2.3 Gauge Boson Masses

The Higgs mechanism gives mass to the gauge bosons associated with broken symmetries. Since the residual symmetry is a linear combination of two symmetries, we can expect the mass spectrum to not be diagonal in W_μ^a and B_μ. Instead, the resulting mass eigenstates will be linear combinations of these gauge bosons. To see this, examine the kinetic term of the Higgs field, and keep only the terms containing the vev:

$$\begin{aligned} V_{mass} = (D_\mu \phi_{vac})^\dagger (D^\mu \phi_{vac}) &= \left| \begin{pmatrix} \partial_\mu - \frac{ig}{2} W_\mu^3 - \frac{ig'}{2} B_\mu & -\frac{ig}{2}(W_\mu^1 - iW_\mu^2) \\ -\frac{ig}{2}(W_\mu^1 + iW_\mu^2) & -\frac{ig}{2} W_\mu^3 + \frac{ig'}{2} B_\mu \end{pmatrix} \phi_{vac} \right|^2 \\ &= \frac{v^2}{8}(g^2|W_\mu^1 - iW_\mu^2|^2 + |gW_\mu^3 - g'B_\mu|^2). \end{aligned} \tag{2.29}$$

We can clearly identify mass terms, but as expected they are not diagonal in the gauge fields. The mass matrix is:

$$M_{ab}^2 = \frac{\partial^2 V_{mass}}{\partial G_\mu^a \partial G_\mu^b} = \begin{pmatrix} g^2 & & & \\ & g^2 & & \\ & & g^2 & -gg' \\ & & -gg' & g'^2 \end{pmatrix}, \quad G_\mu^a, G_\mu^b = W_\mu^1, W_\mu^2, W_\mu^3, B_\mu. \tag{2.30}$$

Diagonalizing gives the following gauge bosons along with their masses:

$$W_\mu^\pm = \frac{1}{\sqrt{2}}(W_\mu^1 \mp W_\mu^2), \quad m_W = \frac{vg}{2}, \tag{2.31}$$

$$Z_\mu^0 = \frac{1}{\sqrt{g^2 + g'^2}}(gW_\mu^3 - g'B_\mu), \quad m_z = \frac{v}{2}\sqrt{g^2 + g'^2}, \tag{2.32}$$

$$A_\mu = \frac{1}{\sqrt{g^2 + g'^2}}(g'W_\mu^3 + gB_\mu), \quad m_\gamma = 0, \tag{2.33}$$

which are just the familiar $W^\pm$ and Z^0 bosons, in addition to the photon, which is massless, as it should be. Seemingly, the Higgs mechanism has correctly generated the masses for the gauge bosons.

2.2.4 Fermion Masses

The fermions obtain their masses through couplings with the Higgs particle in the Yukawa sector. This sector has terms following the form of a Yukawa coupling: $g\overline{\Psi}\phi\Psi$. For the SM this sector is as follows:

$$\mathcal{L}_Y = \lambda_d \overline{Q_L} \phi d_R + \lambda_u \epsilon^{ab} \overline{Q_{La}} \phi_b^\dagger u_R + \lambda_e \overline{E_L} \phi e_R + h.c, \tag{2.34}$$

with ϕ the Higgs field, d_R, u_R, Q_L, E_L and e_R the fermion fields and ϵ^{ab} a 2×2 antisymmetric tensor. Inserting the vev in this expression gives mass terms of the form: $\lambda\langle\phi\rangle\overline{\psi}_L\psi_R$, exactly what we need to give particles a Dirac mass. Since the SM contains three generations of particles we should create Yukawa couplings for each generation. It turns out that the Yukawa sector is actually not diagonal in the three generations. This causes mixing of the flavour states into mass eigenstates. The Yukawa matrix for three generations of quarks is as follows [17]:

$$\mathcal{L}_Y = -Y_{ij}^d \overline{Q_{Li}} \phi d_{Rj} - Y_{ij}^u \overline{Q_{Li}} \epsilon \phi^\dagger u_{Rj} + h.c., \tag{2.35}$$

where $Y^{u,d}$ are the Yukawa matrices for the up and down quarks, and i, j are the generation indices. The Yukawa matrices are 3×3 complex matrices determining the couplings between the Higgs field and the fermions. The fermions in this equation are in the weak flavour eigenstate basis, not in the mass eigenstate basis. To diagonalize the mass matrix for this system, we can apply the following basis transformation:

$$M_{diag}^{2\ u,d} = V_L^{u,d} Y^{u,d} V_R^{u,d} \langle\phi\rangle, \tag{2.36}$$

where $V_{L,R}^{u,d}$ are basis transformation matrices for the up-type and down-type quarks, respectively. This gives rise to the Cabibbo-Kobayashi-Maskawa (CKM) matrix [17]:

$$V_{CKM} = V_L^u V_L^{d\dagger} = \begin{pmatrix} V_{ud} & V_{us} & V_{ub} \\ V_{cd} & V_{cs} & V_{cb} \\ V_{td} & V_{ts} & V_{tb} \end{pmatrix}, \quad \begin{pmatrix} d' \\ c' \\ b' \end{pmatrix} = V_{CKM} \begin{pmatrix} d \\ c \\ b \end{pmatrix} \tag{2.37}$$

which is a 3×3 unitary matrix. The second equation shows how the CKM matrix relates the flavour eigenstate down-type quarks (d', s', b') to their mass eigenstate counterparts (d, s, b). A similar matrix relating the mass and flavour basis of the neutrinos exists, the Pontecorvo-Maki-Nakagawa-Sakata (PMNS) matrix, or V_{PMNS} [17].

2.3 Renormalisation

Loop effects in quantum field theories cause infinities when calculating amplitudes. There is a procedure to get rid of these infinities, called renormalisation. Renormalisation of field theories is dependent on the energy scale μ. This means that the couplings g_i associated with each symmetry group are also dependent on μ. This is the so-called running of the couplings. Eventually the couplings of the individual groups are expected to reach the same value for a certain energy, which is known as the gauge coupling unification. The running of each g_i can be calculated using the β-function. The running of the coupling can easily be computed, up to one-loop, using the following relation [14]:

$$\frac{\mathrm{d}g_i}{\mathrm{d}\ln\mu} = \beta(g_i) = b_i \frac{g_i^3}{4\pi^2} \Rightarrow \frac{4\pi}{g_i^2(\mu_2)} = \frac{4\pi}{g_i^2(\mu_1)} - \frac{b_i}{2\pi}\ln\frac{\mu_2}{\mu_1}, \tag{2.38}$$

where b_i are the β-coefficients. Note that we have expanded the β-function and have only kept the term that is the lowest order in g_i. This corresponds to taking the one-loop β-function, neglecting any corrections from diagrams with more loops. Substituting the coupling for the fine structure constant $\alpha = \frac{g_i^2}{4\pi}$, we obtain:

$$\alpha_i^{-1}(\mu_2) = \alpha_i^{-1}(\mu_1) - \frac{b_i}{2\pi}\ln\frac{\mu_2}{\mu_1}. \tag{2.39}$$

To fully specify how coupling constants evolve, all we have to do, is determine the β-coefficients b_i and find out how the coupling constants relate to each other at a symmetry breaking step. Once we can calculate the evolution of the gauge couplings, we will be able to establish whether a theory allows for unification. Therefore, this will show whether a scenario is a valid GUT to begin with.

2.3.1 β-coefficients

Calculating the β-coefficients is a straightforward procedure. In essence, we need to examine the particle content of a theory and the associated representations. At each energy scale, all particles which are massless contribute to the β-coefficient. To a decent approximation, when a particle gains a mass through the Higgs mechanism at a certain scale, it does not contribute to the running below that scale. In section 6.3, we explain how the effects of massive particles are approximated below their mass scale by an effective field theory. The basic conclusion is that their effects are suppressed by at least $1/M^2$, and more for higher dimension interactions. For this reason they do not contribute significantly to the running.

The influence of the Yukawa couplings on the β-coefficients can be ignored, as they contribute to the β-functions at the two-loop level [18].

Multiple equivalent ways to compute the β-coefficients exist, we use the one employed in [19]:

$$b_i = -\frac{11}{3}\mathcal{C}_2(G) + \frac{2}{3}\sum_{R_f} T(R_F)\prod_{j\neq i} d_j(R_f) + \frac{1}{3}\sum_{R_s} T(R_s)\prod_{j\neq i} d_j(R_s), \tag{2.40}$$

where $\mathcal{C}_2(G)$ is the quadratic Casimir operator for the group to which g_i corresponds:

$$\mathcal{C}_2(G) \equiv \begin{cases} N & \text{if } SU(N), \\ 0 & \text{if } U(1). \end{cases} \tag{2.41}$$

For $SO(N)$, this is $2(N-2)$, so $\mathcal{C}_2 = 16$ for $SO(10)$ [20]. Moving on, $R_{f,s}$ are specific representations of fermions (f) and scalars (s) under the total group of a model. For example, in the SM group $SU(3)_C \times SU(2)_L \times U(1)_Y$, the quarks are represented in $(3, 2, 1/6)$. $T(R_{f,s})$ are the Dynkin indices associated with these representations. The formal definition is as follows:

$$T(R)\delta^{ab} = [T^a, T^b], \tag{2.42}$$

where $T^{a,b}$ are the generators of R.

However, we do not need to engage with this definition, as generally the Dynkin indices are as follows for $SU(N)$:

$$T(R_{f,s}) = \begin{cases} N & \text{if rep = adjoint}, \\ 1/2 & \text{if rep = fundamental}, \\ 0 & \text{if rep = singlet}. \end{cases} \tag{2.43}$$

To expand on our example of the quarks in the SM group, the Dynkin index corresponding to $(3, 2, 1/6)$ for $SU(3)$ would be $1/2$, since it is a fundamental representation of $SU(3)$. The product eq. (2.40) tell us to multiply each Dynkin index with the dimensionality of the representation in the remaining groups. For our example this means multiplying by 2, as that is its dimension under $SU(2)$. The $U(1)_Y$ eigenvalue of the representation is irrelevant, as every irreducible representation is 1-dimensional under $U(1)_Y$. The three generations of quarks and leptons should also be taken into account, therefore any Dynkin index corresponding to fermions must be multiplied by 3. This only applies when $\mu \gg m_{top}$, since we do not take into account particles heavier than μ.

A full example of the β-coefficient b_1, corresponding to $SU(3)_C$ under the SM is given:

$$b_1 = -3(\frac{11}{3}) + 3(\frac{2}{3})\left(2(\frac{1}{2}) + \frac{1}{2} + \frac{1}{2}\right) = -7, \tag{2.44}$$

where we have used the representations $(3, 2, 1/6)$, $(\bar{3}, 1, 1/3)$ and $(3, 1, -2/3)$. The other representations of the SM, $(1, 2, -1/2)$, $(1, 1, 1)$ and $(1, 2, 1/2)$ are irrelevant, as they are $SU(3)_C$ singlets.

Special attention must be given to $U(1)$, as its Dynkin indices are computed slightly differently:

$$T(R_{r,s}) = \lambda_N^2, \tag{2.45}$$

where λ_N is simply the eigenvalue of the normalized operator associated with $U(1)$. It is very important to take into account the normalization of this operator when computing Dynkin indices. The normalization of $U(1)$ operators is in principle arbitrary, so the associated eigenvalues can be arbitrarily scaled. This would directly impact the magnitude of the β-coefficient. To prevent this, we normalize the $U(1)$ operators in the same way as any other operator in a model. For the case of $U(1)_Y$ in an $SO(10)$ theory, it should be normalized like $Y' = \sqrt{\frac{3}{5}}Y$. This ensures that $\mathrm{Tr}(Y^2) = 4$, which is how the other operators in $SO(10)$ are normalized. Applying this normalization means multiplying the β-coefficient by $\frac{3}{5}$, as we use $\lambda'^2 = \frac{3}{5}\lambda^2$.

2.3.2 Matching Conditions

In order to establish how the fine-structure constants of theories relate to each other at a symmetry breaking scale, we need to establish certain matching conditions. In general these conditions are fairly simple. For example, if any group, below the symmetry breaking scale μ, is embedded into a single group above that energy scale, then at μ we have: $\alpha_{below}(\mu) = \alpha_{above}(\mu)$ [16]. This is exactly what happens to the strong force fine-structure constant α_s at the electroweak symmetry breaking scale M_W:

$$\alpha_s(M_W) = \alpha_{3C}(M_W) \tag{2.46}$$

For the fine-structure constant of quantum electrodynamics (QED) we need a slightly more complicated condition. The gauge group of QED, $U(1)_Q$, is embedded into $SU(2) \times U(1)_Y$ at M_W. We can use the operator Q of QED to figure this out, we have:

$$Q = L_3 + Y/2, \tag{2.47}$$

however, this still requires normalization. Recall that the proper normalization of Y is $Y' = \sqrt{\frac{3}{5}}Y$, the normalization of the $U(1)_Q$ operator is: $Q' = \sqrt{\frac{3}{8}}Q$ Plugging this into the above equation yields:

$$Q' = \sqrt{\frac{3}{8}}L_3 + \sqrt{\frac{5}{8}}Y'/2. \tag{2.48}$$

From this relation of operators we can obtain a relation between couplings. In general, we have the following rule: if an operator can be expressed as a linear combination of operators, then we have [16]:

$$T(\mu) = \sum_i p_i T_i(\mu) \quad \Rightarrow \quad \frac{1}{g^2(\mu)} = \sum_i \frac{p_i}{g_i^2(\mu)}, \tag{2.49}$$

where p_i are the coefficients of the linear combination. We can substitute the inverse fine-structure constants right into this equation. For $U(1)_Q$ we can now easily find the relation:

$$\alpha_Q^{-1} = \frac{3}{8}\alpha_{2L}^{-1} + \frac{5}{8}\alpha_Y^{-1}. \tag{2.50}$$

Clearly, whenever a group is embedded into a product of multiple groups at higher energies, the matching condition is no longer trivial. The procedure above can be applied to any such case.

It should be noted that the matching conditions in this section rely on the approximation that symmetry breaking scales are discrete boundaries below which no effects are felt from particles that obtain a mass above it. A more accurate approach, would be to include threshold corrections, which take into account the effects of massive particles close to the symmetry breaking scale.

2.3.3 The Standard Model Running

Applying the concepts in this section to the SM allows us to show the running of the couplings before and after symmetry breaking. The β-coefficients below EW symmetry breaking are [12]:

$$b_s = -\frac{22}{3}, \quad b_Q = \frac{10}{3} \tag{2.51}$$

and above this scale:

$$b_{3C} = -7, \quad b_{2L} = -\frac{19}{6}, \quad b_Y = \frac{41}{10}. \tag{2.52}$$

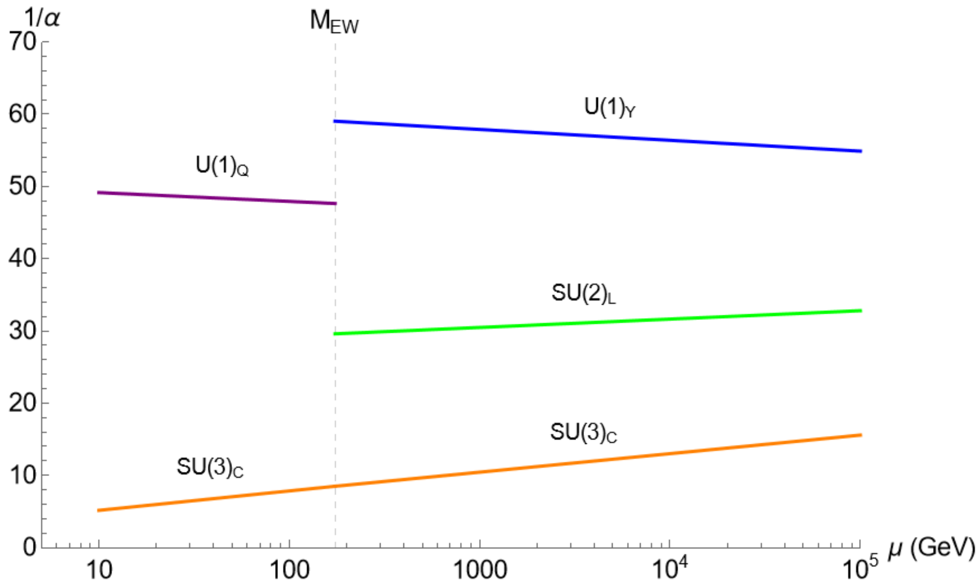

Figure 2.1: The running of the SM above and below the EW symmetry breaking scale $M_{EW} = 174\,\text{GeV}$

Together with the matching condition in eq. (2.50) and the Weinberg angle, we can completely specify the running. A computation of the fine structure constants α_Y and α_{2L} is performed in section 5.4.1. Combining these things we can obtain the running shown in Figure 2.1

The fine structure constant associated with $SU(3)$ clearly just continues past M_{EW}, as it is not affected by the symmetry breaking. The associated β-coefficient does change, due to the top quark becoming massless above M_{EW}. The matching condition in eq. (2.50) is clearly visible in the graph.

Chapter 3

Leptoquarks in Grand Unified Theories

Many extensions of the Standard Model contain particles that carry both baryon number and lepton number, called leptoquarks, which form the main interest of this thesis. These particles can mediate interactions between leptons and quarks in one vertex. Generally, leptoquarks can arise from two sectors: the gauge sector or the scalar sector. In the former case, extending the gauge group of the SM to a larger group will put leptons and quarks into the same representations. The adjoint of this enlarged gauge group will then contain new gauge bosons that couple to leptons and quarks at the same time. The latter case, scalar leptoquarks, arise from Yukawa couplings between new scalar particles, leptons and quarks. Grand unified theories (GUTs) often contain many new scalar particles in order to achieve the desired symmetry breaking down to the SM. The new interaction vertices such particles could possess, dependent on the model they arise from, are shown in Figure 3.1.

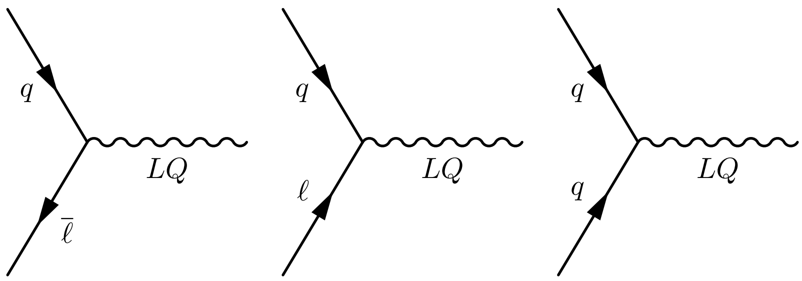

Figure 3.1: Possible couplings of leptoquarks. From l. to r. a coupling between a quark and an anti-lepton, a quark and a lepton, and lastly a diquark coupling that some leptoquarks possess.

We can distinguish between "pure" leptoquarks, which only possess lepton-quark couplings, like the first diagram in Figure 3.1, and B-violating leptoquarks. The B-violating leptoquarks possess diquark couplings along with leptoquark couplings. This allows them to violate baryon number, which could lead to proton decay [21]. For example, the process in Figure 3.2 could mediate proton decay by having a diquark coupling on one side and a leptoquark coupling on the other. The proton lifetime has been measured up to very high precision, so particles that cause proton decay are constrained to exist at extremely high energies ($> 10^{16}$ GeV). These proton decay measurements provide one of the main bounds on GUTs, see e.g. [10] for proton decay constraints on many models including GUTs with leptoquarks.

In this chapter we will examine several non-supersymmetric GUT scenarios and their leptoquark content. This is largely a summary of the conclusions found in [12], which was based on the GUT scenarios classified in [11].

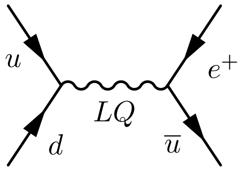

Figure 3.2: Possible diagram leading to proton decay mediated by a leptoquark as shown in [12]

3.1 GUT Scenarios

Multiple GUT scenarios lead to the existence of leptoquarks, however most of these do not provide any leptoquarks on an energy scale low enough to be near current experimental reach (e.g. $\sim$ TeV-scale). The main reasons why, are the bound from proton decay, as mentioned above, and the lack of larger symmetry groups at low energy in many scenarios. Some models simply do not have new physics at low energy scales at all, because solving the β-functions would not allow for coupling unification with low energy intermediate scales, see section 2.3.

In [12], GUTs based on $SU(5)$, $SO(10)$ and trinification ($SU(3)^3$) were considered. These three scenarios will be briefly reviewed in this section. These three gauge groups are all subgroups of E_6, as shown in [11]. All GUTs embedded in E_6 are mapped out in Figure 3.3.

A GUT based on E_6 was first presented in [22]. It was of interest as it contains $SU(3)_C \times SU(3)_L \times SU(3)_R$, the trinification group, which the authors considered a promising model. Furthermore, E_6 is naturally anomaly free, has many options for symmetry breaking down to the SM and can contain all fermions of one generation in its fundamental representation [23]. This fundamental representation can be complex, which is essential for a valid GUT, in order to maintain the chiral nature of the weak interaction [24].

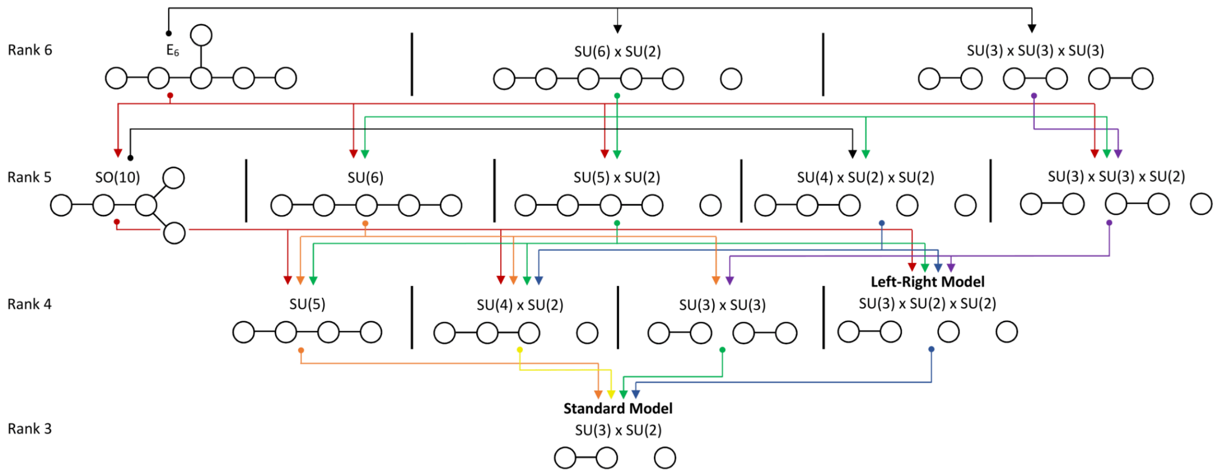

Figure 3.3: Overview of GUTs embedded in E_6, taken from [11]. The Dynkin diagram for each group is shown. The arrows connect a group with the groups it can break to.

The importance of a chiral theory to be anomaly free was identified in [25]. They defined the anomaly of a gauge group as:

$$\mathcal{A}_{abc} = \text{Tr}[t_a\{t_b, t_c\}], \tag{3.1}$$

where t_a are the generators of the group. Essentially, the argument is that certain loop diagrams lead to the non-conservation of axial currents, unless $\mathcal{A}_{abc} = 0$. These anomalies could be cancelled by introducing extra fermions, but this is not desirable if a minimal model is sought after.

E_6 contains more paths down to the SM than just those described in this section. In Figure 3.3 there are paths through $SU(6) \times SU(2)$ or directly to $SU(6)$. These gauge groups could also be models for a GUT themselves. However, looking at the figure, $SU(6) \times SU(2)$ does not provide very different paths down to the SM, compared to the models discussed in this chapter. A potential path is through $SU(5) \times SU(2)$, in section 3.1.1, we will see that $SU(5)$ is restricted to lie at very high energies, therefore $SU(5) \times SU(2)$ is as well. Then there is the option of going through $SU(4)_C \times SU(2)_L \times SU(2)_R$, which $SO(10)$ can break to as well, or breaking to $SU(3) \times SU(3) \times SU(2)$, which can be reached from trinification. Similarly, starting from $SU(6)$, there are only paths identical to those from the models discussed in this chapter. Given that the unification scale is high, it is mainly the intermediate symmetries between the GUT and the SM that are interesting to study in the context of leptoquarks. Therefore, we will not discuss $SU(6)$ based models any further.

3.1.1 The Georgi-Glashow Model: $SU(5)$

A grand unification model based on the $SU(5)$ gauge group was first proposed by Georgi and Glashow [7]. It is one of the simplest models capable of unifying the gauge interactions, as it is the smallest simple Lie group containing the SM. It is rank 4, only one higher than the SM. The fact that it is so minimal was initially seen as one of the major advantages of $SU(5)$. The flip side is that, being such a small group, there are no intermediate symmetries to assist in unifying the couplings.

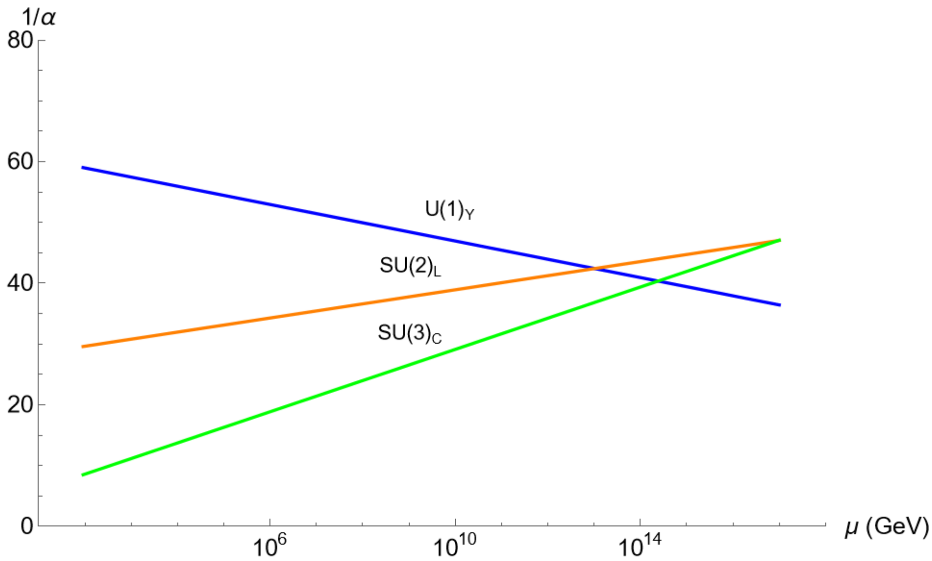

Figure 3.4: Running of the inverse fine-structure constants of the SM as obtained in [12]. Clearly the gauge couplings do not unify.

In fact, $SU(5)$ relies on the couplings of the SM gauge group to unify into a single point, but this does not happen, as can be seen in Figure 3.4. This can be remedied by tweaking the parameters in the SM. Essentially, unification is assumed, and the running is computed, taking the well-known fine-structure constants of the electromagnetic and strong interactions as input. This leaves the precise values of the couplings of $SU(2)_L$ and $U(1)_Y$ as free parameters, constrained by α_{EM} and unification. Therefore, the Weinberg angle is considered an output of this model. The value obtained is [26]:

$$\sin^2\theta_W(M_W) = \frac{g'^2}{g^2 + g'^2} = 0.208, \tag{3.2}$$

with g' the coupling of $U(1)_Y$ and g the coupling of $SU(2)_L$. This value is quite different from the current accepted value of $sin^2\theta_W(M_W) = 0.23121(4)$ [17]. Clearly, minimal $SU(5)$ unification is incompatible with this value, as the measured value has a very small margin of error.

If the running of the SM is significantly altered close to the GUT-scale due to some additional fields, unification is perhaps possible. This in turn would not be minimal $SU(5)$. Minimal $SU(5)$, as the name suggests, relies on using the smallest and fewest representations necessary to be phenomenologically consistent.

The lack of gauge coupling unification is problematic enough by itself, but even assuming the couplings do unify, $SU(5)$ runs into experimental constraints. It is precisely the particles we are interested in, leptoquarks, that further exclude $SU(5)$. All 12 new gauge bosons in $SU(5)$ are leptoquarks, they are referred to as X and Y bosons (though commonly called V_2 in model-independent literature). Their SM representations are:

$$\begin{pmatrix} X_1 & X_2 & X_3 \\ Y_1 & Y_2 & Y_3 \end{pmatrix} \in (\overline{3}, 2, 5/6), \quad \begin{pmatrix} \overline{X}_1 & \overline{X}_2 & \overline{X}_3 \\ \overline{Y}_1 & \overline{Y}_2 & \overline{Y}_3 \end{pmatrix} \in (3, 2, -5/6). \tag{3.3}$$

These leptoquarks possess both diquark and leptoquark couplings, meaning they are of the B-violating type. As stated before, this puts large constraints on these particles. Naturally, because they are gauge bosons of $SU(5)$, their mass is around the unification scale. The unification scale for $SU(5)$, assuming unification will actually happen, is on the order of 10^{15} GeV. This is too low to be compatible with current limits on proton decay [12], which require a unification scale on the order of at least 10^{16} GeV.

In conclusion, while it initially seemed like a simple and minimal model for unification, minimal $SU(5)$ is excluded on one side by precise measurements of the Weinberg angle, preventing unification, and on the other side by proton decay, ruling it out entirely. Furthermore, putting these problems aside, minimal $SU(5)$ does not contain any new physics at the TeV-scale, making it not interesting to study with current collider experiments.

3.1.2 Trinification

Another model described in [12] is trinification. This model is based on the gauge group:

$$SU(3)_C \times SU(3)_L \times SU(3)_R \times \mathbb{Z}_3, \tag{3.4}$$

or $SU(3)^3$ for short. The additional $\mathbb{Z}_3$ symmetry ensures that all three groups have the same gauge coupling, thereby imposing unification. This model does not unify quarks and leptons into a single representation, as opposed to $SU(5)$ and $SO(10)$. Therefore, there are no gauge interactions mixing these particles. In other words, there are no vector leptoquarks in trinification. The benefit of this, is the lack of proton decay due to gauge interactions.

However, the scalar sector of the trinification model does contain leptoquarks, including those mediating proton decay. Bounds due to proton decay on scalar leptoquarks are more relaxed than those on vector leptoquarks. This is due to the fact that the Yukawa couplings Y_u and Y_d, which determine the interaction strength between the quarks and the scalar particles, are generally smaller than the gauge couplings. These smaller couplings suppress the B-violating processes. The bound is estimated to be on the order of 10^{11} GeV [10].

As opposed to $SU(5)$, trinification allows for unification of the gauge couplings, without changing the Weinberg angle. The symmetry breaking pattern that allows for this unification is:

$$SU(3)^3 \times \mathbb{Z}_3 \xrightarrow{M_U} SU(3)_C \times SU(2)_L \times SU(2)_R \times U(1)_{L+R} \xrightarrow{M_I} SM \tag{3.5}$$

with $M_U = 1.3\times10^{16}$ GeV and $M_I = 1.0\times10^{11}$ GeV. This means that, aside from additional Higgs doublets, there is no new physics in this model below 10^{11} GeV, as both the larger gauge group and the scalar leptoquarks are restricted to lie at or above this scale.

In conclusion, while this model is much more promising than $SU(5)$, it does not provide us with TeV-scale leptoquarks. The scale of new physics in this model is so far beyond current experimental reach, that we do not consider it further in this work.

3.1.3 $SO(10)$

The final model considered in [12] is $SO(10)$. A GUT based on this gauge group was first developed in [9]. It is an attractive model, as it is only one rank higher than the clearly excluded $SU(5)$, making it one of the most minimal options left.

$SO(10)$ grand unification allows for many paths down to the SM, as seen in Figure 3.3. The Pati-Salam model, based on $SU(4)_C \times SU(2)_L \times SU(2)_R$ is in some of these paths. This model, originally described in [8], treats leptons as the "fourth colour", thereby allowing gauge interactions that mix leptons and quarks. Therefore, $SO(10)$ includes vector leptoquarks, which might be on the TeV-scale, provided the Pati-Salam model is broken at such energies.

The unified theory itself contains leptoquarks that also possess diquark couplings. These mediate proton decay and push the unification scale up to similar energies as found for $SU(5)$, around 10^{16} GeV. However, the leptoquarks found in the Pati-Salam group are pure leptoquarks. These specific leptoquarks are commonly called U_1 in literature, or are referred to by their SM representation $(3, 1, 2/3)$. In [12] it was found that a specific symmetry-breaking chain could allow for these pure vector leptoquarks at the TeV-scale. This is due to the fact that solving the running of the couplings leaves two free parameters, resulting in a freedom to choose the scale at which the Pati-Salam group breaks. This motivates us to further examine this model in chapter 4.

In short, $SO(10)$ could offer a scenario for TeV-scale pure leptoquarks, which does not immediately run into bounds on proton decay or unification.

3.2 Concluding Remarks

We have shortly reviewed the GUT scenarios established in [11, 12], and the leptoquarks contained in them. These leptoquarks are summarized in Table 3.1. For completeness, we have included the scalar leptoquarks present in $SO(10)$, which we identify in chapter 4. Clearly, reasoning from an interest in low-energy leptoquarks, $SO(10)$ is the model that we need to examine further. Minimal $SU(5)$ is solidly ruled out due to proton decay, and trinification does not give any light leptoquarks. Therefore, we will review and expand upon the work done in [12] to establish a clear scenario for TeV-scale leptoquarks in chapter 4.

Name	SM reps	Q	GUT(s)	Type	Energy Scale	Proton decay
V_2	$(\overline{3}, 2, 5/6)$	$4/3, 1/3$	$SU(5), SO(10)$	Vector	GUT-scale	Yes
$\tilde{V}_2$	$(\overline{3}, 2, -1/6)$	$1/3, -2/3$	$SO(10)$	Vector	GUT-scale	Yes
U_1	$(3, 1, 2/3)$	$2/3$	$SO(10)$	Vector	$\geq 5\,\text{TeV}$	No
S_1	$(\overline{3}, 1, 1/3)$	$1/3$	$SU(5)$	Scalar	$\geq 10^{11}\,\text{GeV}$	Yes
S_3	$(3, 3, 1/3)$	$4/3, 1/3, -2/3$	Trinification	Scalar	$\geq 10^{11}\,\text{GeV}$	Yes
R_2	$(3, 2, 7/6)$	$5/3, 2/3$	$SO(10)$	Scalar	$\geq$ TeV	No
$\tilde{R}_2$	$(3, 2, 1/6)$	$2/3, -1/3$	$SO(10)$	Scalar	$\geq$ TeV	No

Table 3.1: Leptoquarks in three GUTs, some found in [12], others in chapter 4. The particles are listed along with their names, as commonly found in literature.

Chapter 4

$SO(10)$ Representations

In chapter 3 we established that an $SO(10)$ GUT is the only model (aside from the very similar $SU(6) \times SU(2)$) from E_6 that could have leptoquarks at the TeV-scale. In this unifying theory all fermions of one generation fit into a 16-dimensional spinor representation, including a right-handed neutrino [27]. $SO(10)$ contains both $SU(5)$ and $SU(4)_c \times SU(2)_L \times SU(2)_R$ (Pati-Salam) as subgroups. This makes it an attractive GUT as we can break the symmetry down to the SM group in a variety of ways. One of these paths, involving three intermediate energy scales and the Pati-Salam (PS) group [19], is what allows for the existence of leptoquarks at the TeV-scale [12, 28].

The goal of this chapter is to examine all representations we need to build a consistent GUT. In these representations, both scalar and adjoint, we will identify any leptoquarks we come across.

Firstly, we introduce the necessary mathematics to construct representations for $SO(10)$. This will allow us to examine how $SO(10)$ accommodates all fermions and gives rise to new gauge bosons. This first section will follow and elaborate on a lot of the work done in [12, 27].

Secondly, we will discuss the breaking of the symmetry down to the SM. Several Higgs representations of $SO(10)$ will be examined. We will determine which fields need to be given a vacuum expectation value (vev) in order to obtain the symmetry breaking pattern we need. In this section we will also identify any scalar leptoquarks, if they exist. The second section is partially based on [27].

The conclusions in the rest of this work on vector leptoquarks can be applied to $SU(6) \times SU(2)$, but scalar leptoquarks would require their own study, since they are specific to the representations of the GUT group.

4.1 Group Theory and Representations

$SO(10)$ is a Lie group defined by all 10×10 dimensional real matrices that are orthogonal and have determinant 1. This is equivalently stated as:

$$SO(10) = \{O \in GL(10, \mathbb{R}) | O^T O = \mathbf{1}, \det(O) = 1\}, \tag{4.1}$$

where $GL(10, \mathbb{R})$ is the general linear group of degree 10 over the reals, in other words, the group of 10×10 real invertible matrices. Essentially $SO(10)$ is the group of all rotations of real 10 dimensional vectors. The generators Σ_{ab} of $SO(10)$ satisfy the following Lie algebra:

$$[\Sigma_{ab}, \Sigma_{cd}] = \delta_{ad}\Sigma_{bc} + \delta_{bc}\Sigma_{ad} - \delta_{ac}\Sigma_{bd} - \delta_{bd}\Sigma_{ac}. \tag{4.2}$$

In order to examine the particle content of an $SO(10)$ GUT, we need to develop a representation for this theory. We can classify the gauge bosons by looking at the adjoint representation. Furthermore, we need to place all fermions into a spinor representation of $SO(10)$. In actuality, we will construct a representation of $Spin(10)$, which forms a double cover of $SO(10)$. The basic idea is to first represent a general $SO(2N)$ group in a spinor basis. We will construct such a basis following the steps in [27, 29].

4.1.1 $SO(2N)$ Represented in a Spinor Basis

It is well known that $SO(3)$ is locally isomorphic to $SU(2)$, and therefore it can be represented in terms of $SU(2)$ generators. This concept can be applied to $SO(2N)$ for any N, by relating it to $Spin(2N)$. The $SO(2N)$ group rotates vectors in $2N$-dimensional space, leaving their lengths unchanged due to the orthogonality condition of the group. In principle, to define a basis for $SO(2N)$ we need a set of $m = 2N$ objects $\Gamma_1, \Gamma_2, ..., \Gamma_m$, which leaves the length of an m-component vector invariant:

$$x_1^2 + x_1^2 + ... + x_m^2 = (x_1\Gamma_1 + x_2\Gamma_2 + ... + x_m\Gamma_m)^2. \tag{4.3}$$

Examining this expression, it is clear what the conditions on the Γ's are. $\Gamma_a^2 = 1, (a = 1, 2, ..., m)$ and $\Gamma_a\Gamma_b = -\Gamma_b\Gamma_a$, to ensure cancellation of all cross terms, preserving only terms of the form x_a^2. This condition is equivalently written as:

$$\Gamma_a\Gamma_b + \Gamma_b\Gamma_a = 2\delta_{ab}\mathbf{1}, \tag{4.4}$$

which defines a Clifford algebra. The Clifford algebra forms the fundamental representation of $SO(2N)$. We can now use this to create generators of $SO(2N)$ as follows:

$$\Sigma_{ab} = \frac{i}{4}[\Gamma_a, \Gamma_b], \tag{4.5}$$

$$[\Sigma_{ab}, \Sigma_{cd}] = i(\delta_{ad}\Sigma_{bc} + \delta_{bc}\Sigma_{ad} - \delta_{ac}\Sigma_{bd} - \delta_{bd}\Sigma_{ac}), \tag{4.6}$$

with the second equation showing that the Σ's satisfy the Lie algebra of $SO(2N)$. The factor i with respect to eq. (4.2) is down to the fact that this representation is complex instead of real. The generators Σ_{ab} also have the property $\Sigma_{ab} = -\Sigma_{ba}$. It is important to note that each Σ_{ab} labels a separate $(2^N \times 2^N)$ matrix, due to the fact that the representations of the Clifford Algebra are as well. By constructing generators that satisfy the Lie algebra of $SO(2N)$ we can represent $SO(2N)$ itself by exponentiating the generators. The spinor representation of $SO(2N)$ is then

$$R_m = e^{-i\Sigma_{ab}\omega_{ab}}, \tag{4.7}$$

with ω_{ab} the numbers quantifying the transformations. We have now constructed a 2^N dimensional spinor representation of $SO(2N)$. Clearly, the condition for $SO(2N)$ is satisfied:

$$R_m R_m^\dagger = e^{-i\Sigma_{ab}\omega_{ab}} e^{+i\Sigma_{ab}\omega_{ab}} = \mathbf{1}, \tag{4.8}$$

as $\Sigma_{ab}^\dagger = \Sigma_{ab}$, with Σ_{ab} always being real and symmetric or imaginary and antisymmetric [27].

4.1.2 $SO(10)$ Spinor Representation

We have established a general spinor representation for $SO(2N)$. For $SO(10)$ specifically, this procedure gives us the following representation:

$$U = e^{-i\Sigma_{ab}\omega_{ab}}, \tag{4.9}$$

where Σ_{ab} is a 10×10 object with each element being a 32×32 matrix. Therefore, the inner product $\Sigma_{ab}\omega_{ab}$ is also 32×32. An infinitesimal transformation of a spinor is as follows:

$$\Psi \rightarrow \Psi' = U\Psi = (I_{32} - i\Sigma_{ab}\omega_{ab} + ...)\Psi, \tag{4.10}$$

where have neglected higher order terms. A tensor with two upper indices (32×32) will generally transform (under a global transformation) as:

$$T \to T' = UTU^\dagger = (I_{32} - i\Sigma_{ab}\omega_{ab} + ...)T(I_{32} + i\Sigma_{ab}\omega_{ab} + ...) = T - i[\Sigma_{ab}\omega_{ab}, T] + ..., \quad (4.11)$$

where we have once again neglected any higher order terms. This transformation corresponds to the adjoint representation, meaning that the generators Σ_{ab} will also transform like this. We will encounter many 32×32 tensors in this work, which transform exactly like above.

Establishing these transformation rules will allow us to formulate a Lagrangian for the model we treat, which should be invariant under these transformations. However instead of ω_{ab} we will use gW_{ab}, where g is a coupling constant arbitrarily extracted for convenience [14].

4.1.3 Constructing an Explicit Basis for $SO(10)$

Now that we have described a general way to represent $SO(10)$ in a spinor basis we need to explicitly define this basis. As stated before, the basis will involve 32×32 matrices labelled by Σ_{ab} with $a, b = 1, 2, ..., 10$. First we need to find a way to define the Γ's. A straightforward procedure is described in [27]. First consider the usual γ-matrices:

$$\gamma_0 = \sigma_3 \times I_2, \quad \gamma_i = i\sigma_2 \times \sigma_i, \quad i = 1,\ 2,\ 3, \quad (4.12)$$

with σ_i the Pauli spin matrices. These 4×4 matrices form a Clifford algebra. We can construct the Γ_m's, (m=1, 2, ..., 10) in a similar manner:

$$\begin{aligned}
\Gamma_1 &= \sigma_1 \times \sigma_1 \times \sigma_1 \times \sigma_1 \times \sigma_1, & \Gamma_6 &= \sigma_1 \times \sigma_1 \times \sigma_2 \times I_2 \times I_2,\\
\Gamma_2 &= \sigma_1 \times \sigma_1 \times \sigma_1 \times \sigma_1 \times \sigma_2, & \Gamma_7 &= \sigma_1 \times \sigma_1 \times \sigma_3 \times I_2 \times I_2,\\
\Gamma_3 &= \sigma_1 \times \sigma_1 \times \sigma_1 \times \sigma_1 \times \sigma_3, & \Gamma_8 &= \sigma_1 \times \sigma_2 \times I_2 \times I_2 \times I_2,\\
\Gamma_4 &= \sigma_1 \times \sigma_1 \times \sigma_1 \times \sigma_2 \times I_2, & \Gamma_9 &= \sigma_1 \times \sigma_3 \times I_2 \times I_2 \times I_2,\\
\Gamma_5 &= \sigma_1 \times \sigma_1 \times \sigma_1 \times \sigma_3 \times I_2, & \Gamma_{10} &= \sigma_2 \times I_2 \times I_2 \times I_2 \times I_2.
\end{aligned} \quad (4.13)$$

This basis is essentially derived iteratively, for every step in N in $SO(2N)$ we add two Γ's, defined as a tensor product of σ_2 or σ_3 with an appropriately sized identity matrix and multiply the existing Γ_m by σ_1. This procedure requires that one starts with just the three Pauli spin matrices. More compactly:

$$\begin{aligned}
\Gamma_i^{n+1} &= \sigma_1 \times \Gamma_i^n, \quad i = 1, 2, ..., 2n\\
\Gamma_{2n+1}^{n+1} &= \sigma_2 \times I_{2^n},\\
\Gamma_{2n+2}^{n+1} &= \sigma_3 \times I_{2^n}.
\end{aligned} \quad (4.14)$$

Γ_{2n+2}^{n+1} is only included if we want to represent $SO(2N+1)$. This procedure ensures that the Clifford algebra is satisfied at every increment. The two new matrices satisfy the Clifford algebra, as the Pauli spin matrices anticommute. The tensor product of the existing matrices with σ_1 should not affect their anticommutation as $\sigma_i^2 = 1$. This basis is by no means the only one, an equivalent basis can be used by taking the γ matrices as a starting point and expanding these in a similar fashion.

This basis allows for a convenient splitting of the fermion representation into chiral components, as shown in [27]. In order to work towards a representation for the fermions, we should look more closely at the 32-dimensional representation we have discussed. The first step is to notice that we can create a matrix similar to γ_5 for this case:

$$\Gamma_F = -i\Gamma_1\Gamma_2...\Gamma_{10} = \begin{pmatrix} I_{16} & 0 \\ 0 & -I_{16} \end{pmatrix} \quad (4.15)$$

note that Γ_F anticommutes with every Γ_a:

$$\{\Gamma_a, \Gamma_F\} = -i\Gamma_a\Gamma_F - i\Gamma_1\Gamma_2...\Gamma_{10}\Gamma_a = -i\Gamma_a\Gamma_F - i(-1)^9\Gamma_a\Gamma_F = 0. \tag{4.16}$$

Just like γ_5, Γ_F is used to split the representation into a chiral basis. In our choice of basis this is easily visible as Γ_F is a block diagonal matrix. Using this fact we can define the operators and fields:

$$P_\pm = (1 \pm \Gamma_F)/2, \quad \Psi_L = P_+\Psi, \quad \Psi_R = P_-\Psi, \quad \Psi = \begin{pmatrix} \Psi_L \\ \Psi_R \end{pmatrix}, \tag{4.17}$$

where Ψ will contain the fermion fields. Using Γ_F we have split up the 32-dimensional basis into two chiral components. It can be shown that these two components are in fact conjugates of each other.

We would like to construct bilinears of two spinors. A simple bilinear of the form $\Psi^T\Psi$ is not invariant as it transforms to $\Psi^T e^{-i\Sigma^T\omega}e^{-i\Sigma\omega}\Psi$. Therefore, we need some matrix B such that $\Psi^T B\Psi$ is invariant. This bilinear transforms as [13]:

$$\Psi^T B\Psi \to \Psi^T e^{-i\Sigma^T\omega}Be^{-i\Sigma\omega}\Psi \simeq \Psi^T B\Psi + i\omega\Psi^T(\Sigma^T B + B\Sigma)\Psi, \tag{4.18}$$

for this to be invariant we require:

$$\Sigma^T B = -B\Sigma \quad \longrightarrow \quad B^{-1}\Sigma^T B = -\Sigma. \tag{4.19}$$

Since Σ is hermitian we obtain the relation:

$$B^{-1}\Sigma^* B = -\Sigma, \tag{4.20}$$

so B can transform the generators into their negative conjugates. Essentially, by constructing a conjugation matrix B, we have found a way to transform from a space to its conjugate. We should also determine whether B commutes or anticommutes with $P_\pm$. This is equivalent to asking whether it commutes with Γ_F. In section 4.1.4 we will explicitly define B, from this explicit form one can show:

$$\Gamma_F B = -B\Gamma_F. \tag{4.21}$$

We can now define a conjugate spinor as follows:

$$\Psi_c \equiv B^{-1}\Psi^* \to B^{-1}e^{i\Sigma\omega}P_\pm^*\Psi^* = e^{-i\Sigma\omega}P_\mp B^{-1}\Psi^*, \tag{4.22}$$

which transforms just like Ψ. The $P_\pm$ switched to $P_\mp$ this indicates that the conjugate spinor Ψ_c is in fact the right-handed spinor. We have:

$$(\Psi_L)_c = B^{-1}P_-\Psi^* = (\Psi_c)_R. \tag{4.23}$$

We can take this further and show how left- and right-handed spinor spaces transform:

$$B^{-1}\Sigma^* P_\pm B = -\Sigma P_\mp, \tag{4.24}$$

indicating that the charge conjugation matrix B relates the right and left-handed spaces. Therefore, the right- and left-handed spinors are each other's conjugates and the 32-dimensional spinor splits as follows:

$$32 = 16 + \overline{16}. \tag{4.25}$$

This fact will be very useful when placing the fermions in the representation.

4.1.4 A More Convenient Basis for $SO(10)$

The basis presented in section 4.1.3 is easy to derive and has good properties for our purposes. However, there exists a basis for $SO(10)$ shown in [30], that yields a more convenient form for the representation of the fermions and gauge bosons. This basis cannot be generated in the same way as the one in eq. (4.13), and is as follows:

$$\begin{aligned} \Gamma_1 &= \sigma_1 \times \sigma_1 \times I_2 \times I_2 \times \sigma_2, & \Gamma_6 &= \sigma_1 \times \sigma_2 \times I_2 \times \sigma_1 \times \sigma_2, \\ \Gamma_2 &= \sigma_1 \times \sigma_2 \times I_2 \times \sigma_3 \times \sigma_2, & \Gamma_7 &= \sigma_1 \times \sigma_3 \times \sigma_1 \times I_2 \times I_2, \\ \Gamma_3 &= \sigma_1 \times \sigma_1 \times I_2 \times \sigma_2 \times \sigma_3, & \Gamma_8 &= \sigma_1 \times \sigma_3 \times \sigma_2 \times I_2 \times I_2, \\ \Gamma_4 &= \sigma_1 \times \sigma_2 \times I_2 \times \sigma_2 \times I_2, & \Gamma_9 &= \sigma_1 \times \sigma_3 \times \sigma_3 \times I_2 \times I_2, \\ \Gamma_5 &= \sigma_1 \times \sigma_1 \times I_2 \times \sigma_2 \times \sigma_1, & \Gamma_{10} &= \sigma_2 \times I_2 \times I_2 \times I_2 \times I_2. \end{aligned} \tag{4.26}$$

Essentially, this basis is tailor-made for $SO(10)$ to be convenient, but does not readily extend to larger groups. In this basis we have to compute Γ_F again, we obtain:

$$\Gamma_F = \sigma_3 \times I_2 \times I_2 \times I_2 \times I_2 = \begin{pmatrix} I_{16} & 0 \\ 0 & -I_{16} \end{pmatrix}, \tag{4.27}$$

exactly as in eq. (4.15). Once again we have a block diagonal Γ_F, so we can still conveniently represent the fermions as in eq. (4.17).

We will now also explicitly define the conjugation matrix B, in this particular basis we have [27]:

$$B = -i\Gamma_1\Gamma_3\Gamma_5\Gamma_8\Gamma_{10}, \tag{4.28}$$

which clearly anticommutes with $P_\pm$, as it consists of an odd number of Γ_i. This is the basis we will utilize in the rest of this work, due its convenient representation of all particles.

4.1.5 Explicit Fermion Representation

We have established that we can represent $SO(10)$ with two 16-dimensional spinors. Now we need to place the 12 quarks and 3 leptons in it. However, we have another spot left for a right-handed neutrino, which is absent from the SM. Following [27, 30], we can place all fermions into a left-handed and a right-handed spinor. The procedure is as follows: we can define several operators such as Q and U_{B-L} explicitly in terms of Σ_{ab}. The diagonal of the operator will then tell us the eigenvalues associated with each entry in the spinor, thereby revealing how the fermions are placed in the 16-dimensional spinors for our particular choice of basis. For Q we have:

$$Q = \frac{1}{6}(\Sigma_{12} + \Sigma_{34} + \Sigma_{56}) - \frac{1}{2}\Sigma_{78}, \tag{4.29}$$

which amounts to

$$Q_{11} = \mathrm{diag}(\frac{2}{3}, \frac{2}{3}, \frac{2}{3}, 0, -\frac{1}{3}, -\frac{1}{3}, -\frac{1}{3}, -1, \frac{1}{3}, \frac{1}{3}, \frac{1}{3}, 1, -\frac{2}{3}, -\frac{2}{3}, -\frac{2}{3}, 0), \tag{4.30}$$

for the first 16×16 block in Q. U_{B-L} will distinguish between the two neutrinos, allowing us to completely construct the representation, using the alternative basis given in eq. (4.26):

$$\Psi_L = \begin{pmatrix} u_1 \\ u_2 \\ u_3 \\ \nu_e \\ d_1 \\ d_2 \\ d_3 \\ e^- \\ d_1^c \\ d_2^c \\ d_3^c \\ e^c \\ -u_1^c \\ -u_2^c \\ -u_3^c \\ -\nu_e^c \end{pmatrix}_L , \quad \Psi_R = \begin{pmatrix} u_1 \\ u_2 \\ u_3 \\ \nu_e \\ d_1 \\ d_2 \\ d_3 \\ e^- \\ d_1^c \\ d_2^c \\ d_3^c \\ e^c \\ -u_1^c \\ -u_2^c \\ -u_3^c \\ -\nu_e^c \end{pmatrix}_R , \quad \Psi = \begin{pmatrix} \Psi_L \\ \Psi_R \end{pmatrix}. \tag{4.31}$$

The subscripts L and R are to indicate that the fields inside the spinors are left-handed and right-handed respectively. Given that Ψ_R is the conjugate of Ψ_L, the fields in Ψ_R represent antiparticles of those in Ψ_L. Furthermore, the superscript c indicates a conjugated particle, which is simply an antiparticle. Clearly the basis we have chosen gives a very convenient spinor representation. The triplets of quarks are grouped with a lepton. A vector leptoquark (called X or U_1), which will be discussed in section 4.1.6, provides interactions between these quarks and the accompanying lepton.

Decomposing this representation to the SM gives:

$$16 = (3, 1, 1/6) + (\bar{3}, 1, 1/3) + (\bar{3}, 1, -2/3) + (1, 2, -1/2) + (1, 1, 1) + (1, 1, 0) \tag{4.32}$$

As we stated, the 16 dimensions allow us to include a right-handed neutrino, which is not present in the SM. Therefore, we obtain the $(1, 1, 0)$ representation when decomposing.

4.1.6 Gauge Fields

In the context of leptoquarks, one of the most important parts of an $SO(10)$ GUT is the gauge sector. Among the gauge fields are both pure and B-violating vector leptoquarks [12]. In this section we aim to identify these, along with the other gauge bosons present in the theory.

Using the definition of $SO(10)$ in eq. (4.1), we can determine that there are $N(N-1)/2 = 45$ generators in the adjoint, corresponding to the amount of independent orthogonal 10×10 matrices with determinant 1. A maximal subgroup of $SO(10)$ is $SO(6) \times SO(4)$, $SO(6)$ is isomorphic to $SU(4)$ and $SO(4)$ is isomorphic to $SU(2) \times SU(2)$. This shows that the Pati-Salam group is a subgroup of $SO(10)$, with its 21 generators being those from $SO(6) \times SO(4)$. The other 24 generators fall outside this group, and are consequently not present in Pati-Salam theory. These must remain at the GUT-scale. We will use the following convention: in the generators Σ_{ab}, the indices $a, b = 1, 2, ..., 6$ refer to elements belonging to $SO(6)$, and indices $a, b = 7, 8, 9, 10$ to $SO(4)$. Those generators that have one $SO(6)$ index and one $SO(4)$ index fall outside the maximal subgroup.

The Pati-Salam group must contain the 12 generators of the SM. Therefore, we have three categories of gauge boson in this section, the SM, the Pati-Salam and the $SO(10)$ gauge bosons.

The branching rule of the 45 of $SO(10)$ to $SU(4)_C \times SU(2)_L \times SU(2)_R$ is [31]:

$$45 = (15, 1, 1) + (1, 3, 1) + (1, 1, 3) + (6, 2, 2), \tag{4.33}$$

with the first three terms clearly being the adjoint representations of $SU(4)_C$, $SU(2)_L$ and $SU(2)_R$, respectively. The last term corresponds to the bosons only found in $SO(10)$.

We start with the adjoint representation of $SU(4)_C$, the $(15, 1, 1)$, to further examine the bosons contained in this theory. This representation can be further decomposed to gain an idea of what is contained inside. The branching rule to $SU(3)_C \times U(1)_{B-L}$ is as follows [31]:

$$15 = (8, 0) + (3, -4/3) + (\bar{3}, 4/3) + (1, 0), \tag{4.34}$$

where we can clearly recognize the SM gluons in the first term. The second and third term correspond to particles that couple to quarks and have a $B - L$ number of $\pm 4/3$, indicating they also couple to leptons. The last term is a certain $B - L$ conserving boson. To further illustrate this branching consider the decomposition to the SM group:

$$15 = (8, 1, 0) + (3, 1, 2/3) + (\bar{3}, 1, -2/3) + (1, 1, 0), \tag{4.35}$$

this also reveals the charges of each particle. Using this branching rule we can clearly see that we have 8 gluons:

$$G_1, G_2, ..., G_8, \text{ with generators: } U_{G_1}, U_{G_2}, ..., U_{G_8}. \tag{4.36}$$

The remaining 7 bosons are the X vector bosons:

$$X_1 = \bar{X}_4, \quad X_2 = \bar{X}_5, \quad X_3 = \bar{X}_6, \quad X_{B-L}, \tag{4.37}$$

where the latter is the boson corresponding to $B-L$ symmetry. $B-L$ symmetry is inherent to $SO(10)$ [27]. These X bosons, excluding X_{B-L}, are leptoquarks and are commonly referred to as U_1 in literature (not to be confused with the $SU(4)_C$ generator U_1). These leptoquarks were already mentioned in Table 3.1, based on the work done in [12]. The X/U_1 vector leptoquarks are one of the focal points of our research. Therefore, we will define their generators explicitly in terms of the generators of $SO(10)$:

$$U_{X_1} = (U_9 - iU_{10})/2 = (\Sigma_{23} + \Sigma_{14} - i\Sigma_{31} + i\Sigma_{42})/4, \tag{4.38}$$
$$U_{X_2} = (U_{11} - iU_{12})/2 = (\Sigma_{25} + \Sigma_{61} - i\Sigma_{51} - i\Sigma_{62})/4, \tag{4.39}$$
$$U_{X_3} = (U_{13} - iU_{14})/2 = (\Sigma_{45} + \Sigma_{63} - i\Sigma_{53} - i\Sigma_{64})/4, \tag{4.40}$$

where U_i are the generators of $SU(4)$. In general, the generators in this section are linear combinations of multiple $SO(10)$ generators.

Moving on to the other terms in eq. (4.33), we have the $(1, 3, 1)$ and $(1, 1, 3)$, simply corresponding to the left-handed and right-handed gauge bosons:

$$W_L^1, W_L^2, W_L^3, \text{ with generators: } L_1, L_2, L_3, \tag{4.41}$$

and:

$$W_R^1, W_R^2, W_R^3, \text{ with generators: } R_1, R_2, R_3. \tag{4.42}$$

These bosons are usually classified into combinations based on their charge:

$$\begin{aligned} W_L^{\pm} &= (W_L^1 \pm i W_L^2)/2, \qquad & L_{\pm} &= (L_1 \mp i L_2)/\sqrt{2}, \\ Z_L^0 &= W_L^3, & L_0 &= L_3 \end{aligned}, \tag{4.43}$$

and equivalently for the $SU(2)_R$ fields.

We have now classified all bosons from $SO(10)$ that also exist in PS theory. We are left with the $(6,2,2)$ multiplet. This term corresponds to bosons not found at energies below M_U, the GUT-scale, as these only exist in $SO(10)$ and not in its maximal subgroup $SO(6) \times SO(4)$. Further decomposing the $(6,2,2)$ to the SM group gives [27]:

$$(6,2,2) = (3,2,-5/6) + (\bar{3},2,5/6) + (3,2,1/3) + (\bar{3},2,-1/3), \tag{4.44}$$

where we can clearly identify the first two and last two terms each as conjugate pairs. The first two are the Y and Y' bosons:

$$Y_1, Y_2, Y_3, \bar{Y_1}, \bar{Y_2}, \bar{Y_3} \text{ with generators: } D_{Y_1}, D_{Y_2}, D_{Y_3}, D_{\bar{Y_1}}, D_{\bar{Y_2}}, D_{\bar{Y_3}}, \tag{4.45}$$

with a Y' existing for each Y. The A and A' are similarly:

$$A_1, A_2, A_3, \bar{A}_1, \bar{A}_2, \bar{A}_3 \text{ with generators: } D_{A_1}, D_{A_2}, D_{A_3}, D_{\bar{A}_1}, D_{\bar{A}_2}, D_{\bar{A}_3}, \tag{4.46}$$

corresponding to the last two terms in eq. (4.44). We have now fully classified the gauge content of $SO(10)$ by using the branching rules of the adjoint representation. This section is summarized in Table 4.1. It should be noted that two of the PS gauge bosons, X_{B-L} and Z_R will still be present below the PS-scale in this model, due to the elaborate symmetry breaking pattern, see section 4.2. An explicit definition of the generators for all Pati-Salam gauge fields can be found in section A.2

Gauge Boson	SM representation	Category	Note
Gluons	(8,1,0)	SM	
X or U_1	$(3,1,2/3)$	PS	Pure vector leptoquark
X_{B-L}	$(1,1,0)$	PS	Forms $U(1)_Y$ boson together with Z_R
W_L	$(1,3,0)$	SM	
$W_R^{\pm}$	$(1,1,1)$	PS	
Z_R	$(1,1,0)$	PS	Forms $U(1)_Y$ boson together with U_{B-L}
Y or V_2	$(\bar{3},2,5/6)$	$SO(10)$	B-violating leptoquark
A or $\tilde{V}_2$	$(3,2,1/6)$	$SO(10)$	B-violating leptoquark

Table 4.1: Gauge fields in $SO(10)$, listed with their SM representation. Conjugate representations are left out.

4.2 Symmetry Breaking and Higgs Representations

In this work we will discuss a model with multiple intermediate symmetries between the GUT-scale and the SM, as shown in eq. (4.47). Such a model will need many scalar particles to achieve symmetry breaking and reproduce fermion masses. In this section we will examine these scalar representations, their role in symmetry breaking and their leptoquark content. Further discussion about the symmetry breaking scheme in eq. (4.47) is given in section 5.2

$$
\begin{aligned}
SO(10) &\xrightarrow[M_U]{54_H} SU(4)_C \times SU(2)_L \times SU(2)_R \times D \\
&\xrightarrow[M_D]{210_H} SU(4)_C \times SU(2)_L \times SU(2)_R \\
&\xrightarrow[M_{W_R}]{210_H} SU(3)_C \times SU(2)_L \times U(1)_R \times U(1)_{B-L} \\
&\xrightarrow[M_{Z_R}]{16_H} SU(3)_C \times SU(2)_L \times U(1)_Y \\
&\xrightarrow[M_{EW}]{10_H} SU(3)_C \times U(1)_Q.
\end{aligned} \tag{4.47}
$$

In this section we will first engage in a general discussion of scalar representations in $SO(10)$. We will establish which of these can couple directly to fermions and which cannot. This is relevant for two reasons. Scalar representations that couple to fermions can contain both leptoquarks and SM Higgs doublets. The former are the focus of our research, and the latter are necessary for providing the fermions with mass.

Reproducing the correct fermion mass relations in $SO(10)$ is complicated by the fact that the doublet from the 10 representation is unable to give different masses to quarks and leptons. For this reason we need additional Higgs doublets from the 120, the 126 or even both. This is elaborated on in section 5.1.1. The model we initially chose, used one doublet from the 10 and two from the 120. In section 7.3 we will find that this is inconsistent with measurements. Therefore, we will eventually include a doublet from the 126 as well. For this reason, all three of these representations will be discussed.

Secondly, we will discuss several of these representations in more detail. We will explicitly define the representations and identify the fields necessary for symmetry breaking. Any leptoquarks in these representations will be identified as well.

4.2.1 Higgs Multiplets

As described above, several Higgs multiplets from $SO(10)$ are needed to break the intermediate symmetry groups down to the SM. In this section we will examine these Higgs multiplets. The way they are constructed is simply from products of representations [32]:

$$
\begin{aligned}
10 \times 10 &= 1 + 45 + 54 \\
16 \times 16 &= 10 + 120 + 126 \\
16 \times \overline{16} &= 1 + 45 + 210,
\end{aligned} \tag{4.48}
$$

where the 10 is the fundamental representation of $SO(10)$ and the 16 is the spinor representation. The product of two 10's simply splits into a trace, an antisymmetric part and a traceless symmetric part.

To see how the products of the 16 form, we can follow the reasoning in [13]. Take a bilinear form of two 16's and n number of Γ basis matrices:

$$
\begin{aligned}
\Psi^T P_L B \Gamma_i ... \Gamma_n P_L \Psi &= \Psi^T \Gamma_\kappa P_L P_L \Psi = \Psi^T \Gamma_\kappa P_L \Psi, \quad \text{for } n \text{ odd} \\
\Psi^T P_L B \Gamma_i ... \Gamma_n P_L \Psi &= \Psi^T \Gamma_\kappa P_R P_L \Psi = 0 \quad \text{for } n \text{ even.}
\end{aligned} \tag{4.49}
$$

The commutation relations of the chiral projectors with the conjugation matrix B and the Γ matrices will cause the bilinear to disappear for an even amount of Γ matrices. Therefore, 16×16 gives those representations that are built from an odd number of Γ matrices. Conversely, $16 \times \overline{16}$ gives those representations which are built from an odd number of Γ matrices. This can easily be shown by doing the same procedure as in eq. (4.49), but with $\Psi_L^T B \Gamma_1 ... \Gamma_n \Psi_R$ instead.

The 16 representation of fermions contains both particles and antiparticles, and therefore both right-handed and left-handed particles. Counterintuitively, terms of the form $\Psi_L^T B\Phi\Psi_L$, with Φ any scalar field, can give Dirac mass terms, whereas $\Psi_L^T B\Phi\Psi_R$ would give Majorana masses. This means that the Yukawa interactions, the interactions between two fermions and a scalar field, will be of the form 16×16. Looking at how these multiplets are constructed, we can then categorize them into those multiplets that couple to fermions and can give them mass: the 10, 120 and 126, and those that can not: the 45, 54 and 210.

The branching rules of the multiplets constructed in eq. (4.48) to $SU(4)_C \times SU(2)_L \times SU(2)_R$ are [31]:

$$\begin{aligned}
10 &= (1,2,2) + (6,1,1),\\
16 &= (\overline{4},1,2) + (4,2,1),\\
54 &= (1,1,1) + (1,3,3) + (20,1,1) + (6,2,2),\\
120 &= (1,2,2) + (10,1,1) + (\overline{10},1,1) + (6,1,3) + (6,3,1) + (15,2,2),\\
126 &= (6,1,1) + (\overline{10},3,1) + (10,1,3) + (15,2,2),\\
210 &= (1,1,1) + (15,1,1) + (6,2,2) + (15,3,1) + (15,1,3) + (10,2,2) + (\overline{10},2,2).
\end{aligned} \tag{4.50}$$

For each symmetry breaking step, one field from one multiplet will be chosen to break the symmetry. Which field this is, will depend on which symmetries we want to break and the resulting structure. After breaking, the resulting symmetry is the largest subgroup under which the chosen field is a singlet. Furthermore, any multiplet that is not necessary to break the symmetry will be assumed to be superheavy ($m \sim M_U$), this is elaborated on in section 5.4.

Classifying the fields in these Higgs representations is generally an arduous task. The basis in which the representations are convenient to define, is usually not the basis in which fields are conveniently grouped according to SM representations (e.g. an SM Higgs doublet might be a linear combination of many fields in the default basis). The classification of many of these fields was performed in [27]. In the rest of this section we will use this work to identify the fields we need the model we consider.

4.2.2 The 10 Higgs Representation

The 10 Higgs representation serves the role of the SM Higgs doublet in $SO(10)$. It breaks the SM down to $SU(3)_C \times U(1)_Q$. Furthermore, it is essential to providing the fermions with mass. Using the basis in eq. (4.26), the 10 is constructed as follows [27]:

$$\Phi_{10} = \frac{1}{\sqrt{32}}\phi_i\Gamma_i = \frac{1}{4}(\Phi_i \cdot \Gamma'_i + \Phi_i^\dagger \cdot \Gamma_i'^\dagger), \; \frac{1}{32}\,\mathrm{Tr}\big[(\phi_i\Gamma_i)^2\big] = \sum \phi_i^2, \; i = 1,2,...,10, \tag{4.51}$$

where we have written down an alternative basis in terms of 10 independent Γ'_i. This basis is convenient as it allows us to separate the 10 easily into its multiplets under the PS group. We have the following branching rule for the PS group and the SM group, respectively:

$$10 = (2,2,1) + (1,1,6) = (1,2,-1/2) + (1,2,1,1/2) + (3,1,-1/3) + (\bar{3},1,1/3), \tag{4.52}$$

where, clearly, we are interested in the SM doublet, originating from the $(2,2,1)$. The Φ_i and Γ'_i corresponding to the $(2,2,1)$ are:

$$\Phi_4 = (\phi_7 + i\phi_8)/2, \quad \Gamma'_4 = (\Gamma_7 - i\Gamma_8)/2, \tag{4.53}$$

$$\Phi_5 = (\phi_9 + i\phi_{10})/2, \quad \Gamma'_5 = (\Gamma_9 - i\Gamma_{10})/2. \tag{4.54}$$

In our convention the indices 7, .., 10 correspond to the $SU(2) \times SU(2)$ part of $SO(10)$, therefore these matrices correspond to the $SU(4)$ singlets. The symmetry breaking we want to achieve is $SU(2)_L \times U(1)_Y \to U(1)_Q$. Φ_4 carries electric charge [27], therefore we can not use it to break to $U(1)_Q$, since it would give the photon a mass. That leaves Φ_5, which is a colour singlet and carries zero charge. Giving some vev to Φ_5 will then break the electroweak symmetry, just like in the SM. Setting $\langle \Phi_5 \rangle = v$, we get:

$$\phi_{vac} = \frac{1}{4}(v \cdot \Gamma'_5 + v^\dagger \cdot \Gamma'^\dagger_5). \tag{4.55}$$

Now to see which generators we have broken, we simply need to check with which generators ϕ_{vac} commutes. Since ϕ_{vac} transforms as:

$$\phi_{vac} \to \phi'_{vac} = (I_{32} - i[W \cdot \Sigma, \phi_{vac}] + ...)\phi_{vac}, \tag{4.56}$$

any combination of generators that commutes with the vev will be left unbroken. Any generator that does not commute will transform ϕ_{vac} and is therefore broken. It can straightforwardly (computationally) be checked that:

$$\begin{aligned} &[U_{G_1}, \phi_{vac}] = ... = [U_{G_8}, \phi_{vac}] = 0, \\ &[L_1, \phi_{vac}] = [L_2, \phi_{vac}] = [L_3, \phi_{vac}] \neq 0, \\ &[Y/2, \phi_{vac}] \neq 0, \end{aligned} \tag{4.57}$$

clearly, both $SU(2)_L$ and $U(1)_Y$ have been broken. However, there is one linear combination that leaves the vev unaltered:

$$[L_3 + Y/2, \phi_{vac}] = 0, \quad Q = L_3 + Y/2, \tag{4.58}$$

this is precisely the charge operator associated with $U(1)_Q$. This symmetry breaking is equivalent to EW breaking in the SM, shown in section 2.2.1. Just like the SM Higgs doublet, this doublet will also enter the Yukawa potential and give the fermions a mass with its vev.

In eq. (4.52) we can identify the $(\overline{3}, 1, 1/3)$ representation and its conjugate. This is the S_1 leptoquark, which can mediate proton decay and is therefore restricted to lie at very high energies ($\geq 10^{11}$ GeV). These are also present in $SU(5)$, as we stated in Table 3.1. In the model we discuss these leptoquarks are kept at the GUT-scale.

4.2.3 The 16 Higgs Representation

To break to the SM, we utilize a Higgs field from the 16 of $SO(10)$. In this process the $U(1)_R \times U(1)_{B-L}$ symmetry is broken to $U(1)_Y$. Therefore, we can use this Higgs multiplet to find out how the operator Y is written in terms of $SO(10)$ generators. In terms of quantum numbers, the 16 is just like the spinor representation for the fermions (except for spin of course). Since we have chargeless and colourless states in the spinor, we should be able to identify fields that are SM singlets. We can write the following Higgs field [27]:

$$\phi^{\pm} = (1 \pm \Gamma_F)\phi, \quad \phi = \begin{pmatrix} \phi^+ \\ \phi^-, \end{pmatrix} \tag{4.59}$$

where we have used the basis described in eq. (4.26). Recall from section 4.1.5 that the spinor representation has neutrinos as the 4th and 16th elements in $\Psi_{L/R}$, these are exactly the chargeless and colourless states we could use for a Higgs field. Therefore, we can give an expectation value to one pair of these values in the Higgs multiplet, for example the 16th element of ϕ^+ and the 4th element of ϕ^-. In the fermion representation, these correspond to $\overline{\nu}_e$. This is the $(1,1,1/2,-1)$ multiplet of the 16. Equivalently we can pick the positions of ν_e instead. Choosing the first option, we get the following vev for ϕ:

$$\phi^+_{vac} = \begin{pmatrix} 0 \\ 0 \\ 0 \\ 0 \\ 0 \\ 0 \\ 0 \\ 0 \\ 0 \\ 0 \\ 0 \\ 0 \\ 0 \\ 0 \\ 0 \\ -\langle\varphi_0\rangle \end{pmatrix}, \quad \phi^-_{vac} = \begin{pmatrix} 0 \\ 0 \\ 0 \\ \langle\varphi_0\rangle^* \\ 0 \\ 0 \\ 0 \\ 0 \\ 0 \\ 0 \\ 0 \\ 0 \\ 0 \\ 0 \\ 0 \\ 0 \end{pmatrix}, \quad \phi_{vac} = \begin{pmatrix} \phi^+_{vac} \\ \phi^-_{vac} \end{pmatrix}, \tag{4.60}$$

where we have labelled the field φ_0. Now we can examine which generators (or linear combinations of generators) leave the vev unaltered. To check this we want to see which infinitesimal generators of symmetry groups do not change the vev, up to first order:

$$\left(I_{32} - ia^iT^i\right)\phi_{vac} = \phi_{vac}, \tag{4.61}$$

where T^i are the generators. So more practically, we demand:

$$a^iT^i\phi_{vac} = 0. \tag{4.62}$$

Since we are breaking from $SU(3)_C \times SU(2)_L \times U(1)_R \times U(1)_{B-L}$ to the SM group, we have the following generators to consider:

$$U_{G_1}\phi_{vac} = ... = U_{G_8}\phi_{vac} = 0, \tag{4.63}$$

$$L_1\phi_{vac} = L_2\phi_{vac} = L_3\phi_{vac} = 0, \tag{4.64}$$

$$U_{B-L}\phi_{vac} \neq 0, \tag{4.65}$$

$$R_3\phi_{vac} \neq 0, \tag{4.66}$$

$$Y/2\phi_{vac} = (U_{B-L}/2 + R_3)\phi_{vac} = 0. \tag{4.67}$$

Clearly, the generators for $SU(3)_C$ and $SU(2)_L$ are unbroken, this is good as we want to break to the SM group. Furthermore, R_3 and U_{B-L} are individually broken, as desired, but a linear combination of them does not affect the vev. Therefore, we are left with one $U(1)_Y$ symmetry. These results can be obtained by explicitly writing the basis for $SO(10)$

and then constructing all individual generators. We have now obtained an important result for the rest of our work:

$$Y/2 = U_{B-L}/2 + R_3. \tag{4.68}$$

This means that for Q we have, following the well known relation to L_3 and $Y/2$ [14]:

$$Q = Y/2 + L_3 = U_{B-L}/2 + R_3 + L_3, \tag{4.69}$$

this result can be used to derive the placement of fermions in section 4.1.5.

4.2.4 The 120 Higgs Representation

The 120-dimensional Higgs representation is constructed from three Γ matrices. Given that this is an odd number, it is one of the representations that can be used to provide the fermions with masses, along with the 10 and 126, following the reasoning in section 4.2.1. The representation can be constructed in the following way:

$$\Phi_{120} = \frac{1}{\sqrt{32}}\phi_{ijk}\Gamma_i\Gamma_j\Gamma_k, \quad \frac{1}{32}\operatorname{Tr}\left[(\phi_{ijk}\Gamma_i\Gamma_j\Gamma_k)^2\right] = \sum \phi_{ijk}^2. \tag{4.70}$$

This representation is real and antisymmetric. Therefore, any couplings between it and two fermions of the same generation must disappear. To see this, note that an antisymmetric bilinear form of two identical vectors is always zero:

$$(\Psi_L^a)^T\Phi_{120}\Psi_L^b = -(\Psi_L^b)^T\Phi_{120}\Psi_L^a \quad \rightarrow \quad (\Psi_L^a)^T\Phi_{120}\Psi_L^a = 0, \tag{4.71}$$

where a, b are generation indices. This condition means we can set Y_{120}, the Yukawa matrix, to be antisymmetric, without loss of generality. Therefore, all terms with fermions of the same generation disappear.

This representation is not classified in [27], meaning we need to use commutation relations with generators to manually identify the fields. In section 5.3.3 we use this approach to identify two SM Higgs doublets from this representation:

$$\Sigma_1 = \frac{1}{\sqrt{2}}(\phi_{7810} + i\phi_{789}), \tag{4.72}$$

$$\Sigma_2 = \phi_{1210} + \phi_{3410} + \phi_{5610} + i(\phi_{129} + \phi_{349} + \phi_{569}), \tag{4.73}$$

with the first originating from the $(1, 2, 2)$ and the second from the $(15, 2, 2)$ representation under the PS group. When these acquire vev's they will contribute to the fermion masses through the Yukawa sector. We need these doublets, along with the doublet from the 10, to obtain different masses for the leptons and quarks.

The $(15, 2, 2)$ representation branches to the standard model as follows:

$$\begin{aligned}(15, 2, 2) = {} & (8, 2, -1/2) + (8, 2, 1/2) + (3, 2, 1/6) + (3, 2, 7/6) \\ & + (\overline{3}, 2, -7/6) + (\overline{3}, 2, -1/6) + (1, 2, -1/2) + (1, 2, 1/2)\end{aligned} \tag{4.74}$$

Note the $(3, 2, 1/6)$ and $(3, 2, 7/6)$ representations along with their conjugates. These particles are known as the $\tilde{R}_2$ and R_2 scalar leptoquarks [21], respectively. These do not mediate proton decay, as they are pure leptoquarks. Depending on the symmetry breaking and the mechanism by which these particles obtain mass, it is possible that this model has TeV-scale scalar leptoquarks, as well as the vector leptoquarks described in section 4.1.6. In chapter 7 we will establish that TeV-scale scalar leptoquarks can in fact exist in this model. In this respect, our findings differ from [12].

4.2.5 The 126 Higgs Representation

Another representation often used to provide the fermions with mass is the 126. It is defined as follows [27]:

$$\Phi_{126} = \frac{1}{\sqrt{32}}\phi_{ijklm}\Gamma_i\Gamma_j\Gamma_k\Gamma_l\Gamma_m, \; \frac{1}{32}\,\mathrm{Tr}\big[(\phi_{ijklm}\Gamma_i\Gamma_j\Gamma_k\Gamma_l\Gamma_m)^2\big] = \sum \phi^2_{ijklm}. \tag{4.75}$$

This representation is complex and symmetric, as opposed to the 120 which is real and antisymmetric. The branching of the $(15, 2, 2)$, which contains an SM doublet that could be used for fermion masses, is identical to the same multiplet from the 120, shown in eq. (4.74). Therefore, this representation contains the same leptoquarks. Since this representation is symmetric, it is a bit easier to see the leptoquark couplings, as the couplings within a generation do not disappear in this case.

The R_2 and $\tilde{R}_2$ leptoquarks correspond to the $(3, 2, 7/6)$ and $(3, 2, 1/6)$ representations, respectively. Therefore, they are colour triplets, as any leptoquark should be [21], and $SU(2)$ doublets, as opposed to the vector leptoquarks found in section 4.1.6, which were singlets. Logically, each representation totals 6 particles. The fact that they are doublets means that each leptoquark representation admits two sets of particles with different charges. For R_2 we have particles with $Q = Y/2 + L_3 = 7/6 \pm 1/2 = 5/3,\ 2/3$, and for $\tilde{R}_2$ we have $Q = 1/6 \pm 1/2 = 2/3,\ -1/3$. In vector form:

$$R_2 = \begin{pmatrix} R_2^{5/3} \\ R_2^{2/3} \end{pmatrix}, \quad \tilde{R}_2 = \begin{pmatrix} \tilde{R}_2^{2/3} \\ \tilde{R}_2^{-1/3} \end{pmatrix}, \tag{4.76}$$

where colour indices are left implicit. We can use this to derive the leptoquark couplings with fermions. Since the 126 is found in the product of the 16 with itself, we can write down the Yukawa Lagrangian:

$$\mathcal{L} = Y_{126}\Psi_L^T\Phi_{126}\Psi_L. \tag{4.77}$$

To see that this describes leptoquarks we must expand this Lagrangian [21]:

$$\begin{aligned}\mathcal{L} =& Y_{126}(\overline{u}\nu_e R_2^{2/3} + \overline{u}e^- R_2^{5/3} + \overline{d}\nu_e R_2^{2/3*} + \overline{e^+}u R_2^{5/3*} \\ &+ \overline{d}e^-\tilde{R}_2^{2/3} + \overline{d}\nu_e\tilde{R}_2^{-1/3} + \overline{u}\nu_e\tilde{R}_2^{2/3} + \overline{d}\nu_e\tilde{R}_2^{-1/3}) + h.c,\end{aligned} \tag{4.78}$$

where we have dropped all other scalar particles in the $(15, 2, 2)$. Clearly, R_2 and $\tilde{R}_2$ have vertices with both leptons and quarks.

This representation contains an SM doublet, which can be used to provide the fermions with mass. At first, we do not include this representation in the model we discuss, as we did not deem it necessary. In section 7.3, we find that models without the 126 do not reproduce fermion masses consistent with measurement, and therefore we will eventually include this representation in chapter 7. The inclusion of the 126 also means we include the R_2 and $\tilde{R}_2$ with symmetric couplings in the model, as opposed to the antisymmetric couplings that the 120 has.

4.2.6 The 210 Higgs Representation

Two symmetry breaking steps are accomplished by giving a vev to specific fields from the 210. Specifically, breaking D-parity and breaking the PS group down to $SU(3)_C \times SU(2)_L \times U(1)_R \times U(1)_{B-L}$. The 210 is constructed as follows [27]:

$$\Phi_{210} = \frac{1}{\sqrt{32}}\phi_{ijkl}\Gamma_i\Gamma_j\Gamma_k\Gamma_l = \frac{1}{16}(\Gamma'\cdot\Phi + \Gamma'^{\dagger}\cdot\Phi^{\dagger}), \; \frac{1}{32}\,\mathrm{Tr}\big[(\phi_{ijkl}\Gamma_i\Gamma_j\Gamma_k\Gamma_l)^2\big] = \sum \phi^2_{ijkl}, \tag{4.79}$$

where $i \neq j \neq k \neq l$ and $i, j, k, l = 1, 2, ..., 10$ The second part of the equation tells us how to normalize the representation. To see that this is indeed 210-dimensional, note that the Clifford algebra anticommutes. This means that any sequence of 4 Γ's is equal to an even permutation of itself, and differs by a minus sign from an odd permutation, e.g:

$$\Gamma_1\Gamma_2\Gamma_3\Gamma_4 = -\Gamma_1\Gamma_2\Gamma_4\Gamma_3 = \Gamma_2\Gamma_1\Gamma_4\Gamma_3. \tag{4.80}$$

Clearly permutations are not independent elements of the representation. Therefore, we have $\frac{10!}{6!4!} = 210$ linearly independent combinations of ϕ_{ijkl}. This type of calculation applies to the other representations in this chapter as well. The 210 independent combinations are labelled Φ, with corresponding matrices Γ′. As stated before, the 210 decomposes under the PS group as follows:

$$210 = (1, 1, 1) + (1, 1, 15) + (2, 2, 6) + (3, 1, 15) + (1, 3, 15) + (2, 2, 10) + (2, 2, \overline{10}). \tag{4.81}$$

To break D-parity we use the singlet (1,1,1), which has the desired parity-oddness, without affecting the resulting PS symmetry group. Then, to break the PS group we will utilize a field from the (15,1,3), which decomposes as [33]:

$$\begin{aligned}(15, 1, 3) = &(8, 1, 1, 0) + (8, 1, 0, 0) + (8, 1, -1, 0)\\ &+ (3, 1, 1, 4/3) + (3, 1, 0, 4/3) + (3, 1, -1, 4/3)\\ &+ (\bar{3}, 1, 1, -4/3) + (\bar{3}, 1, 0, -4/3) + (\bar{3}, 1, -1, -4/3)\\ &+ (1, 1, 1, 0) + (1, 1, 0, 0) + (1, 1, -1, 0),\end{aligned} \tag{4.82}$$

clearly we want to endow the field corresponding to the $(1, 1, 0, 0)$ representation with a vev, as it branches to a singlet. This field will break $SU(4)_C$ to $SU(3)_C \times U(1)_{B-L}$ and $SU(2)_R$ to $U(1)_R$. $SU(2)_L$ is unaffected as the field is a singlet under this group.

We can call this specific field $\Phi^{15}_{0\hat{0}}$, using the conventions from [27], where the hat on the right index indicates that this is the singlet of the $SU(2)_R$ triplet. A full classification of fields from the 210, and their placement in the resulting explicit 32×32 matrix, can be found in [27]. By explicitly constructing the 210 and comparing the entries to the aforementioned source, we can identify the $\Phi^{15}_{0\hat{0}}$ field as:

$$\Phi^{15}_{0\hat{0}} = (\phi_{1278} - \phi_{12910} + \phi_{3478} - \phi_{34910} - \phi_{5678} + \phi_{56910})/\sqrt{6}, \tag{4.83}$$

this is consistent with what is stated in [34], where they have verified the transformation properties of this field. If we give this field a vev (e.g. $\langle\Phi^{15}_{0\hat{0}}\rangle = u$), then the term from the 210 we are interested in is:

$$\phi_{vac} \equiv \frac{1}{16}(\Phi^{15}_{0\hat{0}}\Gamma^{15}_{0\hat{0}} + \Phi^{15\dagger}_{0\hat{0}}\Gamma^{15\dagger}_{0\hat{0}}) = \frac{u + u^\dagger}{16}\Gamma^{15}_{0\hat{0}}, \tag{4.84}$$

where we have:

$$\Gamma^{15}_{0\hat{0}} = \sqrt{2}(\Gamma_1\Gamma_2\Gamma_7\Gamma_8 - \Gamma_1\Gamma_2\Gamma_9\Gamma_{10} + \Gamma_3\Gamma_4\Gamma_7\Gamma_8 - \Gamma_3\Gamma_4\Gamma_9\Gamma_{10} - \Gamma_5\Gamma_6\Gamma_7\Gamma_8 + \Gamma_5\Gamma_6\Gamma_9\Gamma_{10}). \tag{4.85}$$

The combinations of Γ's are simply those that correspond to the fields that make up $\Phi^{15}_{0\hat{0}}$. The factor in front is to ensure that we have the following normalization:

$$\frac{1}{16}\,\mathrm{Tr}\Big[((u + u^\dagger)\Gamma^{15}_{0\hat{0}})^2\Big] = u^2. \tag{4.86}$$

Now that we have explicitly constructed the Higgs representation, we can easily verify the following:

$$[U_{G_1}, \phi_{vac}] = ... = [U_{G_8}, \phi_{vac}] = 0, \tag{4.87}$$
$$[L_i, \phi_{vac}] = 0, \tag{4.88}$$
$$[R_3, \phi_{vac}] = 0, \tag{4.89}$$
$$[U_{B-L}, \phi_{vac}] = 0, \tag{4.90}$$
$$[R_1, \phi_{vac}] = [R_2, \phi_{vac}] \neq 0, \tag{4.91}$$
$$[U_{X_i}, \phi_{vac}] \neq 0, \tag{4.92}$$

meaning that exactly those generators are broken that we expected to break.

4.3 Conclusions

In this chapter, we have developed the basic mathematical formalism needed to represent fermions, gauge bosons and scalar particles in a GUT based on $SO(10)$. We have explicitly defined a spinor basis and placed all fermions in it. We have also shown how to construct specific higher dimensional representations needed to represent the Higgs sector of this model.

Furthermore, we have briefly laid out a symmetry breaking pattern, with three intermediate scales between the GUT-scale and the SM. To this end, we have identified the scalar fields in the Higgs representations, which are needed to perform the many symmetry breaking steps.

We have identified three types of pure leptoquarks in this chapter. The vector leptoquark X, known in literature as U_1, with SM representation $(3, 1, 2/3)$, and the scalar leptoquarks R_2 and $\tilde{R}_2$, corresponding to the $(3, 2, 7/6)$ and $(3, 2, 1/6)$ representations, respectively. All of these leptoquarks obtain masses at the Pati-Salam scale, and could therefore be relatively light, similarly to the W_R boson. In chapter 6 we will see that the PS-scale is pushed up to 2 PeV. This affects the mass of the vector leptoquarks, but not necessarily of the scalar leptoquarks, as discussed in chapter 7.

Name	SM representation	Type	Energy Scale	Proton decay
V_2	$(\overline{3}, 2, 5/6)$	Vector	GUT-scale	Yes
$\tilde{V}_2$	$(\overline{3}, 2, -1/6)$	Vector	GUT-scale	Yes
U_1	$(3, 1, 2/3)$	Vector	$> 2\,\mathrm{PeV}$	No
S_1	$(\overline{3}, 1, 1/3)$	Scalar	GUT-scale	Yes
R_2	$(3, 2, 7/6)$	Scalar	$\geq$ TeV	No
$\tilde{R}_2$	$(3, 2, 1/6)$	Scalar	$\geq$ TeV	No

Table 4.2: Leptoquarks in $SO(10)$, along with their minimal mass-scale

This GUT also contains the B-violating A and Y vector leptoquarks and the S_1 scalar leptoquark, but these have masses on the order of the GUT-scale in the model we treat, thereby avoiding proton decay constraints. These results are summarized in Table 4.2.

In short, we have developed much of the group theoretical formalism needed to build a model for a GUT with several TeV-scale leptoquarks.

Chapter 5

The $SO(10)$ Model

We have gathered the group theoretical tools needed to build a coherent model for grand unification in chapter 4. In this chapter we focus on building that model and resolving any clashes or inconsistencies that may occur.

In the first section, we discuss the field theoretical aspects of $SO(10)$. A Lagrangian will be constructed based on Yang-Mills theory. We also take a brief look at the Yukawa sector. This section is partially based on the work done in [27].

In the second section we will elaborate on the symmetry breaking pattern and intermediate scales.

In the third section we will write down the Higgs sector of the model, including the potentials that mix the different scalar representations. Furthermore, we will give an example of how the masses of scalar fields in a certain representation can split due to symmetry breaking, akin to the doublet-triplet splitting problem [15]. Another point that we will resolve are the vev's and masses of the additional Higgs doublets needed for the correct fermion masses.

Finally, in the fourth section, we will compute the running of the couplings and show that with three intermediate scales, we can obtain a theory with the TeV-scale leptoquarks from Table 4.2. This is largely based on the work of [12, 19].

5.1 An $SO(10)$ Lagrangian

In order to make predictions with an $SO(10)$ GUT we need to move beyond just group theory and actually construct a Lagrangian. By doing this, we can determine Feynman rules and eventually amplitudes for interactions. We will use the definitions established in chapter 4 to construct a model. We will largely follow the steps as shown in [27]. In section 4.1.2 we developed a spinor basis for $SO(10)$. Specifically, we showed that spinors can be transformed as follows:

$$\psi_i = \left(e^{-ig\Sigma_{ab}W^{ab}}\right)_{ij}\psi_j = U_{ij}\psi_j, \tag{5.1}$$

where U_{ij} is a unitary matrix. The unitarity of this matrix was established in eq. (4.8). This fact means that we can use Yang-Mills theory to write down a Lagrangian, using $SO(10)$ as the non-abelian gauge group.

Firstly, we must define a derivative that is covariant under $SO(10)$:

$$D_\mu = \partial_\mu + igW_\mu{}^{ab}\Sigma_{ab}, \tag{5.2}$$

where $W_\mu{}^{ab}$ are the gauge fields associated with the generators Σ_{ab} and g is the coupling constant of associated with the gauge group. $D_\mu\Psi$ transforms as follows:

$$D_\mu\Psi \to UD_\mu\Psi, \tag{5.3}$$

exactly like we need it to. Now we can define a field strength tensor:

$$F^{\mu\nu\ ab} = \frac{i}{g}[D_\mu, D_\nu] = \partial_\mu W_\nu{}^{ab} - \partial_\nu W_\mu{}^{ab} - g(W_\mu{}^{ac} W_\nu{}^{cb} - W_\nu{}^{ac} W_\mu{}^{cb}). \tag{5.4}$$

Combining $F_{\mu\nu}$ with the Dirac Lagrangian we obtain:

$$\mathcal{L} = \bar{\Psi} i\gamma^\mu D_\mu \Psi - \frac{1}{4} F^{\mu\nu\ ab} F_{\mu\nu}{}^{ab}. \tag{5.5}$$

The Lagrangian can be further split into kinetic and interaction terms as follows:

$$\mathcal{L} = \bar{\Psi} i\gamma^\mu \partial_\mu \Psi + g\bar{\Psi}\gamma^\mu (W_\mu \cdot \Sigma)\Psi - \frac{1}{4} F^{\mu\nu} \cdot F_{\mu\nu}, \tag{5.6}$$

where the first term is the fermion kinetic term, the second is the interaction term and the third is the gauge field kinetic term. Examining the interaction term further we can identify the interactions with all the different gauge bosons:

$$\begin{aligned} +i\frac{g}{\sqrt{2}} W^{ab}\Sigma_{ab} = &+ ig\sqrt{2}\big(G \cdot U_G + (X_\alpha \cdot U_{X_\alpha} + h.c) + \frac{\sqrt{3}}{4} X_{B-L} \cdot U_{B-L} \\ &+ W_L^\pm L_\pm + \frac{W_L^0}{\sqrt{2}} L_0 + W_R^\pm R_\pm + \frac{W_R^0}{\sqrt{2}} R_0 + \\ &(D_{A_\alpha} \cdot A_\alpha + D_{A'_\alpha} \cdot A'_\alpha + D_{Y_\alpha} \cdot Y_\alpha + D_{Y'_\alpha} \cdot Y'_\alpha + h.c.)\big), \end{aligned} \tag{5.7}$$

with the terms describing interactions, respectively, with gluons, X/U_1 leptoquarks, the X_{B-L} boson, the left-handed and right-handed W bosons, A bosons and Y bosons.

Now that we have a basic Lagrangian for an $SO(10)$ GUT, we can move on to the Yukawa sector, after which we will discuss the symmetry breaking path further, and eventually discuss the whole scalar potential.

5.1.1 Yukawa Sector and Fermion Masses

The masses of the fermions are obtained through a vev of a scalar field. The relevant Higgs representations are the 10, the 120, and the 126, as they are the only ones that can couple to a 16×16 term in the potential, as discussed in section 4.2.1. Since we break the electroweak symmetry with the 10, we would expect this multiplet to generate the masses through a simple Yukawa interaction Lagrangian. However, it turns out that this is not enough, and we should also use the 120 [35]. The reason for this is that the $(1, 2, 1/2)_{10}$ Higgs doublet comes from the $(1, 2, 2)_{10}$ representation under the PS group; it is an $SU(4)_C$ singlet, and cannot differentiate between leptons and quarks. Obviously, we want different masses for leptons and quarks, so we need an additional Higgs multiplet. The minimal extension of our Yukawa sector is done by adding a multiplet from the 120. Specifically, the $(15, 2, 2)$ and $(1, 2, 2)$ PS representations of the 120 are used, as they both contain SM doublets. We will obtain 9 real Yukawa couplings in this case [35]. The form of the Yukawa Lagrangian is as follows:

$$\mathcal{L}_Y = \Psi^T B(Y_{10}\Phi_{10} + Y_{10'}\Phi_{10'} + Y_{120}\Phi_{120})\Psi, \tag{5.8}$$

where Y_{10}, $Y_{10'}$ and Y_{120} are 3×3 matrices spanning the generations of fermions. The $10'$ is there to make the real 10 complex. The vev's that the doublets from these Higgs representations acquire, will provide the fermions with mass terms.

This Yukawa Lagrangian also provides the direct interaction between scalar particles and fermions. Only the scalar representations in this Lagrangian, the 10 and 120 can directly interact with fermions. For this reason scalar leptoquarks can only come from these representations. In section 4.2 we described these representations and some of their particle content. Both the 120 and 126 contain the R_2 and $\tilde{R}_2$ scalar leptoquarks. The masses of these particles, and therefore their viability as light leptoquarks, will be determined in section 7.2. To keep things minimal, we do not include the 126 for now, exactly like the first model described in [19]. However, in section 7.3, we will find that it is not possible to get a correct fermion mass spectrum without the 126, and will therefore eventually include it.

5.2 Intermediate Symmetry Groups

In order to obtain the SM from this $SO(10)$ GUT, we need to spontaneously break the symmetry. We will use the Higgs mechanism to achieve this, as discussed in section 2.2. Furthermore, we want to have additional intermediate symmetry breaking scales between the GUT-scale and the SM, as shown in [12, 19, 28]. There is an amount of freedom in choosing intermediate energy scales, as can be seen in Figure 3.3. Possible other paths not discussed in this work are shown in [27, 28]. The specific intermediate energy scales we choose, will allow us to have new physics at the TeV-scale. The specific scalar fields associated with the symmetry breaking steps are discussed in section 4.2. A schematic overview of the procedure:

$$\begin{aligned} SO(10) &\xrightarrow[M_U]{54_H} SU(4)_C \times SU(2)_L \times SU(2)_R \times D \\ &\xrightarrow[M_D]{210_H} SU(4)_C \times SU(2)_L \times SU(2)_R \\ &\xrightarrow[M_{W_R}]{210_H} SU(3)_C \times SU(2)_L \times U(1)_R \times U(1)_{B-L} \\ &\xrightarrow[M_{Z_R}]{16_H} SU(3)_C \times SU(2)_L \times U(1)_Y \\ &\xrightarrow[M_{EW}]{10_H} SU(3)_C \times U(1)_Q. \end{aligned} \tag{5.9}$$

At the Grand Unification scale M_U, the $SO(10)$ symmetry will be broken by a PS singlet from the 54 of $SO(10)$, the resulting group is a product of the PS group with D-parity. This D-parity ensures symmetry between the left-handed and right-handed fields. Then at M_D this D-parity is broken by a parity-odd PS singlet from the 210. Breaking D-parity separately from $SU(2)_R$ was first proposed in [36], in order to obtain lower energy scales for the subsequent intermediate theories. This separation also allows for consistency with cosmological findings [28], without requiring the PS group to break close to M_U.

From M_D onward to M_{W_R} we have the PS group, in which the U_1 leptoquarks are still present. The symmetry breaking scale M_{W_R} will therefore determine the energy at which we can expect to see new physics involving these leptoquarks. The breaking at M_{W_R} is done with another field from the 210, the result is a product of the SM group with $U(1)_{B-L}$. This group corresponds to the $B-L$ (baryon number minus lepton number) symmetry and was split of from $SU(4)_C$ in the breaking of the symmetry. The $B-L$ symmetry, together with $B+L$ conservation, which always holds, preserves B and L separately. Therefore, there can be no proton decay at this level.

To obtain the SM once again, we break the symmetry with a Higgs from the 16 at M_{Z_R}. This is the lowest energy scale of new physics in this theory. Lastly, the electroweak symmetry is broken, using an SM Higgs doublet from the 10.

In the next we will discuss what the Higgs sector needs to look like to achieve this symmetry breaking pattern.

5.3 The Higgs Sector

This model for an $SO(10)$ GUT makes extensive use of spontaneous symmetry breaking through the Higgs mechanism. No fewer than 5 Higgs representations are used to achieve the desired symmetry breaking and fermion mass relations. We should now explicitly define what the Higgs sector of the Lagrangian looks like. This section is partially based on [27]. We start by writing down a kinetic term:

$$\mathcal{L}_{kin} = \mathrm{Tr}\Big[(D_\mu \Phi)^\dagger (D_\mu \Phi)\Big], \tag{5.10}$$

for every Higgs representation. The covariant derivative is not the same as the one for the fermions, except for Φ_{16}, as it transforms like a vector. The other Higgs representations transform like a rank 2 tensor, therefore we have:

$$D_\mu \Phi = \partial_\mu \Phi + \frac{ig}{\sqrt{2}}[W_\mu^{ab}\Sigma_{ab}, \Phi]. \tag{5.11}$$

The kinetic term is responsible for giving the gauge bosons mass, after the Higgs potential breaks the symmetry and gives a vev to a Higgs field. This will be explicitly shown in section 5.3.1.

In section 2.2.1 we defined a potential for a Higgs doublet that breaks the electroweak symmetry. In principle, we can construct a similar potential for every Higgs representation we have used. Every term in such a potential has to be invariant. To see which terms are invariant we simply have to look at representation theory. A simple procedure is described in [37]. If the product of the representations contains a singlet, then the corresponding term is invariant:

$$D_1 \otimes D_2 = 1 \oplus ..., \tag{5.12}$$

where D_i are arbitrary representations (not necessarily different from each other). For more complicated terms we might have a tensor product of the form:

$$D_1 \otimes D_2 = D_3 \oplus ..., \tag{5.13}$$

then:

$$(D_1 \otimes D_2) \otimes \overline{D}_3 = (D_3 \otimes \overline{D}_3) \oplus ... = 1 \oplus ..., \tag{5.14}$$

where $\overline{D}_3$ is the conjugate of D_3. The product between a representation and its conjugate always contains a singlet. This procedure is easily applied to products of four representations. So if we have a table of the tensor products of all the relevant $SO(10)$ representations (see Table 42 in [31]), we can easily identify all the invariant terms. The 10, 54, 120 and 210 are self conjugate. Therefore, terms of the form Φ^2, $\Phi^2\Phi^2$ and Φ^4 are invariant. The 16 is not self-conjugate, terms need to be of the form $\overline{16} \times 16$. The potentials without mixing between the representations are as follows:

$$V_{54} = -\frac{1}{2}m_{54}^2 \,\mathrm{Tr}\Big[\Phi_{54}^\dagger \Phi_{54}\Big] + \lambda_{54}\,\mathrm{Tr}\Big[(\Phi_{54}^\dagger \Phi_{54})^2\Big] + \nu_{54}\,\mathrm{Tr}\Big[\Phi_{54}^\dagger \Phi_{54}\Big]^2, \tag{5.15}$$

$$V_{210} = -\frac{1}{2}m_{210}^2 \,\mathrm{Tr}\Big[\Phi_{210}^\dagger \Phi_{210}\Big] + \lambda_{210}\,\mathrm{Tr}\Big[(\Phi_{210}^\dagger \Phi_{210})^2\Big] + \nu_{210}\,\mathrm{Tr}\Big[\Phi_{210}^\dagger \Phi_{210}\Big]^2, \tag{5.16}$$

$$V_{120} = -\frac{1}{2}m_{120}^2 \,\mathrm{Tr}\Big[\Phi_{120}^\dagger \Phi_{120}\Big] + \lambda_{120}\,\mathrm{Tr}\Big[(\Phi_{120}^\dagger \Phi_{120})^2\Big] + \nu_{120}\,\mathrm{Tr}\Big[\Phi_{120}^\dagger \Phi_{120}\Big]^2, \tag{5.17}$$

$$V_{16} = -\frac{1}{2}m_{16}^2 \Phi_{16+}^\dagger \Phi_{16+} + \lambda_{16}(\Phi_{16+}^\dagger \Phi_{16+})^2 + \nu_{16}(\overline{\Phi}_{16-}\Gamma_i \Phi_{16+})(\overline{\Phi}_{16+}\Gamma_i \Phi_{16-}), \tag{5.18}$$

$$V_{10} = -\frac{1}{2}m_{10}^2 \,\mathrm{Tr}\Big[\Phi_{10}^\dagger \Phi_{10}\Big] + \lambda_{10}\,\mathrm{Tr}\Big[(\Phi_{10}^\dagger \Phi_{10})^2\Big] + \nu_{10}\,\mathrm{Tr}\Big[\Phi_{10}^\dagger \Phi_{10}\Big]^2, \tag{5.19}$$

these are principally responsible for the fields obtaining a vev (except for the 120). The Higgs representations used are defined in section 4.2. The term containing Γ_i for the 16 is needed to create a non-zero invariant term connecting the + and − parts of the 16. The invariant potential terms that contain multiple representations are as follows:

$$V_{16}^{210} = \alpha_1 \Phi_{16+}^\dagger \Phi_{16+} \operatorname{Tr}\left[\Phi_{210}^\dagger \Phi_{210}\right] + \beta_1 \Phi_{16+}^\dagger \Phi_{210}^\dagger \Phi_{210} \Phi_{16+} + \gamma_1 \Phi_{16+}^\dagger \Phi_{210} \Phi_{16+}, \quad (5.20)$$

$$V_{54}^{210} = \alpha_2 \operatorname{Tr}\left[\Phi_{54}^\dagger \Phi_{54}\right] \operatorname{Tr}\left[\Phi_{210}^\dagger \Phi_{210}\right] + \beta_2 \operatorname{Tr}\left[\Phi_{54}^\dagger \Phi_{210}^\dagger \Phi_{210} \Phi_{54}\right], \quad (5.21)$$

$$V_{10}^{210} = \alpha_3 \operatorname{Tr}\left[\Phi_{10}^\dagger \Phi_{10}\right] \operatorname{Tr}\left[\Phi_{210}^\dagger \Phi_{210}\right] + \beta_3 \operatorname{Tr}\left[\Phi_{10}^\dagger \Phi_{210}^\dagger \Phi_{210} \Phi_{10}\right], \quad (5.22)$$

$$V_{10}^{54} = \alpha_4 \operatorname{Tr}\left[\Phi_{54}^\dagger \Phi_{54}\right] \operatorname{Tr}\left[\Phi_{10}^\dagger \Phi_{10}\right] + \beta_4 \operatorname{Tr}\left[\Phi_{54}^\dagger \Phi_{10}^\dagger \Phi_{10} \Phi_{54}\right], \quad (5.23)$$

$$V_{16}^{54} = \alpha_5 \Phi_{16+}^\dagger \Phi_{16+} \operatorname{Tr}\left[\Phi_{54}^\dagger \Phi_{54}\right] + \beta_5 \Phi_{16+}^\dagger \Phi_{54}^\dagger \Phi_{54} \Phi_{16+}, \quad (5.24)$$

$$V_{10}^{16} = \alpha_6 \Phi_{16+}^\dagger \Phi_{16+} \operatorname{Tr}\left[\Phi_{10}^\dagger \Phi_{10}\right] + \beta_6 \Phi_{16+}^\dagger \Phi_{10}^\dagger \Phi_{10} \Phi_{16+} + \gamma_6 \Phi_{16-}^\dagger \Phi_{10} \Phi_{16+}, \quad (5.25)$$

$$V_{210}^{120} = \alpha_7 \operatorname{Tr}\left[\Phi_{120}^\dagger \Phi_{120}\right] \operatorname{Tr}\left[\Phi_{210}^\dagger \Phi_{210}\right] + \beta_7 \operatorname{Tr}\left[\Phi_{120}^\dagger \Phi_{210}^\dagger \Phi_{210} \Phi_{120}\right]. \quad (5.26)$$

These potentials should, in theory, be responsible for giving the fields their appropriate masses. However, these mixing potentials will also make calculating the vev much more complicated. We will now examine the masses of the gauge bosons, before moving on to an example of the scalar fields obtaining masses through these mixing potentials.

5.3.1 Gauge Boson Masses

In this section we discuss how several new gauge bosons achieve their masses through spontaneous symmetry breaking. We have the new Z_R, W_R, X_{B-L} and U_1 vector bosons between the SM and the GUT-scale. Z_R and U_{B-L} achieve their masses through the breaking of the $SU(3)_C \times SU(2)_L \times U(1)_R \times U(1)_{B-L}$ symmetry by the $(1, 1, 0)$ (SM representation) field of the 16. We will show this first. Then we will show how the breaking of the Pati-Salam group by the $(1, 1, 0, 0)$ (3211 representation) field from the 210 gives W_R and the U_1 leptoquarks a mass. The relevant Higgs fields are discussed in section 4.2.3 for the 16 and in section 4.2.6 for the 210. As we stated above, the gauge bosons gain their mass through the kinetic term of the scalar fields in the Lagrangian.

Starting with the symmetry breaking due to the 16 at M_{Z_R}:

$$SU(3)_C \times SU(2)_L \times U(1)_R \times U(1)_{B-L} \xrightarrow{16} SU(3)_C \times SU(2)_L \times U(1)_Y, \quad (5.27)$$

where, as mentioned in section 4.2.3, a linear combination of generators is broken. This slightly complicates the calculation of the masses. The specific bosons are X_{B-L}, associated with the generator U_{B-L}, and Z_R^0, associated with R_3. The mass term resulting from symmetry breaking is:

$$Tr[(D_\mu \phi_{vac}^{16})^\dagger (D^\mu \phi_{vac}^{16})] \to \frac{1}{2} v^2 (g_{1R} Z_R^0 - \sqrt{\frac{3}{2}} g_{B-L} X_{B-L})^\dagger (g_{1R} Z_R^0 - \sqrt{\frac{3}{2}} g_{B-L} X_{B-L}), \quad (5.28)$$

where ϕ_{vac}^{16} is the 16 representation after obtaining a vev, as defined as in section 4.2.3. v is the value of the vev. For ease of reading, we started by using the covariant derivative at the GUT-scale, even though by this point it has split up into distinct parts. The mixing means we have a mass for some boson $Z_{mix} = \frac{1}{\sqrt{g_{1R}^2 + \frac{3}{2} g_{B-L}^2}} (g_{1R} Z_R^0 - \sqrt{\frac{3}{2}} g_{B-L} X_{B-L})$, with mass:

$$M_{Z_{mix}} = \frac{v}{\sqrt{2}} \sqrt{g_{1R}^2 + \frac{3}{2} g_{B-L}^2}, \quad (5.29)$$

where g_{1R} and g_{B-L} are the coupling constants associated with $U(1)_R$ and U_{B-L}, respectively.

Moving on to the breaking of the PS group due to a field from the 210 at M_{W_R}:

$$SU(4)_C \times SU(2)_L \times SU(2)_R \xrightarrow{210} SU(3)_C \times SU(2)_L \times U(1)_R \times U(1)_{B-L} \tag{5.30}$$

Computing the masses of the X/U_1 and $W_R^\pm$ bosons is straightforward, we use the kinetic term of the Higgs field Lagrangian (see section 5.3):

$$\begin{aligned} Tr[(D_\mu \phi^{210}_{vac})^\dagger (D^\mu \phi^{210}_{vac})] &= Tr[(\partial_\mu \phi^{210}_{vac} - \frac{ig}{\sqrt{2}}[W\cdot\Sigma, \phi^{210}_{vac}])^\dagger (\partial^\mu \phi^{210}_{vac} + \frac{ig}{\sqrt{2}}[W\cdot\Sigma, \phi^{210}_{vac}])] \\ \to \frac{1}{2} g^2 Tr\big([W\cdot\Sigma, \phi^{210}_{vac}]^\dagger [W\cdot\Sigma, \phi^{210}_{vac}]\big) &= \frac{4}{3} g_{4C}^2 u^2 (X_r^2 + X_g^2 + X_b^2) + g_{2R}^2 u^2 (W_R^\pm)^2, \end{aligned} \tag{5.31}$$

where u is the vev, g_{4C} is the coupling of $SU(4)_C$, as that is the group the X/U_1 leptoquarks belong to and g_{2R} is the coupling of $SU(2)_R$. ϕ^{210}_{vac} defined as in section 4.2.6. We obtain a mass term for the X/U_1 and $W_R^\pm$ bosons, with masses of:

$$M_{U_1} = \frac{2}{\sqrt{3}} g_{4C} u, \quad M_{W_R^\pm} = g_{2R} u \tag{5.32}$$

The value for g and g' can be obtained by running the couplings of $SU(4)_C$ and $SU(2)_R$, which will be done in section 5.4. Furthermore, if a numerical value for the masses is desired, the vev u would have to be determined based on the effective potential of the 210 Higgs at the Pati-Salam scale.

5.3.2 Higgs Mass Splitting

At every symmetry breaking scale μ, certain Higgs fields are left behind in accordance with the extended survival hypothesis, see section 5.4. At the GUT-scale this is simply assumed. However, at subsequent symmetry breaking steps, the unnecessary Higgs fields need to acquire a mass through some mechanism. This is accomplished by having the different Higgs representations coupled to each other in the potential. When one Higgs field from a representation acquires a vev at a scale μ, then all the desired Higgs fields from a different representation can acquire a mass on the order of μ. The remaining fields in that representation are needed to break the symmetry at a lower energy scale and thus need to remain massless. This puts certain bounds on the parameters in the Higgs sector.

In this section we will treat one example: the breaking of the PS group by a field from the $(15, 1, 3)$ of the 210 will give mass to all fields in the $(\overline{4}, 1, 2)$ of the 16, except for the $(1, 1, 1/2, 1)$ field, which breaks the $SU(3)_C \times SU(2)_L \times U(1)_R \times U(1)_{B-L}$ group to the SM. Much of the work in this section draws on the procedures described in [38–40], where a potential including the 16 and 45 of $SO(10)$ is considered. Furthermore, the work done in [15] on the doublet-triplet splitting problem in $SU(5)$ GUTs, has heavily inspired the procedure we use in this section.

To start off, we will combine the potentials for the 210, the 16 and their mixing terms in one potential function. Furthermore, we ignore any effects from mixing with other representations than the 16 or the 210, or from symmetry breaking at higher energy scales. All fields not in the $(15, 1, 3)$ or the $(\overline{4}, 1, 2)$ are simply ignored entirely. We deem this assumption acceptable, because any interactions with fields at higher energy scales will be heavily suppressed due to their high mass. The potential reads:

$$\begin{aligned} V = &-\frac{1}{2}m_{210}^2 \operatorname{Tr}\Big[\Phi_{210}^\dagger\Phi_{210}\Big] + \lambda_{210}\operatorname{Tr}\Big[(\Phi_{210}^\dagger\Phi_{210})^2\Big] + \nu_{210}\operatorname{Tr}\Big[\Phi_{210}^\dagger\Phi_{210}\Big]^2 \\ &- \frac{1}{2}m_{16}^2\Phi_{16+}^\dagger\Phi_{16+} + \lambda_{16}(\Phi_{16+}^\dagger\Phi_{16+})^2 + \nu_{16}(\overline{\Phi}_{16-}\Gamma_i\Phi_{16+})(\overline{\Phi}_{16+}\Gamma^i\Phi_{16-}) \\ &+ \alpha_1\Phi_{16+}^\dagger\Phi_{16+}\operatorname{Tr}\Big[\Phi_{210}^\dagger\Phi_{210}\Big] + \beta_1\Phi_{16+}^\dagger\Phi_{210}^\dagger\Phi_{210}\Phi_{16+} + \gamma_1\Phi_{16+}^\dagger\Phi_{210}\Phi_{16+}, \end{aligned} \tag{5.33}$$

where Γ^i are the usual basis matrices of $SO(10)$. To find the vacuum expectation value of $\Phi_{0\hat{0}}^{15}$ field from the $(15,1,3)$, we take the derivative of its potential with respect to that field:

$$\begin{aligned} \frac{\partial V}{\partial(\Phi_{0\hat{0}}^{15})^2} = &-\frac{1}{2}m_{210}^2\operatorname{Tr}\left[\frac{1}{64}\Gamma_{0\hat{0}}^{\prime 15\dagger}\Gamma_{0\hat{0}}^{\prime 15}\right] + 2\lambda_{210}\operatorname{Tr}\left[\frac{1}{64}\Phi_{210}^\dagger\Phi_{210}\Gamma_{0\hat{0}}^{\prime 15\dagger}\Gamma_{0\hat{0}}^{\prime 15}\right] \\ &+ 2\nu_{210}\operatorname{Tr}\Big[\Phi_{210}^\dagger\Phi_{210}\Big]\operatorname{Tr}\left[\frac{1}{64}\Gamma_{0\hat{0}}^{\prime 15\dagger}\Gamma_{0\hat{0}}^{\prime 15}\right] \\ = &-\frac{1}{2}m_{210}^2 + \frac{7}{24}\lambda_{210}(\Phi_{0\hat{0}}^{15})^2 + 2\nu_{210}(\Phi_{0\hat{0}}^{15})^2 = 0, \end{aligned} \tag{5.34}$$

where we have ignored the interactions with the 16, as it has not developed a vev yet. The $\Gamma_{0\hat{0}}^{\prime 15}$'s arise from taking the derivative of $\Phi_{210} = \frac{1}{8}\Phi^i\Gamma^{\prime i}$, with respect to $\Phi_{0\hat{0}}^{15}$. Due to our choice of normalization we have: $\operatorname{Tr}\left[\frac{1}{64}\Gamma_{0\hat{0}}^{\prime 15\dagger}\Gamma_{0\hat{0}}^{\prime 15}\right] = 1$. This leads to the following vev:

$$\langle(\Phi_{0\hat{0}}^{15})^2\rangle = \frac{m_{210}^2}{\frac{7}{48}\lambda_{210} + \nu_{210}} \equiv u^2, \tag{5.35}$$

which we have labelled u^2 for convenience. Now that we have obtained this vev we can calculate the Higgs mass spectrum as follows [14]:

$$m_{AB}^2 = \left.\frac{\partial^2 V}{\partial\phi_A\partial\phi_B}\right|_{\langle\Phi_{0\hat{0}}^{15}\rangle}, \quad A, B = 1, 2, ..., 16, \tag{5.36}$$

which basically means that the terms quadratic in the field ϕ_A correspond to the mass terms, as long as m_{AB}^2 is diagonal. If there are off-diagonal terms, we need to compute the eigenvalues to find the masses. For the fields 8 fields ϕ_A. $A = 9, 10, ...16$ in Φ_{16+}, which were still present at this PS-scale, we obtain the following masses:

$$M^2(\overline{3}, 1, -1/2, -1/3) = -m_{16}^2 + 2\alpha_1 u^2 + \frac{\beta_1 u^2}{24} + \frac{\gamma_1 u}{2\sqrt{3}}, \tag{5.37}$$

$$M^2(\overline{3}, 1, 1/2, -1/3) = -m_{16}^2 + 2\alpha_1 u^2 + \frac{\beta_1 u^2}{24} - \frac{\gamma_1 u}{2\sqrt{3}}, \tag{5.38}$$

$$M^2(1, 1, 1/2, 1) = -m_{16}^2 + 2\alpha_1 u^2 + \frac{3\beta_1 u^2}{8} - \frac{1}{2}\sqrt{3}\gamma_1 u, \tag{5.39}$$

$$M^2(1, 1, -1/2, 1) = -m_{16}^2 + 2\alpha_1 u^2 + \frac{3\beta_1 u^2}{8} + \frac{1}{2}\sqrt{3}\gamma_1 u, \tag{5.40}$$

where the fields are labelled according to their representation under $SU(3)_C \times SU(2)_L \times U(1)_R \times U(1)_{B-L}$. As indicated before, we want the fields in the first three representations above to have mass, and the last one to be massless. This puts certain constraints on the potential. Clearly, we need $M^2(1, 1, 1/2, 1) < 0$, so that we can still have it acquire a vev at a lower scale. The rest of the masses should be greater than zero. Combining these conditions allows us to determine the following set of constraints:

$$\begin{aligned}
\gamma_1 &< 0, \\
\beta_1 &< -\frac{\sqrt{3}}{u}\gamma_1, \\
\alpha_1 &> \frac{m_{16}^2}{2u^2} - \frac{\beta_1}{48} - \frac{\gamma_1}{4\sqrt{3}u}, \\
-\frac{1}{2}\sqrt{3}\gamma_1 u > -m_{16}^2 &+ 2\alpha_1 u^2 + \frac{3\beta_1 u^2}{8} > +\frac{1}{2}\sqrt{3}\gamma_1 u.
\end{aligned} \tag{5.41}$$

These conditions are required in order to get the symmetry breaking pattern we need. We can also state the effective potential after symmetry breaking:

$$V_{\text{eff}}(\varphi_0) = \big(-m_{16}^2 + 2\alpha_1 u^2 + \frac{3\beta_1 u^2}{8} + \frac{1}{2}\sqrt{3}\gamma_1 u\big)(\varphi_0^\dagger \varphi_0) + \lambda_{16}(\varphi_0^\dagger\varphi_0)^2 + \text{interactions}, \tag{5.42}$$

where φ_0 is the remaining massless field. By taking the derivative of V_{eff} with respect to φ_0, we can find the following vev:

$$\langle(\varphi_0^\dagger\varphi_0)\rangle = \frac{1}{2\lambda_{16}}\big(m_{16}^2 - 2\alpha_1 u^2 - \frac{3\beta_1 u^2}{8} - \frac{1}{2}\sqrt{3}\gamma_1 u\big) \equiv v^2. \tag{5.43}$$

We need to ensure that there exists a hierarchy between v and u. Inspecting the expression for v it would seem that v is on the order of u, unless the terms involving u cancel each other. Since we intend to have the two symmetry breaking steps occur at two very close energies, we do not require a precise cancellation. However, $v < u$ is still very much a requirement, otherwise the symmetry breaking would happen in reverse, meaning that the PS group would be broken immediately to the SM, without any intermediate symmetry.

When the field φ_0 from the 16 acquires a vev, the symmetry breaks to the SM. This will impact the scalar mass spectrum, for the fields in the 16 we get:

$$M^2(\overline{3}, 1, 1/3) = -\frac{\beta_1 u^2}{3} - \frac{\gamma_1 u}{\sqrt{3}}, \tag{5.44}$$

$$M^2(\overline{3}, 1, -2/3) = -\frac{\beta_1 u^2}{3} - \frac{2\gamma_1 u}{\sqrt{3}}, \tag{5.45}$$

$$M^2(1, 1, 1) = -\sqrt{3}\gamma_1 u, \tag{5.46}$$

$$M^2(1, 1, 0) = 8\lambda_{16} v^2, \tag{5.47}$$

where we have now labelled the fields in terms of their SM representations. These masses are obtained based on the assumption that the scalar fields from the 210 and 16 do not mix. For every field the mass of the real and imaginary component fields are the same, except for the $(1, 1, 0)$. The field belonging to the complex phase remains massless. This field is a Goldstone boson and any term involving it can be transformed away using a $U(1)_Y$ gauge transformation. The existence of one Goldstone boson is expected as we break one linear combination of generators.

We have now shown that the mass splitting of the Higgs multiplets can work for the scenario treated above. It is expected that this procedure extends to other Higgs representations as well, so that the scalar spectrum described in Table 5.1 is accurate.

5.3.3 The Vev of the 120 Doublets

The 120 representation is special in the sense that we want its two doublets to acquire a vev at the electroweak scale, while having a mass at the PS-scale. In [41], it was argued that in a model using one doublet from the 126 representation for fermion mass and another multiplet for breaking the PS group to the SM, a potential term of the form $\Phi_{126}^3\Phi_{10}$ could endow the doublet with a vev at around $\sim 100\,\text{MeV}$, while still having a mass at the PS-scale. This potential term would contain $\Delta_R\overline{\Delta}_R\Sigma\Phi$, with Δ_R the multiplet responsible for breaking the PS symmetry, and Σ and Φ the Higgs doublets from the 126 and 10, respectively. When Δ_R and Φ obtain a vev, so does Σ:

$$\frac{\partial}{\partial\Sigma}\big(\frac{1}{2}m^2\Sigma^2 + \lambda\langle\Delta_R\rangle\langle\overline{\Delta}_R\rangle\Sigma\langle\Phi\rangle + \mathcal{O}(\Sigma^3)\big) = 0 \;\rightarrow\; \langle\Sigma\rangle \simeq \lambda\frac{\langle\Delta_R\rangle^2}{m^2}\langle\Phi\rangle. \tag{5.48}$$

Since $\langle\Delta_R\rangle$ and m are of the same order, this vev will be on the order of $\langle\Phi\rangle$, exactly what we want. We can take inspiration from this to construct a similar mechanism for the 120 Higgs doublets. We break the PS group with the 210, a natural first try would be a term of the form $\Phi_{210}^2\Phi_{120}^\dagger\Phi_{10}$, another option is a similar term that is linear in Φ_{210}. This would give us the potential:

$$V_{120}^{\text{mix}} = \alpha\,\text{Tr}\Big[\Phi_{210}^\dagger\Phi_{210}\Phi_{120}^\dagger\Phi_{10}\Big] + \beta\,\text{Tr}\Big[\Phi_{210}\Phi_{120}^\dagger\Phi_{10}\Big]. \tag{5.49}$$

There are two doublets that we would like to give a vev, one from the $(1,2,2)$, called Σ_1 and one from the $(15,2,2)$, called Σ_2. Plugging in the vev's of the 10 and 210 in fact gives:

$$V_{120}^{\text{mix}} = \alpha\langle\Phi_{210}\rangle^2\Sigma_1\langle\Phi_{10}\rangle + \beta\langle\Phi_{210}\rangle\Sigma_2\langle\Phi_{10}\rangle \tag{5.50}$$

We need to prove that this is actually the case. Doing the calculation explicitly allows us to identify the fields that gain a vev. Assuming these are Σ_1 and Σ_2, we get:

$$\Sigma_1 = \frac{1}{\sqrt{2}}(\phi_{7810} + i\phi_{789}), \tag{5.51}$$

$$\Sigma_2 = \phi_{1210} + \phi_{3410} + \phi_{5610} + i(\phi_{129} + \phi_{349} + \phi_{569}). \tag{5.52}$$

To check that these are the SM Higgs doublets, we can examine their Y and L_3 eigenvalues, and see if they commute with the $SU(3)_C$ generators:

$$[\Sigma_i, Y/2] = \frac{1}{2}\Sigma_i, \quad [\Sigma_i, L_3] = \frac{1}{2}\Sigma_i, \quad [\Sigma_i, U_j] = 0, \tag{5.53}$$

with $i = 1,2$ and $j = 1,2,...,8$. Clearly these fields are $(1,2,1/2)$ representations of the SM group. Furthermore, we can check that both commute with U_{B-L} and that:

$$[U_k, \Sigma_1] = 0, \quad [U_k, \Sigma_2] \neq 0, \quad k = 9,10,...,14, \tag{5.54}$$

indicating that Σ_1 is an $SU(4)$ singlet, and Σ_2 is not. Therefore, we conclude that Σ_2 belongs to the $(15,2,2)$.

There is a point of concern with this method. Namely, having terms linear in $\Sigma_{1,2}$ seemingly does not respect the residual $U(1)_Q$ symmetry after EW breaking. In the EW breaking in the SM, a term linear in the Higgs field would break the residual symmetry. We need to examine the effective potentials at several stages to confirm that no symmetry is unintentionally broken. At the SM scale we have the following effective potential for the doublets from the 120, up to second order:

$$\begin{aligned} V_{\text{eff}}^{\text{SM}} = \frac{1}{2}M_{120}^2\Sigma_{1,2}^\dagger\Sigma_{1,2} &+ \alpha u^2(\Sigma_1^\dagger\Phi_{10} + \Phi_{10}^\dagger\Sigma_1) \\ &+ \beta u(\Sigma_2^\dagger\Phi_{10} + \Phi_{10}^\dagger\Sigma_2), \end{aligned} \tag{5.55}$$

where M_{120} is the mass obtained due to a vev from the 210. Clearly this potential is $SU(2)_L \times U(1)_Y$ invariant, as all terms are products of a doublet and a conjugate doublet. After EW breaking, Φ_{10} obtains a vev. We parameterize the fields as follows:

$$\Sigma_{1,2} = \begin{pmatrix} \Sigma^+_{1,2} \\ \Sigma^0_{1,2} \end{pmatrix}, \quad \Phi_{10} = \frac{1}{\sqrt{2}} \begin{pmatrix} \Phi^+_{10} \\ \Phi^0_{10} \end{pmatrix} \to \frac{1}{\sqrt{2}} \begin{pmatrix} 0 \\ (v+h)e^{i\theta/v} \end{pmatrix}, \tag{5.56}$$

where v is the vev, h the resulting Higgs boson and θ represents the arbitrary phase. Having this freedom to choose a phase is essential for keeping $U(1)_Q$ symmetry. Plugging this in, the resulting effective potential is as follows:

$$\begin{aligned} V^{\text{EW}}_{\text{eff}} = \frac{1}{2} M^2_{120} \Sigma^\dagger_{1,2} \Sigma_{1,2} + \alpha_7 u^2 (\Sigma^{0\dagger}_1 (v+h) e^{i\theta/v} + (v+h) e^{-i\theta/v} \Sigma^0_1) \\ + \beta_7 u (\Sigma^{0\dagger}_2 (v+h) e^{i\theta/v} + (v+h) e^{-i\theta/v} \Sigma^0_2), \end{aligned} \tag{5.57}$$

which should still respect the $U(1)_Q$ symmetry. If we transform θ, $\Sigma^{0\dagger}_{1,2}$ transforms oppositely to compensate. For the last step $\Sigma_{1,2}$ obtain vev's:

$$\Sigma_{1,2} \to (v_{1,2} + h_{1,2}) e^{i\theta_{1,2}/v_{1,2}}, \tag{5.58}$$

plugging this in we obtain the effective potential after all doublets have gained vev's:

$$\begin{aligned} V^{\text{final}}_{\text{eff}} = + \alpha u^2 ((v_1+h_1) e^{-i\theta_1/v_1} (v+h) e^{i\theta/v} + (v+h) e^{-i\theta/v} (v_1+h_1) e^{i\theta_1/v_1}) \\ + \beta u ((v_2+h_2) e^{-i\theta_2/v_2} (v+h) e^{i\theta/v} + (v+h) e^{-i\theta/v} (v_2+h_2) e^{i\theta_2/v_2}), \end{aligned} \tag{5.59}$$

where we have omitted the mass terms. Inspecting this potential, we see that we can change θ, but must then change $\theta_{1,2}$ to compensate. In principle, we still have a residual $U(1)_Q$ symmetry. The combination of the two fields allows for the symmetry to be unbroken. Note that only one phase can be rotated away at a time. If we set θ to zero, then the other two doublets will have a physical phase.

We have established that the mechanism does not have unintended consequences for the residual symmetry. Now we can conclude that the neutral components of the two doublets from the 120 obtain the following vev's after EW symmetry breaking:

$$\langle \Sigma^0_1 \rangle \sim \alpha \frac{\langle \Phi_{210} \rangle^2}{M^2_{120}} \langle \Phi_{10} \rangle, \quad \langle \Sigma^0_2 \rangle \sim \beta \frac{\langle \Phi_{210} \rangle}{M^2_{120}} \langle \Phi_{10} \rangle. \tag{5.60}$$

Since $\langle \Phi_{210} \rangle$ and m_{120} are of the same order, we get exactly what we want for $\langle \Sigma_1 \rangle$: a vev on the same order as $\langle \Phi_{10} \rangle$. However, for $\langle \Sigma_2 \rangle$ we seem to have a suppression of $\sim \frac{1}{M_{120}}$, which would lower the vev. This could in principle be tuned away with the dimensionful coupling β. This coupling would have to be on the order of M_{120}.

5.4 Running and Unification of the Couplings

In section 2.3 we described how the particle content of a theory can be used to calculate the β-coefficients. These β-coefficients specify the running of the couplings of the gauge group. Combined with the procedure for finding matching conditions, provided in the same section, we are now equipped with most of the knowledge needed to compute the running and unification of the couplings for an $SO(10)$ GUT with three intermediate scales.

The only missing piece of the puzzle is the particle content at each intermediate scale. In Table 5.1 we display the fermion and scalar content of each relevant symmetry group. The last column corresponds to the β-coefficients in the same order as the groups are written in the first column. Each representation in the second and third column will contribute to the β-coefficients through eq. (2.40). To reproduce the β-coefficients, one can follow the steps in section 2.3.1 using the representations listed in Table 5.1.

Group	Fermions	Scalars	b_i
$SU(3)_C \times SU(2)_L \times U(1)_Y$	$(3,1,1/6)$, $(\bar{3},1,1/3)$, $(\bar{3},1,-2/3)$, $(1,2,-1/2)$, $(1,1,1)$	$\Phi(1,2,1/2)_{10}$	$\begin{pmatrix} -7 \\ -19/6 \\ 41/10 \end{pmatrix}$
$SU(3)_C \times SU(2)_L \times U(1)_R \times U(1)_{B-L}$	$(3,2,0,1/3)$, $(\bar{3},1,1/2,1/3)$, $(\bar{3},1,-1/2,1/3)$, $(1,2,0,-1)$, $(1,1,-1/2,-1)$, $(1,1,1/2,-1)$	$\Phi_1(1,2,1/2,0)_{10}$, $\Phi_2(1,2,-1/2,0)_{10'}$, $H_R(1,1,1/2,-1)_{16}$	$\begin{pmatrix} -7 \\ -3 \\ 53/12 \\ 33/8 \end{pmatrix}$
$SU(4)_C \times SU(2)_L \times SU(2)_R$	$(4,2,1),(\bar{4},1,2)$	$\Phi_1(1,2,2)_{10}$, $\Phi_2(1,2,2)_{10'}$, $H_R(\bar{4},1,2)_{16}$, $\Sigma_R(15,1,3)_{210}$	$\begin{pmatrix} -19/3 \\ -8/3 \\ 8 \end{pmatrix}$
$SU(4)_C \times SU(2)_L \times SU(2)_R \times D$	$(4,2,1),(\bar{4},1,2)$	$\Phi_1(1,2,2)_{10}$, $\Phi_2(1,2,2)_{10'}$, $H_R(\bar{4},1,2)_{16}$, $H_L(4,2,1)_{16}$, $\Sigma_R(15,1,3)_{210}$, $\Sigma_L(15,3,1)_{210}$, $\sigma(1,1,1)_{210}$	$\begin{pmatrix} -2 \\ 8 \\ 8 \end{pmatrix}$

Table 5.1: β-coefficients along with fermion and scalar content of each symmetry group [12, 19]

.

Extended Survival Hypothesis

It is important to note that we only take into account those Higgs representations, which are needed in order to break the symmetry at each step. Every other multiplet is assumed to have a very large mass M_U. This is the extended survival hypothesis as discussed in [42]. An argument for this hypothesis can be made based on the principle of minimal fine-tuning [43]. The core of the argument is that, if one wants to fine-tune the least amount of parameters, it is required that all irrelevant Higgs multiplets are superheavy. In section 5.3.2 we discussed an example of how certain multiplets can be kept heavy at intermediate scales.

Matching Conditions for Three Intermediate Scales

Now that we have the β-coefficients we need to figure out the matching conditions for the specific model we treat. Following the prescription in section 2.3.2 we can see that for the most part these conditions are simple. At the unification scale all groups are embedded into one group: $SO(10)$. Therefore, the fine-structure constants have to be equal at M_U:

$$\alpha_{4C}^{-1}(M_U) = \alpha_{2LR}^{-1}(M_U) = \alpha_U^{-1}(M_U), \tag{5.61}$$

where α_U is the fine-structure constant corresponding to $SO(10)$. One should keep in mind that above the D-parity scale M_D we have $\alpha_{2L} = \alpha_{2R} = \alpha_{2LR}$, since D-parity enforces left-right symmetry.

At M_D nothing happens to $SU(4)_C$, but as stated left-right symmetry is enforced above it, therefore the matching conditions are:

$$\alpha_{4C'}^{-1}(M_D) = \alpha_{4C}^{-1}(M_D), \tag{5.62}$$

$$\alpha_{2L}^{-1}(M_D) = \alpha_{2R}^{-1}(M_D) = \alpha_{2LR}^{-1}(M_D), \tag{5.63}$$

where the prime corresponds to the coupling constant below the symmetry breaking scale.

Moving on to the next symmetry breaking scale M_{W_R}, we can see that $SU(4)_C$ breaks to $SU(3)_C \times U(1)_{B-L}$. Therefore, the couplings of the latter should be equal to that of $SU(4)_C$. Furthermore, we have $SU(2)_L$ unaffected by the symmetry breaking, yielding a trivial matching condition. $SU(2)_R$ breaks to $U(1)_R$, forcing their couplings to be equal at M_{W_R}:

$$\alpha_{3C}^{-1}(M_{W_R}) = \alpha_{B-L}^{-1}(M_{W_R}) = \alpha_{4C'}^{-1}(M_{W_R}), \tag{5.64}$$

$$\alpha_{2L'}^{-1}(M_{W_R}) = \alpha_{2L}^{-1}(M_{W_R}), \tag{5.65}$$

$$\alpha_{1R}^{-1}(M_{W_R}) = \alpha_{2R}^{-1}(M_{W_R}). \tag{5.66}$$

For the last symmetry breaking, we break to the SM at M_{Z_R}. We have two trivial matching conditions for $SU(3)_C$ and $SU(2)_L$. The last matching condition, corresponding to $U(1)_R \times U(1)_{B-L}$ breaking to $U(1)_Y$ is the only more complicated matching condition in this section. We have a product of two groups breaking to a single group. In section 4.2.3 we have established that the operator for $U(1)_Y$ is expressed in terms of the other operators as follows:

$$Y/2 = U_{B-L}/2 + R_3 \tag{5.67}$$

Enforcing $\mathrm{Tr}(Y^2/4) = \mathrm{Tr}(U_{B-L}^2) = 4$, we get the normalized operators $Y' = \sqrt{\frac{3}{5}}Y$ and $U'_{B-L} = \sqrt{\frac{3}{8}}U_{B-L}$. Therefore, the normalized relation is $Y'/2 = \sqrt{\frac{2}{5}}U'_{B-L} + \sqrt{\frac{3}{5}}R'_3$. We then obtain:

$$\alpha_Y^{-1}(M_{Z_R}) = \frac{2}{5}\alpha_{B-L}^{-1}(M_{Z_R}) + \frac{3}{5}\alpha_{1R}^{-1}(M_{Z_R}), \tag{5.68}$$

$$\alpha_{3C'}^{-1}(M_{Z_R}) = \alpha_{3C}^{-1}(M_{Z_R}), \tag{5.69}$$

$$\alpha_{2L''}^{-1}(M_{Z_R}) = \alpha_{2L'}^{-1}(M_{Z_R}). \tag{5.70}$$

The left-hand side of all these three equations correspond to the SM fine-structure constants. These will be used as input in our running. This means that the theory uses input from lower energy measurements to make predictions about higher-energies, as opposed to the $SU(5)$ case we discussed in section 3.1.1, where the SM parameters are an output of the running.

Aside from initial conditions, we have now established everything we need to compute the running of the couplings from the SM up to the gauge coupling unification.

5.4.1 Results

In total, we have 11 independent conditions, one corresponding to each equation in the matching conditions (except for the condition on α_U^{-1}, as it is only a result). However, we have 13 parameters to fix:

$$\begin{gathered} M_{Z_R},\ M_{W_R},\ M_D,\ M_U, \\ \alpha_{4C},\ \alpha_{4C'},\ \alpha_{3C},\ \alpha_{2LR},\ \alpha_{2L},\ \alpha_{2L'},\ \alpha_{2R},\ \alpha_{1R},\ \alpha_{B-L}, \end{gathered} \tag{5.71}$$

one parameter corresponding to each symmetry breaking scale, and one for each fine-structure constant not fixed by experiment. We have $13 - 11 = 2$ free parameters, this means we can pick any two parameters and vary them, thereby creating a vast parameter space of valid solutions. Since we want to state a theory with leptoquarks at the TeV-scale, we will pick M_{Z_R} and M_{W_R} as the input parameters. This means we can fix these energy scales in order to lower the mass of the U_1 leptoquark as much as possible, hopefully in range of collider experiment.

We can now proceed by doing either one of two things: algebraically work out the matching conditions and running of the couplings to obtain values for M_U and α_U as in [19], or we numerically compute the running as done in [12]. We will choose the second option for now, fixing $M_{Z_R} = 5\,\text{TeV}$ and $M_{W_R} = 10^{8.3}$ GeV. These values are the same as in [12, 19]. We choose to keep these values, as $M_{Z_R} = 5\,\text{TeV}$ is approximately as low as it can be, taking into account experimental constraints. Choosing $M_{W_R} = 10^{8.3}$ GeV allows for a clear graph of the running. Furthermore, we have non-normalized input values [17]:

$$\alpha_s^{-1} = 8.4817, \quad \alpha_{em}^{-1} = 127.951, \quad \sin^2\theta_W = 0.23121 \tag{5.72}$$

at $\mu = M_{W_Z}$, the Z_0 boson mass. From these inputs the fine-structure constants of the SM can be straightforwardly computed:

$$\alpha_{em} = \frac{e^2}{4\pi}, \quad e = \frac{gg'}{\sqrt{g'^2+g^2}}, \quad \sin\theta_W = \frac{g'}{\sqrt{g'^2+g^2}}, \quad \cos\theta_W = \frac{g}{\sqrt{g'^2+g^2}}, \tag{5.73}$$

where g is the coupling for $SU(2)_L$ and g' the coupling for $U(1)_Y$. After some algebra and using the fact that $SU(3)_C$ is unchanged at the electroweak scale, we obtain the normalized SM fine-structure constants:

$$\alpha_{3C}^{-1} = 8.4817, \quad \alpha_{2L''}^{-1} = 29.5836, \quad \alpha_{Y}^{-1} = 59.0205, \tag{5.74}$$

where we have used $Y' = \sqrt{\frac{3}{5}}Y$ to obtain the normalized result.

Using our input values, matching conditions and β-coefficients, we obtain the following results:

$$M_U = 1.6\times10^{16}\,\text{GeV}, \ M_D = 4.3\times10^{15}\,\text{GeV}, \ \alpha_U^{-1} = 42.2. \tag{5.75}$$

The result of this procedure is also summarized graphically in Figure 5.1. This figure agrees with the one obtained before in [12].

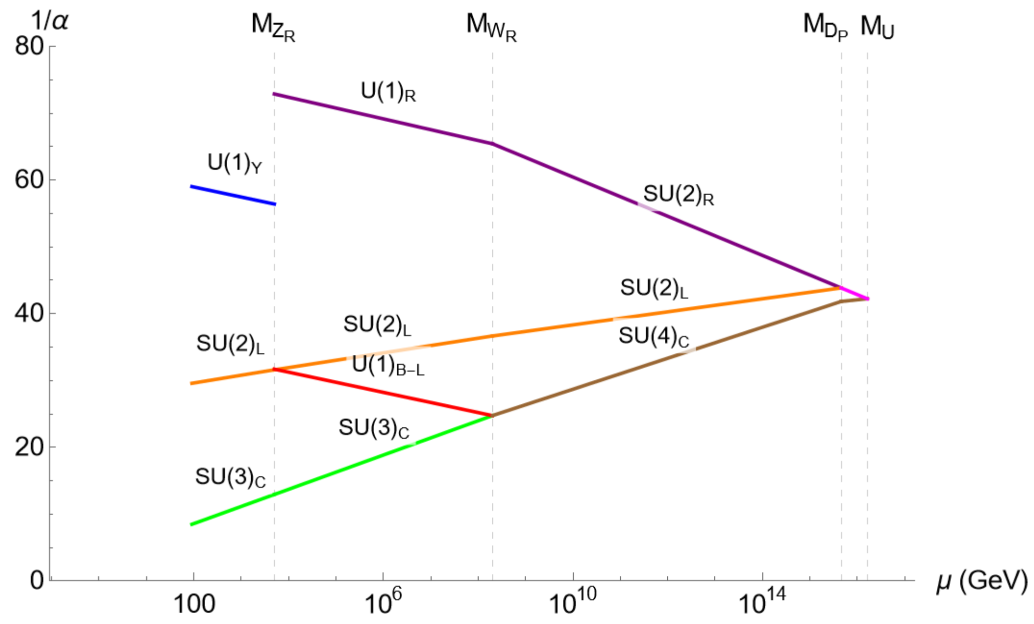

Figure 5.1: Running of the couplings from M_W to M_U, obtained using code from [12].

The running of the couplings and the matching conditions are clearly visible in Figure 5.1. This procedure has shown that we can obtain an $SO(10)$ GUT with three intermediate symmetry scales. Now we can arbitrarily change M_{W_R} to obtain a lower mass for the U_1 leptoquarks. M_{Z_R} is kept fixed at 5 TeV, while M_{W_R} is varied. The resulting M_U is plotted in Figure 5.2. Clearly, we can make M_{W_R} very low, while still attaining an acceptable value for M_U.

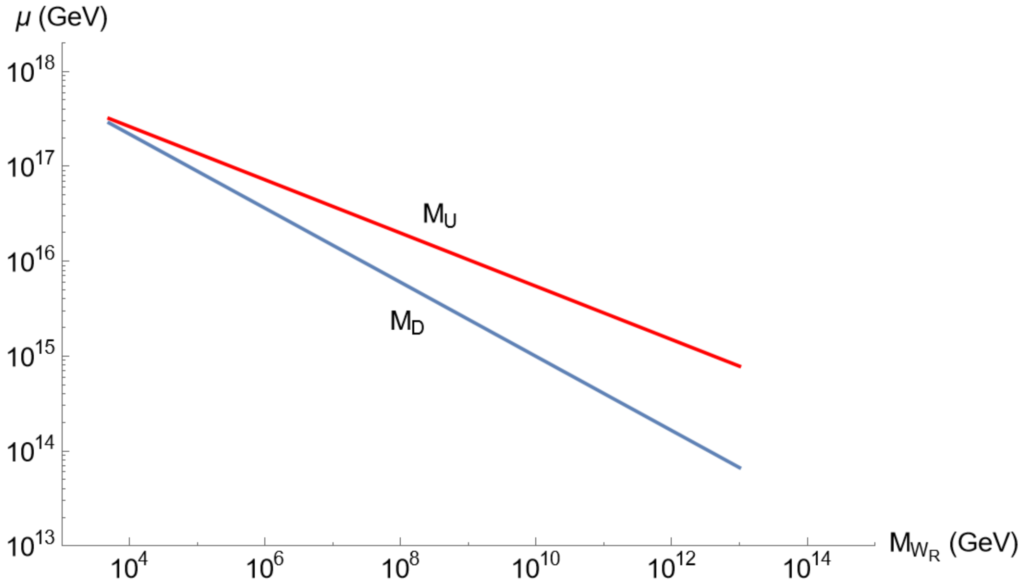

Figure 5.2: M_U and M_D as a function of M_{W_R}, the scale at which U_1 leptoquarks can exist. For this graph we have set: $M_{Z_R} = 5\,\text{TeV}$.

Some approximations should be noted. The running of couplings below a certain symmetry breaking scale will be influenced by massive particles above that scale. As we discussed in section 2.3.1, this effect is suppressed by a factor $\sim \frac{1}{M^2}$. For this reason we have entirely ignored it. Furthermore, the running we computed was valid up to one-loop level, as we did not take two-loop corrections into account. Two-loop contributions are much smaller than one-loop contributions, since they are proportional to a higher order of the coupling constant. For all curves in Figure 5.1 we have $\alpha/4\pi < 1$, therefore higher orders in the coupling are suppressed.

Another approximation is the fact that the running starts at M_Z. Technically, EW symmetry breaking has occurred at this scale, therefore we would not have three coupling constants. Furthermore, this is below the mass of the top quark, so its effects should not be taken into account. Overall we do not deem these effects to be significant enough to warrant changing the procedure with respect to [12].

We have now established a clear case: it is possible to have vector leptoquarks at the scale of 5 TeV by fixing M_{W_R} at that energy scale. Furthermore, scalar leptoquarks could occur at a similar scale, provided there is a mechanism providing them with mass, which in section 7.2 we argued there is.

Algebraic Computation of the Unification Scale

As opposed to the numerical solution offered in the previous section, it is possible to obtain M_U, M_D and α_U^{-1} algebraically. Basically, we have to use the running of the couplings in eq. (2.39) and the matching conditions to express each desired variable in terms of our input. We still have two free variables, M_{W_R} and M_{Z_R}. Like in [19] we obtain the following equations for the running from SM to M_U:

$$\begin{aligned}\alpha_{3C'}^{-1}(M_W) = \alpha_U^{-1}(M_U) &+ \frac{b_{3C'}}{2\pi}\ln\left(\frac{M_{Z_R}}{M_W}\right) + \frac{b_{3C}}{2\pi}\ln\left(\frac{M_{W_R}}{M_{Z_R}}\right)\\ &+ \frac{b_{4C'}}{2\pi}\ln\left(\frac{M_D}{M_{W_R}}\right) + \frac{b_{4C}}{2\pi}\ln\left(\frac{M_U}{M_D}\right),\end{aligned} \tag{5.76}$$

$$\begin{aligned}\alpha_{2L''}^{-1}(M_W) = \alpha_U^{-1}(M_U) &+ \frac{b_{2L''}}{2\pi}\ln\left(\frac{M_{Z_R}}{M_W}\right) + \frac{b_{2L'}}{2\pi}\ln\left(\frac{M_{W_R}}{M_{Z_R}}\right)\\ &+ \frac{b_{2L}}{2\pi}\ln\left(\frac{M_D}{M_{W_R}}\right) + \frac{b_{2LR}}{2\pi}\ln\left(\frac{M_U}{M_D}\right),\end{aligned} \tag{5.77}$$

$$\begin{aligned}\alpha_Y^{-1}(M_W) = \alpha_U^{-1}(M_U) &+ \frac{b_Y}{2\pi}\ln\left(\frac{M_{Z_R}}{M_W}\right)\\ &+ \frac{1}{2\pi}(\frac{2}{5}b_{B-L} + \frac{3}{5}b_{1R})\ln\left(\frac{M_{W_R}}{M_{Z_R}}\right)\\ &+ \frac{1}{2\pi}(\frac{2}{5}b_{4C'} + \frac{3}{5}b_{2R})\ln\left(\frac{M_D}{M_{W_R}}\right)\\ &+ \frac{1}{2\pi}(\frac{2}{5}b_{4C} + \frac{3}{5}b_{2LR})\ln\left(\frac{M_U}{M_D}\right),\end{aligned} \tag{5.78}$$

now we have three equations and three unknowns.

Through the linear combinations $\alpha_{2L''}^{-1}(M_W) - \alpha_Y^{-1}(M_W)$ and $\alpha_{2L''}^{-1}(M_W) - \alpha_{3C'}^{-1}(M_W)$ one can cancel α_U^{-1} and find a system of equations with only M_U and M_D. With some algebra one can then find $\ln\left(\frac{M_D}{M_W}\right)$ in terms of initial conditions. From this follows $\ln\left(\frac{M_U}{M_W}\right)$. Having obtained these values, $\alpha_U^{-1}(M_U)$ can be computed from any of the three equations in eq. (5.76). We obtain:

$$\begin{aligned}\ln\left(\frac{M_D}{M_W}\right) &= \left((C_3 - C_4) - \frac{C_4}{D_4}(D_3 - D_4)\right)^{-1}\\ &\left(2\pi(\alpha_{2L''}^{-1} - \alpha_Y^{-1}) - (C_1 - C_2)\ln\left(\frac{M_{Z_R}}{M_W}\right) - (C_2 - C_3)\ln\left(\frac{M_{W_R}}{M_W}\right)\right.\\ &\left. - \frac{C_4}{D_4}\left(2\pi(\alpha_{2L''}^{-1} - \alpha_{3C'}^{-1}) - (D_1 - D_2)\ln\left(\frac{M_{Z_R}}{M_W}\right) - (D_2 - D_3)\ln\left(\frac{M_{W_R}}{M_W}\right)\right)\right),\end{aligned} \tag{5.79}$$

$$\begin{aligned}\ln\left(\frac{M_U}{M_W}\right) &= \frac{1}{D_4}\left(2\pi(\alpha_{2L''}^{-1} - \alpha_{3C'}^{-1}) - (D_1 - D_2)\ln\left(\frac{M_{Z_R}}{M_W}\right)\right.\\ &\left. - (D_2 - D_3)\ln\left(\frac{M_{W_R}}{M_W}\right) - (D_3 - D_4)\ln\left(\frac{M_D}{M_W}\right)\right),\end{aligned} \tag{5.80}$$

where C_i and D_i are linear combinations of β-coefficients. These coefficients can be found in section A.3. Using these relations we, reassuringly, obtain the exact same results as before:

$$M_U = 1.6 \times 10^{16}\,\text{GeV},\ M_D = 4.3 \times 10^{15}\,\text{GeV},\ \alpha_U^{-1} = 42.2. \tag{5.81}$$

In principle, it should not be a surprise we obtained the same results. We used the exact same matching conditions, running formulas and input values. The only thing that changed w.r.t. the previous method is that we solved the equations analytically instead of numerically.

5.4.2 Inclusion of the 120

In previous literature describing this specific path from $SO(10)$ down to the SM [12, 19], the influence of the 120 Higgs representation on the running was not considered. The $(15, 2, 2)$

and the $(1,2,2)$ multiplets are used in the Yukawa sector to generate masses. Both these multiplets contain SM doublets. These fields should have a significant influence. Indeed, as stated in [32], the $(15,2,2)$ and $(1,2,2)$ give rise to a sizeable change in the β-coefficients at the PS-scale, as seen in Table 5.2. Below the Pati-Salam scale we do not have to take into account the running of the Higgs doublets from the $(15,2,2)$ and $(1,2,2)$, as these multiplets obtain a mass at the PS-scale, as discussed in section 5.3.3

Δb_i	$SU(4)_C$	$SU(2)_L$	$SU(2)_R$
$(15,2,2)$	$\frac{16}{3}$	5	5
$(1,2,2)$	0	$\frac{1}{3}$	$\frac{1}{3}$

Table 5.2: Influence of 120 Higgs multiplets on β-coefficients, as found in [32]

We have to include these representations in the running from M_U till M_{W_R}. The running is plotted in Figure 5.3. It is clearly visible that α_U^{-1} has been shifted downward with

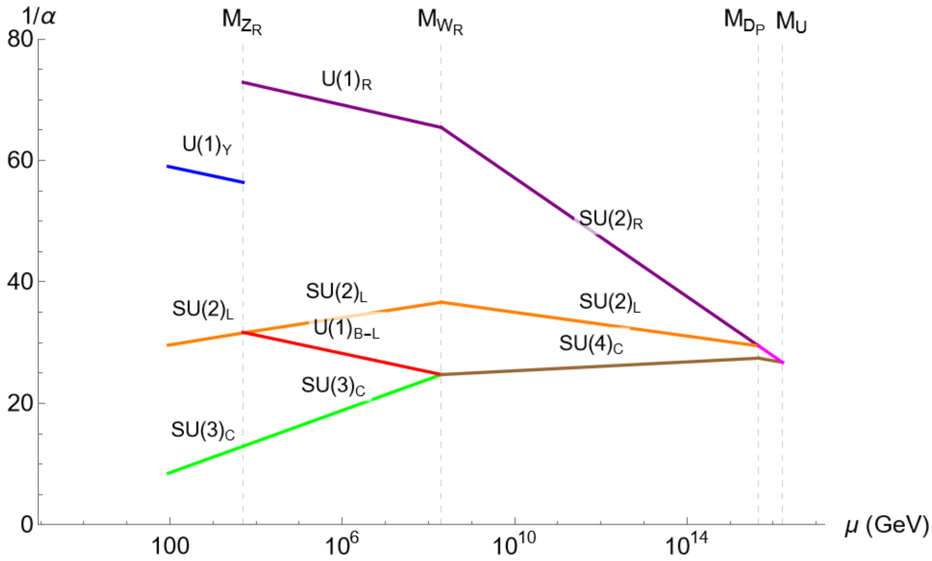

Figure 5.3: Running of the Couplings from M_W to M_U, including the effect of the 120.

respect to the previous scenario in Figure 5.1. This is due to the fact that the β-coefficient of every coupling has been increased, making the trends more downward. The results for this scenario are, using $M_{W_R} = 10^{8.3}$ GeV and $M_{Z_R} = 5$ TeV:

$$M_U = 1.6 \times 10^{16}\,\text{GeV},\;\; M_D = 4.6 \times 10^{15}\,\text{GeV},\;\; \alpha_U^{-1} = 26.8. \tag{5.82}$$

Clearly the effect on M_U is minimal, while there is some change in M_D. The most dramatic change is in α_U^{-1}, which is much lower than the previous found value of 42.2. The values of M_U and M_D as a function of M_{W_R}, keeping M_Z fixed at 5 TeV, have been plotted in Figure 5.4. This graph is fairly similar to Figure 5.2, reflecting the fact that these values were not significantly altered by the inclusion of the 120. From the graph it can be seen that the scenario is valid for energies as low as 5 TeV, as $M_D < M_U$ still holds.

This scenario, with three intermediate energy scales, including the Higgs multiplets from the 120, is what we will base our work on for now. In chapter 7 we will add the 126 representation for fermion as well. We will choose M_{W_R} to be as low as possible, according to current experimental bounds. For completeness, an updated table with the particle content and β-coefficients is provided in Table 5.3.

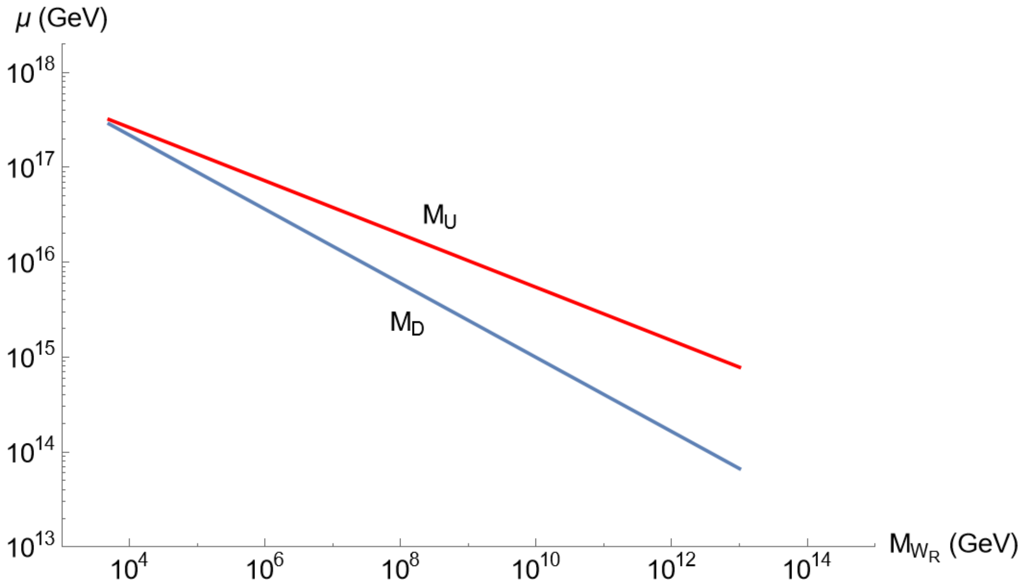

Figure 5.4: Values for M_U and M_D as a function of M_{W_R}, including the effects of the 120. For this graph we have set: $M_{Z_R} = 5\,\text{TeV}$.

Group	Fermions	Scalars	b_i
$SU(3)_C \times SU(2)_L \times U(1)_Y$	$(3, 1, 1/6)$, $(\bar{3}, 1, 1/3)$, $(\bar{3}, 1, -2/3)$, $(1, 2, -1/2)$, $(1, 1, 1)$	$\Phi(1, 2, 1/2)_{10}$	$\begin{pmatrix} -7 \\ -19/6 \\ 41/10 \end{pmatrix}$
$SU(3)_C \times SU(2)_L \times U(1)_R \times U(1)_{B-L}$	$(3, 2, 0, 1/3)$, $(\bar{3}, 1, 1/2, 1/3)$, $(\bar{3}, 1, -1/2, 1/3)$, $(1, 2, 0, -1)$, $(1, 1, -1/2, -1)$, $(1, 1, 1/2, -1)$	$\Phi_1(1, 2, 1/2, 0)_{10}$, $\Phi_2(1, 2, -1/2, 0)_{10'}$, $H_R(1, 1, 1/2, -1)_{16}$	$\begin{pmatrix} -7 \\ -3 \\ 53/12 \\ 33/8 \end{pmatrix}$
$SU(4)_C \times SU(2)_L \times SU(2)_R$	$(4, 2, 1), (\bar{4}, 1, 2)$	$\Phi_1(1, 2, 2)_{10}$, $\Phi_2(1, 2, 2)_{10'}$, $H_R(\bar{4}, 1, 2)_{16}$, $\Sigma_R(15, 1, 3)_{210}$, $\Phi^1_{120}(1, 2, 2)_{120}$, $\Phi^2_{120}(15, 2, 2)_{120}$	$\begin{pmatrix} -1 \\ 8/3 \\ 40/3 \end{pmatrix}$
$SU(4)_C \times SU(2)_L \times SU(2)_R \times D$	$(4, 2, 1), (\bar{4}, 1, 2)$	$\Phi_1(1, 2, 2)_{10}$, $\Phi_2(1, 2, 2)_{10'}$, $H_R(\bar{4}, 1, 2)_{16}$, $H_L(4, 2, 1)_{16}$, $\Sigma_R(15, 1, 3)_{210}$, $\Sigma_L(15, 3, 1)_{210}$, $\sigma(1, 1, 1)_{210}$, $\Phi^1_{120}(1, 2, 2)_{120}$, $\Phi^2_{120}(15, 2, 2)_{120}$	$\begin{pmatrix} 10/3 \\ 40/3 \\ 40/3 \end{pmatrix}$

Table 5.3: β-coefficients along with Fermion and Scalar content of each symmetry group, including the multiplets of the 120.

5.4.3 Experimental Constraints

In order to further examine the validity of the scenario we discuss, we need to compare it to current experimental bounds. An important experimental bound for any GUT is the proton lifetime. GUTs generally predict a mechanism of proton decay due to the existence of particles with both leptoquark and diquark couplings, which mediate such decays, see chapter 3. The current estimate of the proton lifetime is $\tau_p > 1.6 \times 10^{34}\,\mathrm{s}$ for the $p \to e^+\pi^0$ decay, as measured in the Super-Kamiokande [44]. A power law relating the unification scale M_U and the proton lifetime can be found [45]:

$$\tau_p = 6.9 \times 10^{35}\,\mathrm{s} \times \left(\frac{M_U}{10^{16}\mathrm{GeV}}\right)^4, \tag{5.83}$$

using this relation one finds that $M_U \gtrsim 4 \times 10^{16}$ GeV. This in turn gives us an upper bound on M_{W_R}: examining Figure 5.3, we can see that $M_{W_R} \lesssim 10^7$GeV. If M_{W_R} is any higher, M_U becomes too low. A lower bound on M_{W_R} can also be found from collider searches that constrain the right-handed W boson. The most recent value is 5 TeV [46]. Aside from collider experiments, the cosmic microwave background puts a lower bound of 4 TeV on the mass of the right-handed W_R boson [47]. Taking these constraints into account, we decide to set $M_{W_R} \geq 5$ TeV for the rest of this work.

5.5 Conclusions

In this chapter we have discussed a specific $SO(10)$ model and showed that it is able to achieve unification of the gauge couplings at a scale consistent with experimental bounds. Furthermore, we have established a scenario for new physics at energies as low as 5 TeV. Specifically, the existence of leptoquarks at this scale is of interest. The associated phenomenology will be the topic of further chapters.

By using the representations defined in chapter 4, we have formulated a Lagrangian for an $SO(10)$ model, including an elaborate scalar potential. The main difference between this model and the one in [12, 19], is that we take into account the $(15, 2, 2)$ and $(1, 2, 2)$ multiplets from the 120 of $SO(10)$ in the running of the couplings.

We have taken the symmetry breaking pattern from section 4.2 and performed the running of the couplings for this scenario. Through the computation of the β-coefficients and the determination of the matching conditions, we have managed to show this running from the SM to the GUT-scale. This successfully showed that the scenario is a valid GUT, even with the PS-scale at relatively low energies. This was precisely possible due to the existence of three intermediate scales.

However, this scenario also brings challenges with it, which we have attempted to address. The Higgs representations we use in this theory are very large. Many of the fields are irrelevant, therefore only the smallest possible multiplets of representations are kept massless at each scale. All the other fields are assumed to be superheavy (a mass on the order of the GUT-scale). There are fields that do need to be lighter than that, because they are in the same representations as necessary fields, but serve no other purpose. These need to obtain a mass due to symmetry breaking. We have shown that such a mechanism is possible, by explicitly treating an example. In this example, the breaking of the PS symmetry with a field from the 210 made the desired fields of the 16 massive, while keeping one massless.

Essentially, the doublet-triplet splitting problem and the hierarchy problem have been turned into features rather than issues of the theory. Some scalar particles becoming heavy due to interactions with other scalars is actually desirable in the model we discuss. These mechanisms are possible due to the freedom we have in assigning couplings strength for the interactions between scalar fields. The explicit splitting of masses in the scalar sector in this way is an important, yet oft neglected, part of making GUTs consistent.

Another problem has to do with the Yukawa sector of the theory. Using a single Higgs doublet from the 10 does not provide the right mass relations. Therefore, two doublets from the 120 were added. This immediately brings a new problem with it: we only see one doublet at the SM scale. Ideally, the doublets from the 120 should be heavier, while its vev's remains low. This was solved through a similar mechanism to the mass splitting, involving couplings of the 120 to both the 210 and the 10.

In short, we have developed a reasonably convincing scenario for a GUT, that could have low-energy consequences, which may be within reach of current collider experiments. This scenario contains both vector leptoquarks (X/U_1) and scalar leptoquarks (R_2, $\tilde{R}_2$) at 5 TeV, giving us reason to continue with examining the associated phenomenology. In the next chapter we will discuss the U_1 vector leptoquarks, and find that they are ruled out at the TeV-scale.

Chapter 6

Vector Leptoquarks

We have established a model for $SO(10)$ Grand Unification with vector and scalar leptoquarks at the TeV-scale that is consistent from a theoretical perspective. In this chapter we move on to the phenomenological aspects of vector leptoquarks. The relevant vector leptoquark in this model is U_1 (sometimes called X), with SM representation $(3, 1, 2/3)$. The other vector leptoquarks live at the GUT-scale and are therefore not studied in this chapter.

Firstly, we will identify a process involving U_1 that could possibly be observed at the Large Hadron Collider (LHC). Then we will look at effective field theory to examine current bounds on the new interactions associated with vector leptoquarks. This will point us towards rare meson decays, which will lead to the exclusion of U_1 vector leptoquarks at the TeV-scale. This renders the aforementioned observable impossible to measure at LHC. Several attempts to circumvent the bounds due to these decays will then be discussed.

6.1 Interaction Lagrangian

To examine the phenomenology of the vector leptoquark, we start with the interaction Lagrangian. We can easily extract the possible interactions of the U_1 leptoquark, from eq. (5.7). Expanding the relevant term we obtain [27]:

$$\begin{aligned} \mathcal{L}_X^{int} &= +ig\sqrt{2}\big(-X_\alpha \cdot U_{X_\alpha}\big) \\ &= +i\frac{g}{\sqrt{2}}\{-X_\alpha^\mu(\bar{d}^c_{\alpha\ L}\gamma_\mu e^c_L + \bar{u}^c_{\alpha\ L}\gamma_\mu \nu^c_L) + \bar{X}^\mu_\alpha(\bar{d}_{\alpha\ L}\gamma_\mu e_L + \bar{u}_{\alpha\ L}\nu_L) + h.c.\}, \end{aligned} \tag{6.1}$$

where α are the colour indices and X_α is the leptoquark field. The second and third generations have an equivalent interaction Lagrangian.

In essence, we have three U_1 leptoquarks and their conjugates, each coupling to a current with their respective colour: $J^X_{\alpha,\ \mu}$. This interaction Lagrangian confirms that U_1 is a pure leptoquark: there are no couplings to two quarks or two leptons. Therefore, the U_1 boson cannot mediate proton decay. Furthermore, it is $B-L$ conserving, carrying a $B-L$ charge of $4/3$. The Feynman diagram vertices we can obtain are shown in Figure 6.1

These diagrams form the main building blocks of any process that the leptoquark can be involved in.

6.2 Phenomenology

The U_1 leptoquark, could provide interesting phenomenology for collider experiments, provided the bounds established later in this chapter would not be an issue. Due to the fact that U_1 is a pure leptoquark, s-channel production is not possible. A B-violating leptoquark could be produced by the fusion of two quarks, but this is clearly not possible for a pure

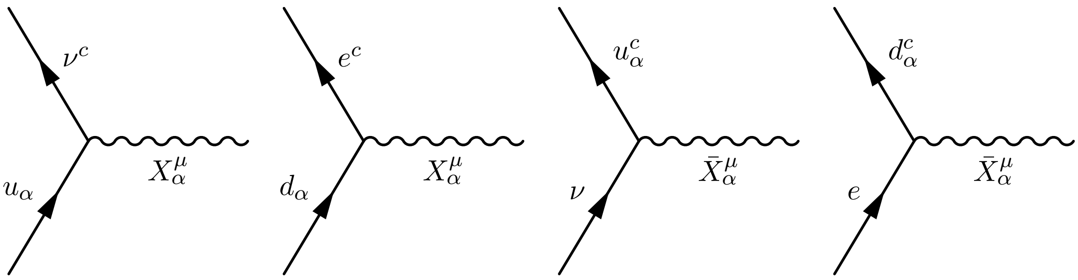

Figure 6.1: Vertices of the U_1 leptoquark, corresponding to the interaction Lagrangian in eq. (6.1)

leptoquark. The only (first generation) possibility for s-channel production would be the fusion of a down quark and a positron, however the positron would have to be produced first, for example from a photon, similarly to the process described in [48]. The process in [48], which uses a τ instead of a positron, is sensitive to leptoquarks with masses of about 2 TeV, at a coupling strength of 1.5. This is clearly too low for 5 TeV leptoquarks.

A more promising process is a t-channel exchange of a leptoquark in $d\bar{d} \to e\bar{e}$, an example of a Drell-Yan process. In Figure 6.2 the diagram for this process is shown on the left-hand side. Since U_1 is a pure leptoquark, a dd t-channel process is not possible, as it would violate baryon number.

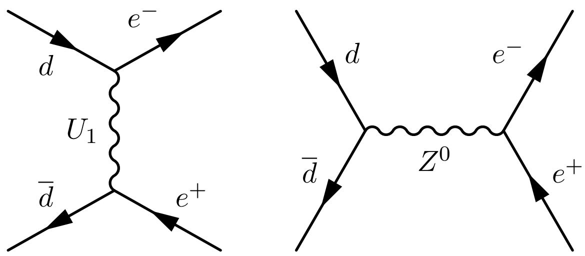

Figure 6.2: t-channel $d\bar{d} \to e^-e^+$ process mediated by U_1 leptoquarks, along with a source of background due to s-channel Z^0 exchange.

A major source of background would be an s-channel process mediated by a Z boson as shown on the right-hand side of Figure 6.2. Due to the fact that the leptoquark process is a t-channel, it might be possible to distinguish it from the background based on the spatial distribution of the resulting electron pair.

The amplitude of the leptoquark process shown in Figure 6.2 is:

$$i\mathcal{M} = -\frac{g_4^2}{2}[\overline{u}_{s;j}(p)\gamma^\mu T^\alpha_{ij} u_{s';j}(p')]\frac{-i(g_{\mu\nu} - k_\mu k_\nu/M^2_{U_1})}{k^2 - M^2_{U_1}}\delta^{\alpha\beta}[\overline{u}_{r;k}(q)\gamma^\nu T^\beta_{kl} u_{r';l}(q')], \tag{6.2}$$

where r, s are spin states, p, q, k are momenta, with $k = p - p'$, and T^α_{ij} are $SU(4)$ generators with α corresponding to the colour.

A very rough estimate on the suppression of such a process at LHC can be obtained by estimating that the input momentum is about 2 TeV, mostly from the d quark. This quark should have about 1/3 of the proton momentum, which has half the 14 TeV collision energy of the LHC. If half the input momentum goes to the leptoquark, this would give a suppression of $1^2/5^2 = 1/25$.

We can make a slightly more informed estimate, using parton distribution functions. A parton distribution function (pdf) determines the fraction of the proton momentum that a part (e.g. a quark or a gluon) of the proton gets. A calculation of these pdf's can be found in [49]. These pdf's determine the probability to find a parton (a specific particle in the proton) with a certain fraction x of the proton's momentum. Essentially, there is a trade-off between energy and probability. We want the momentum of the incoming d and $\overline{d}$ quarks to be as high as possible, without the associated probability being too low.

Using the pdf's, the momentum associated with a quark is:

$$E_q = \frac{\sqrt{s}}{2}x, \tag{6.3}$$

where s is the centre of mass energy. Roughly, the ratio of the signal, from the diagram on the left hand of Figure 6.2 and the background, due to the diagram on the right hand, would be:

$$\text{S/B} \sim \frac{1}{2}\frac{E_q^2}{M_{U_1}^2} = \frac{s}{8}\frac{x_d x_{\overline{d}}}{M_{U_1}^2} \sim x_d x_{\overline{d}} \ll 1. \tag{6.4}$$

It so happens that the other factors approximately cancel out in this case. The estimate for the ratio would be on the order of 10^{-2}. This makes such a process difficult to detect.

Another source of suppression is the size of the pdf's at x_d and $x_{\overline{d}}$. Their product would be:

$$f_d f_{\overline{d}} \sim 10^{-2} \tag{6.5}$$

Together these suppressions make detection rather difficult.

We will not do any further calculations related to this process, as they would be rendered irrelevant due to the bounds in the rest of this chapter greatly increasing this suppression.

6.3 Effective Field Theory

Effective field theory (EFT) is an approach to particle physics that is often employed to approximate more complicated theories. The basics of effective field theory are straightforward: at some energy scale $\mu \ll \Lambda$, where Λ is a cut-off energy associated with a UV completion, we expand or integrate out any contributions from the theory above the cut-off. What is left after this procedure are EFT operators. These ignore the underlying processes at high energy, and only consider the effects we see at low energy. This significantly simplifies calculations.

A prime example of an EFT is the Fermi theory of β-decay, where the decay is mediated by a contact interaction between four fermions. Of course, we now know the weak interaction explains β-decay using a W-boson. In hindsight, Fermi theory is an EFT approximation to the weak interaction. A basic interaction Lagrangian for Fermi theory is as follows:

$$\mathcal{L}_F = \frac{G_F}{\sqrt{2}}(\overline{p}\gamma_\mu n)(\overline{e}\gamma^\mu \nu_e) + h.c., \tag{6.6}$$

where we have G_F, the Fermi constant. Fermi theory predates the quark model and therefore contains neutrons and protons instead. This theory can be derived from the weak interaction in the limit that the gauge boson mass goes to infinity. That is exactly what you would expect when looking at interactions far below the scale Λ associated with the theory that describes those interactions.

To see that this is indeed the EFT associated with the weak interaction, look at the Feynman diagram in Figure 6.3. This diagram is the leading-order contribution to beta-decay of a neutron into a proton. Following the steps in [50], the amplitude associated with such a diagram is:

$$i\mathcal{M} = \left(\frac{g_w}{2\sqrt{2}}\right)^2[\overline{u}_s(p)\gamma^\mu(1-\gamma^5)\cos\theta_c u_{s'}(p')]\frac{-i(g_{\mu\nu}-k_\mu k_\nu/M_W^2)}{k^2-M_W^2}[\overline{u}_r(q)\gamma^\nu(1-\gamma^5)u_{r'}(q')], \tag{6.7}$$

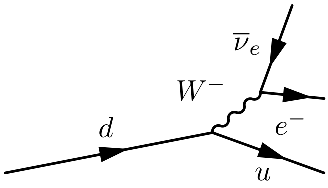

Figure 6.3: β-decay in the Standard Model.

where g_w is the weak coupling constant, θ_c is the Cabibbo angle, $u_s(p)$ is a fermion spinor with spin s and momentum p, and M_W is the mass of the W boson. Furthermore, as the W boson is an internal line in the diagram, we have its propagator: $\frac{-i(g_{\mu\nu}-k_\mu k_\nu/M_W^2)}{k^2-M_W^2}$, with $k = p - p'$. Note that this momentum will generally be on the order of 1 MeV (see Figure 10.2 in [50]), much lower than M_W, which is approximately 80.4 GeV [17]. Using this fact we can approximate the propagator:

$$\frac{-i(g_{\mu\nu} - k_\mu k_\nu/M_W^2)}{k^2 - M_W^2} \quad \rightarrow \quad \frac{ig_{\mu\nu}}{M_W^2} \quad k^2 \ll M_W^2, \tag{6.8}$$

combining this with the Feynman rules for each vertex we get:

$$i\left(\frac{g_w}{2\sqrt{2}M_W}\right)^2 = i\frac{G_F}{\sqrt{2}}, \tag{6.9}$$

which contains the familiar Fermi constant, just like in eq. (6.6). Reinserting this back into our amplitude yields:

$$i\mathcal{M} = i\frac{G_F}{\sqrt{2}}[\overline{u}_s(p)\gamma^\mu(1-\gamma^5)\cos\theta_c u_{s'}(p')][\overline{u}_r(q)\gamma_\mu(1-\gamma^5)u_{r'}(q')], \tag{6.10}$$

which is a 4-point interaction corresponding to the diagram in Figure 6.4, and corresponds to the interactions in eq. (6.6).

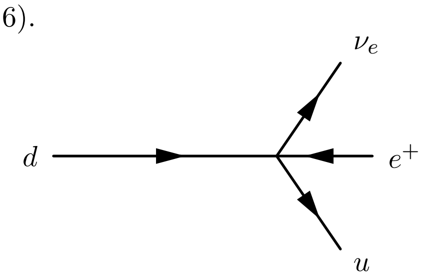

Figure 6.4: β-decay in the EFT approximation of weak interactions. The W boson has been replaced by a 4-point interaction vertex.

By simply making the assumption that the energy of the W boson is much greater than the energy scale of the interaction, we have obtained an EFT approximation, which is similar to the Fermi theory. The EFT ignores the underlying structure of the high energy theory, only keeping the results visible at lower energies. This is a powerful tool, as it allows us to constrain new physics without having to specify an actual theory. Conversely, one can take a UV completion, integrate out (when there are loops) or expand the contributions from high energy particles, and be left with just EFT operators. The operators can then be constrained by experiment. These two approaches are known as bottom-up and top-down, respectively.

6.3.1 Standard Model Effective Field Theory

A popular EFT framework in the context of new physics is the Standard Model Effective Field Theory (SMEFT). SMEFT is an EFT at the level of the SM, consisting of the SM

Lagrangian with any contribution from new physics captured in higher dimension EFT operators. SMEFT only contains the particles of the SM, but the new, higher dimensional operators introduce additional interactions between them. Therefore, the effects of new particles are only felt through these effective operators of known particles. The SMEFT Lagrangian can be defined as [51]:

$$\mathcal{L}_{SMEFT} = \mathcal{L}_{SM}^{(d=4)} + \sum_i \frac{c_i}{\Lambda_i^{d-4}} \mathcal{O}_i^{(d\geq 5)}, \tag{6.11}$$

where, c_i are the Wilson coefficients associated with each operator $\mathcal{O}_i$, Λ_i is the associated energy scale and d is the dimension of the operators. Usually, SMEFT is truncated beyond dimension-six. Higher order operators are further suppressed, therefore they contribute less and can be ignored in most cases [52]. Furthermore, dimension-five operators are not useful to us, as they only consist of couplings between the Higgs field and leptons. These operators are mainly relevant for neutrino mass generation [52]. That leaves us with the following model:

$$\mathcal{L} = \mathcal{L}_{SM}^{(d=4)} + \sum_i \mathcal{C}_i \mathcal{O}_i^{(d=6)}, \tag{6.12}$$

with the constant defined as:

$$C_i = \frac{c_i}{\Lambda_i^2} \tag{6.13}$$

Operators in SMEFT are essentially the same as in any QFT, except they treat complicated processes as contact interactions between SM particles. Just like how Fermi theory treats the weak interaction as a contact interaction between four fermions. Broadly, dimension-six SMEFT operators can be classified into several categories: four fermion operators, bosonic operators, scalar operators and mixed operators. In Table 6.1 we have summarized all four fermion operators, classified according to their chirality.

All the operators in this table can be split into separate operators linking particles of specific generations. There are 2778 operators in SMEFT up to dimension-six [53], 81 if you restrict them to 1 generation. Most of these operators are irrelevant for our purposes. Thankfully, by integrating out contributions from new particles, dictionaries linking BSM physics to SMEFT operators exist, such as [51]. In Table 6.2 we have extracted the relevant parts of such a dictionary, by displaying the operators associated with the new gauge bosons. For future reference, we also list the operators associated with the scalar leptoquarks.

Now that we have the relevant operators, we can start compiling bounds on these. This is a rather elaborate task, as bounds come from many experiments, scattered across many publications. Some bounds come from best fits of SMEFT operators to a multitude of experimental data, others come from single experiments. Among the experimental data, are results from ATLAS, CMS and electroweak precision observables.

An important thing to note is that bounds are in principle set on a Wilson coefficient $C_i = \frac{c_i}{\Lambda_i^2}$. To find bounds on Λ, the scale of new physics, a choice for c_i has to be made. There is no consistent standard for this in literature. For example, ATLAS publications employ coefficients of the form $\frac{g^2}{\Lambda^2}$ with $g^2/4\pi = 1$, see [54]. This results in a rather large value for g^2, thereby inflating the value of Λ as a result. The value of $g^2/4\pi$ at 5 TeV in our case is approximately 1/(11.6), which leads to a bound on Λ that is only a 0.29 of the published figure. Clearly there are some very high bounds on the operators constraining the U_1 leptoquark, seemingly excluding the scenario at the TeV-scale. These high bounds, far beyond the reach of collider experiment, primarily come from rare meson decays. We will discuss these in section 6.4.

The bounds on R_2 and $\tilde{R}_2$ are much more relaxed in comparison and are not excluded up to the same energy scale. Our attention will turn to these particles in chapter 7.

Chirality	Symbol	Operator	Symbol	Operator
$(\overline{L}L)(\overline{L}L)$	$\mathcal{O}_{ll}$	$(\bar{l}_L\gamma_\mu l_L)(\bar{l}_L\gamma^\mu l_L)$		
	$\mathcal{O}_{qq}^{(1)}$	$(\overline{q}_L\gamma_\mu q_L)(\overline{q}_L\gamma^\mu q_L)$	$\mathcal{O}_{qq}^{(3)}$	$(\overline{q}_L\gamma_\mu\sigma_i q_L)(\overline{q}_L\sigma_i\gamma^\mu q_L)$
	$\mathcal{O}_{lq}^{(1)}$	$(\bar{l}_L\gamma_\mu l_L)(\overline{q}_L\gamma^\mu q_L)$	$\mathcal{O}_{lq}^{(3)}$	$(\bar{l}_L\gamma_\mu\sigma_i l_L)(\overline{q}_L\sigma_i\gamma^\mu q_L)$
$(\overline{R}R)(\overline{R}R)$	$\mathcal{O}_{ee}$	$(\overline{e}_R\gamma_\mu e_R)(\overline{e}_R\gamma^\mu e_R)$		
	$\mathcal{O}_{uu}$	$(\overline{u}_R\gamma_\mu u_R)(\overline{u}_R\gamma^\mu u_R)$	$\mathcal{O}_{dd}$	$(\overline{d}_R\gamma_\mu d_R)(\overline{d}_R\gamma^\mu d_R)$
	$\mathcal{O}_{ud}^{(1)}$	$(\overline{u}_R\gamma_\mu u_R)(\overline{d}_R\gamma^\mu d_R)$	$\mathcal{O}_{ud}^{(8)}$	$(\overline{u}_R\gamma_\mu T_A u_R)(\overline{d}_R\gamma^\mu T_A d_R)$
	$\mathcal{O}_{eu}$	$(\overline{e}_R\gamma_\mu e_R)(\overline{u}_R\gamma^\mu u_R)$	$\mathcal{O}_{ed}$	$(\overline{e}_R\gamma_\mu e_R)(\overline{d}_R\gamma^\mu d_R)$
$(\overline{L}L)(\overline{R}R)$	$\mathcal{O}_{le}$	$(\bar{l}_L\gamma_\mu l_L)(\overline{e}_R\gamma^\mu e_R)$	$\mathcal{O}_{qe}$	$(\overline{q}_L\gamma_\mu q_L)(\overline{e}_R\gamma^\mu e_R)$
	$\mathcal{O}_{lu}$	$(\bar{l}_L\gamma_\mu l_L)(\overline{u}_R\gamma^\mu u_R)$	$\mathcal{O}_{ld}$	$(\bar{l}_L\gamma_\mu l_L)(\overline{d}_R\gamma^\mu d_R)$
	$\mathcal{O}_{qu}^{(1)}$	$(\overline{q}_L\gamma_\mu q_L)(\overline{u}_R\gamma^\mu u_R)$	$\mathcal{O}_{qu}^{(8)}$	$(\overline{q}_L\gamma_\mu T_A q_L)(\overline{u}_R\gamma^\mu T_A u_R)$
	$\mathcal{O}_{qd}^{(1)}$	$(\overline{q}_L\gamma_\mu q_L)(\overline{d}_R\gamma^\mu d_R)$	$\mathcal{O}_{qd}^{(8)}$	$(\overline{q}_L\gamma_\mu T_A q_L)(\overline{d}_R\gamma^\mu T_A d_R)$
$(\overline{L}R)(\overline{R}L)$	$\mathcal{O}_{ledq}$	$(\bar{l}_L e_R)(\overline{d}_R q_L)$		
$(\overline{L}R)(\overline{L}R)$	$\mathcal{O}_{quqd}^{(1)}$	$(\overline{q}_L u_R)i\sigma_2(\overline{q}_L d_R)^T$	$\mathcal{O}_{quqd}^{(8)}$	$(\overline{q}_L T_A u_R)i\sigma_2(\overline{q}_L T_A d_R)^T$
	$\mathcal{O}_{lequ}^{(1)}$	$(\bar{l}_L e_R)i\sigma_2(\overline{q}_R u_L)^T$	$\mathcal{O}_{lequ}^{(3)}$	$(\bar{l}_L\sigma_{\mu\nu} e_R)i\sigma_2(\overline{q}_R\sigma^{\mu\nu} u_L)^T$

Table 6.1: Overview of relevant dimension-six four fermion operators as found in [51]. T_A are the Gell-Mann matrices, and $\sigma_{\mu\nu} = -\frac{i}{4}[\gamma^\mu, \gamma^\nu]$ is the spin representation of the Lorentz Lie algebra.

Boson	Operators
Z_R	$\mathcal{O}_{ll}, \mathcal{O}_{qq}^{(1)}, \mathcal{O}_{lq}^{(1)}, \mathcal{O}_{ee}, \mathcal{O}_{dd}, \mathcal{O}_{uu}, \mathcal{O}_{ed}, \mathcal{O}_{eu}, \mathcal{O}_{ud}^{(1)}, \mathcal{O}_{le}, \mathcal{O}_{ld}, \mathcal{O}_{lu}, \mathcal{O}_{qu}^{(1)}, \mathcal{O}_{qd}^{(1)},$ $\mathcal{O}_{\phi D}, \mathcal{O}_{\phi\Box}, \mathcal{O}_{e\phi}, \mathcal{O}_{d\phi}, \mathcal{O}_{u\phi}, \mathcal{O}_{\phi l}^{(1)}, \mathcal{O}_{\phi q}^{(1)}, \mathcal{O}_{\phi e}, \mathcal{O}_{\phi d}, \mathcal{O}_{\phi u}$
W_R	$\mathcal{O}_{\phi 4}, \mathcal{O}_{ud}^{(1)}, \mathcal{O}_{ud}^{(8)}, \mathcal{O}_{\phi}, \mathcal{O}_{\phi D}, \mathcal{O}_{\phi\Box}, \mathcal{O}_{e\phi}, \mathcal{O}_{d\phi}, \mathcal{O}_{u\phi}, \mathcal{O}_{\phi ud},$
U_1	$\mathcal{O}_{lq}^{(3)}, \mathcal{O}_{lq}^{(1)}, \mathcal{O}_{ed}, \mathcal{O}_{ledq}$
R_2	$\mathcal{O}_{lu}, \mathcal{O}_{qe}, \mathcal{O}_{lequ}^{(1)}, \mathcal{O}_{lequ}^{(3)}$
$\tilde{R}_2$	$\mathcal{O}_{ld}$

Table 6.2: Operators generated by new gauge bosons and scalar leptoquarks present in Pati-Salam theory [51].

6.4 Rare Meson Decays

Mesons such as the B-meson, kaon and pion have decays mediated by U_1 leptoquarks. These decays have long been known to put significant constraints on the Pati-Salam model, see for example [59, 60]. The rare decays shown in Figure 6.5, $K_L^0 \to e^\pm\mu^\mp$, $\pi^+ \to e^-\nu_e$ and $B_s \to e^\pm\mu^\mp$, provide some of the more stringent bounds, depending on the flavour structure of the leptoquark. The kaon and B-meson decays are examples of lepton flavour violation and do not occur in the SM. These decays can generally be measured to high precision [61].

Note that, of the three decays in Figure 6.5, the first two do not mix generations in their vertices, whereas the last one does. In the most simple case, where the leptoquark

Operator	Precision Experiment [TeV]	Collider [TeV]	Reference
$\mathcal{O}_{lq}^{(1)}$	4.2	7.6(26.0)	[54, 55]
$\mathcal{O}_{lq}^{(3)}$	9.2		[55]
$\mathcal{O}_{lq}^{(3)[1111]}$	5.5		[56]
$\mathcal{O}_{ed}$	3.6	7.8(26.5)	[54, 55]
$\mathcal{O}_{ed}^{[1111]}$	1.2		[56]
$\mathcal{O}_{ed}^{[1212]}$	319		[56]
$\mathcal{O}_{qe}$	4.6	6	[57, 58]
$\mathcal{O}_{qe}^{[3333]}$		0.3	[56]
$\mathcal{O}_{lu}$	7.6	5.2	[57, 58]
$\mathcal{O}_{ld}$	8.1	5.0	[57, 57]
$\mathcal{O}_{ledq}^{[1111]}$	220		[56]
$\mathcal{O}_{ledq}^{[1112]}$	1205		[56]
$\mathcal{O}_{ledq}^{[1113]}$	31		[56]
$\mathcal{O}_{ledq}^{[1123]}$	7.4		[56]
$\mathcal{O}_{ledq}^{[2112]}$	1840		[56]
$\mathcal{O}_{ledq}^{[1313]}$	5.2		[56]
$\mathcal{O}_{ledq}^{[2212]}$	227		[56]
$\mathcal{O}_{lequ}^{[2112]}$	7.0		[56]
$\mathcal{O}_{lequ}^{[3333]}$	2.1		[58]
$\mathcal{O}_{lu}^{[3333]}$	1.4		[58]

Table 6.3: Bounds on Λ for several operators related to U_1, R_2 and $\tilde{R_2}$ leptoquarks, assuming $c_i = 1$,

is forbidden from mixing generations at tree level, the last one will not occur. Therefore, these decays constrain different parts of the parameter space of the theory. The current experimental observations and SM predictions are listed in Table 6.4. The ratio between pion decay to a muon and decay to an electron is measured to high accuracy (10^{-7}), and is about 1σ from the SM prediction. The kaon and B-meson decays are also measured up to high precision.

To relate these observables to our case, look at the interaction Lagrangian, taking into account the three generations of fermions:

$$\mathcal{L}_{int} = \frac{g_4}{\sqrt{2}}(\overline{q_{Li}}\gamma_\mu V_L l_L^i + \overline{q_{Rj}}\gamma_\mu V_R l_R^j)X^\mu + h.c., \tag{6.14}$$

where q_L, q_R, l_L, l_R are the left- and right-handed quarks and leptons, $i = 1,2$ is an $SU(2)_L$ index and $j = 1,2$ is and $SU(2)_R$ index. This expression contains all generations, as $q_{L1} = (u,c,t)$, and similarly for the other fermions. The matrices $V_{L,R} \in U(3)$ determine which generations the leptoquarks will couple to. This structure, together with the mass of the leptoquarks, forms a parameter space. In [61] they constrain this parameter space for

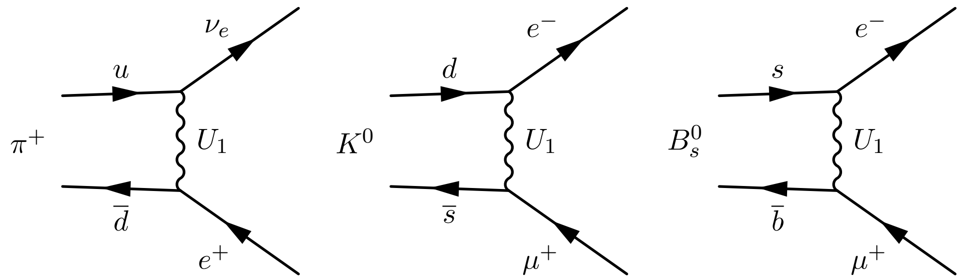

Figure 6.5: Rare meson decays mediated by U_1 leptoquarks. From l. to r.: $\pi^+ \to e^-\nu_e$, $K^0 \to e^-\mu^+$ and $B_s^0 \to e^-\mu^+$.

Observable	Measurement	SM prediction
$R_{e/\mu}(\pi^+ \to \ell^+\nu_l)$	$1.2327(23) \times 10^{-4}$	$1.2352(1) \times 10^{-4}$
$BR(K_L^0 \to e^\pm\mu^\mp)$	$< 4.7 \times 10^{-12}$	0
$BR(B_s^0 \to e^\pm\mu^\mp)$	$< 5.4 \times 10^{-9}$	0

Table 6.4: Branching ratios for several rare meson decays as reported in [61]

a very similar model based on $SU(4)_C \times SU(2)_L \times U(1)_R$. This model contains the exact same leptoquark, but the right-handed fermions are in slightly different representations, as there is no $SU(2)_R$ symmetry. In their case, one has the following interaction Lagrangian:

$$\mathcal{L}_{int} = \frac{g_4}{\sqrt{2}}(\overline{q_{Li}}\gamma_\mu V_L l_L^i + \overline{d_R}\gamma_\mu V_R e_R + \overline{u_R}\gamma_\mu V_R' \nu_R)X^\mu + h.c., \tag{6.15}$$

where V_L, V_R and V_R' are 3×3 matrices linking the different generations. This can be restated by using chiral projectors $P_{L,R}$ and expanding the i index [61]:

$$\mathcal{L}_{int} = \frac{g_4}{\sqrt{2}}(\bar{d}\gamma_\mu[P_L V_L + P_R V_R]e + \overline{u_L}\gamma_\mu V_{CKM} V_L \tilde{\nu}_L)X^\mu + h.c., \tag{6.16}$$

where only SM fermions are kept, leaving out the right-handed neutrinos. They then match these interactions to SMEFT operators and find predictions for rare meson decays due to leptoquarks. In this way they find bounds on the leptoquark mass for different choices of parameters. Depending on these choices, the decay that delivers the most stringent constraint also changes. The highest mass constraint is obtained when setting $V_L = V_R = I_3$. In this case a 90% C.L. upper bound on $K_L^0 \to e^\pm\mu^\mp$ gives a lower bound of 2074 TeV for the mass of U_1. The overall lowest mass bound is for the following set of parameters:

$$V_L = \begin{pmatrix} 0 & -0.04 - 0.06i & -0.09 - 0.99i \\ 0 & 0.20 - 0.98i & -0.05 + 0.06i \\ 1 & 0 & 0 \end{pmatrix}, V_R = \begin{pmatrix} 0 & -0.06 + 0.04i & -0.23 - 0.97i \\ 0 & 0.12 - 0.99i & -0.06 - 0.04i \\ 1 & 0 & 0 \end{pmatrix},$$

in which case the mass is constrained by the $B_s \to e^\pm\mu^\mp$ decay, giving a lower bound of 90 TeV. Clearly, these constraints apply to our case as well, since we have the exact same leptoquarks. A similar lower bound was earlier obtained in [62]. Therefore, we must conclude that experimental constraints rule out the 5 TeV vector leptoquark scenario, unless these leptoquarks couple in ways that evade these constraints.

Along with the leptoquarks, these constraints push the Pati-Salam theory up to energies as high as 2 PeV. Since the scalar leptoquarks obtain their mass at this scale, it would be expected that these are ruled out along with the vector leptoquarks. However, these scalar leptoquarks can evade the bounds from rare meson decays, while being relatively light, due to fact that their couplings to first and second generation fermions are small. Therefore, if we can find a way to make them lighter than the Pati-Salam scale, there is still a scenario for light leptoquarks. We will establish a mechanism for light scalar leptoquarks in section 7.2.

6.5 Nonunitary Models

In the previous section the parameter space for the U_1 leptoquarks was constrained under the assumption that the generation structure is determined by unitary matrices:

$$V_L, V_R \in U(3),$$

in similar fashion to the CKM and PMNS matrix for flavour-changing weak interactions, see section 2.2.4. If there are only three generations, this assumption seems reasonable, as these matrices relate mass eigenstates to flavour eigenstates. A change of basis from one orthonormal basis to another should be unitary, unless there are additional dimensions, like a fourth generation of fermions. Furthermore, when a W boson changes a down quark into either an up, charm or top, the total probability to end up in either of these states should theoretically be 1:

$$|V_{ud}|^2 + |V_{cd}|^2 + |V_{td}|^2 = 1, \tag{6.17}$$

experimentally this has been verified to be 0.9985(7), a 2.2σ deviation from the SM [17]. As we stated, if there are 4 generations, the subspace of three generations does not need to be unitary. This could be one possibility for creating a nonunitary model for the vector leptoquarks.

A unitary $V_{L,R}$ is clearly not viable for a model with TeV-scale vector leptoquarks, as shown in section 6.4. Therefore, we could simply try the following matrix at tree level:

$$V_{L,R} = \begin{pmatrix} 0 & 0 & 0 \\ 0 & 1 & 0 \\ 0 & 0 & 1 \end{pmatrix}, \tag{6.18}$$

however, this leads to a problem. The leptoquarks are in the adjoint of $SU(4)$, as are the gluons. Therefore, at the PS-scale, the gluons and leptoquarks should couple to all matter in the exact same way. Gluons couple identically to each generation, logically the vector leptoquarks should too. This means we need some mechanism to create differences in couplings below the PS-scale, explicitly breaking the symmetry, as well as spontaneously.

Another potential issue with a nonunitary model, is whether it actually evades the bounds. After all, due to flavour-changing interactions, there could still be effective interactions with first generation leptons, due to higher order diagrams. For example the penguin diagram in Figure 6.6 shows how forbidden decays could still occur even with the generation structure in eq. (6.18). These higher order corrections are much smaller than 1, however.

To show that higher order corrections to $V_{L,R}$ are not significant, we need to make an estimate of the effective first generation coupling of the leptoquark due to a diagram like in Figure 6.6. A simple estimate would be:

$$\mathcal{M} = \frac{1}{16\pi^2}\frac{G_F}{\sqrt{2}} m_{K^0}^2 V_{cd}^{CKM} U_{e2}^{PMNS} \approx 2 \times 10^{-9} \tag{6.19}$$

where we have taken into account the $1/16\pi^2$ factor from a loop integral, the Fermi constant for weak interactions, and the mixing matrices for quarks and leptons. This number is so

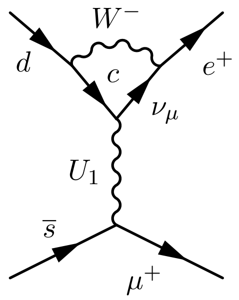

Figure 6.6: Penguin diagram of $K^0 \to e^-\mu^+$ decay, mediated by a U_1 leptoquark

small that contributions from flavour-changing processes like this should not lead to conflicts with bounds on these decays. This is under the assumption that an effective coupling of 1 to first generation matter leads to a bound of 2 PeV, therefore a coupling on the order 10^{-9} leads to a bound of $\sim 20\,\text{MeV}$, approximately.

Nevertheless, obtaining a nonunitary model from a GUT, or at all, is rather complicated. Some attempts are made in [63–66]. These models often involve separate gauge groups for each generation [64] or a separate group for the third generation [65]. This prevents the whole theory from being embedded in a single copy of $SO(10)$. Others introduce groups like $Sp(4)$ to include a flavour symmetry in their model [63]. These theories often reduce to the 4321 model at a certain scale, corresponding to the gauge group:

$$SU(4)_C^3 \times SU(3)_C^{2+1} \times SU(2)_L \times U(1)_Y, \tag{6.20}$$

where the superscripts indicate to which generations $SU(3)$ and $SU(4)$ couple. These models essentially only let the third generation couple to the U_1 leptoquarks at lower energies. This allows them to evade the stringent bounds. Some theories that do not rely on this mechanism introduce extra particles, for example vector-like fermions [66]. These vector-like fermions mix with the ordinary fermions, resulting in nonunitary couplings.

The added complexity of these models, and their inability to be embedded in a minimal GUT makes them unattractive candidates. Therefore, we will not explore these theories any further in this work.

6.6 Conclusions

In this chapter we have examined some phenomenology associated with the U_1 leptoquark. The observable shown in section 6.2 is ruled out at low energies due to rare meson decays, as shown in section 6.4. Therefore, we are left with either of the following cases:

- The specific Pati-Salam model we have discussed is valid at energies of 2 PeV or larger,
- The U_1 Leptoquark is light, but does not couple (strongly) to first generation fermions.
- The model is not an accurate description of physics at high energies.

In the first case it would be impossible to measure effects of the leptoquark with current colliders, as LHC operates at $E_{CM} = 14\,\text{TeV}$, or even at future colliders such as the Future Circular Collider with $E_{CM} = 100\,\text{TeV}$.

In the second case we need to either establish a mechanism to create these different couplings in the model we treat, or let go of the model entirely, in order to examine observables with second and third generation fermions.

The option that the Pati-Salam model simply does not describe physics at higher energies has of course always been an option, but one that is impossible to verify currently.

Further examination of the collider phenomenology associated with U_1 leptoquarks does not seem like a useful exercise. Constraining the flavour structure of U_1 leptoquark through experiments such as meson decay measurements is still viable, however.

The conclusions in this chapter lead us to shift our focus to the scalar leptoquarks contained in the GUT.

Chapter 7

Scalar Leptoquarks

In section 4.2 we identified several scalar leptoquarks, coming from the 10, 120, and 126 representations. The latter two contain pure leptoquarks that do not mediate proton decay, these are R_2 and $\tilde{R}_2$, with SM representations $(3, 2, 7/6)$ and $(3, 2, 1/6)$, respectively. Both leptoquarks exist in the 120 and the 126, the key difference being that those in the 120 have antisymmetric couplings whereas those in the 126 have symmetric couplings.

The bounds on the Pati-Salam scale, established in section 6.3.1, exclude the existence of vector leptoquarks up to 2 PeV in the model we discuss. In principle, the scalar leptoquarks, R_2 and $\tilde{R}_2$, obtain their mass at this scale too, if the extended survival hypothesis is followed. In this chapter, we will examine whether it is possible to make these leptoquarks light (TeV-scale). Firstly, we will attempt to do this by adjusting the parameters in the scalar potential. Secondly, we will attempt to do so by relaxing the extended survival hypothesis. Before discussing the mass of the scalar leptoquarks, we spend some time on fine-tuning.

After establishing a mechanism to obtain TeV-scale scalar leptoquarks, we will discuss the couplings of these leptoquarks to fermions. In this section we will determine that the Yukawa couplings of the scalar leptoquarks are similar to the Yukawa couplings in the SM. The findings in this section lead us to add the 126 representation to the model.

As stated, several changes will be made to the model in this chapter. The resulting model is given in an overview in section 7.4. In this section we compute the running of the couplings once more to show that the model can still achieve unification.

Lastly, we will move on to studying the phenomenology of these scalar leptoquarks. We will collect important bounds on the model and identify interesting collider observables for our scenario. The hierarchy in the couplings of the leptoquarks allows them to evade the bounds set due to rare meson decays. As a result of this hierarchy, we focus on observables with third generation fermions.

7.1 Fine-Tuning

Due to the high Pati-Salam scale (2 PeV), we will need very small couplings to achieve small masses for scalar leptoquarks. Usually, we want couplings to be of order 1, and could consider the coupling we will compute in eq. (7.5) to be fine-tuning.

The main argument against fine-tuning comes from the principle of "naturalness", that any coupling defined in terms of some cut-off scale Λ must be of order 1 [67]. This is a heuristic argument and not an established law. It functions as a guiding principle in formulating theories, stemming from an appeal to "beauty". Whether this is a good guiding principle remains a topic of debate.

Another definition of naturalness is that in order to be considered natural, a theory must be stable with respect to small changes in its fundamental parameters. That is to say, if we change a parameter by a small amount, the theory should not be incredibly different.

Very small parameters are clearly more susceptible to such changes.

Theories of BSM physics are often compared to each other by the amount of fine-tuning necessary. Several benchmarks exist that attempt to quantify fine-tuning. Following these measures, a theory with less fine-tuning is considered more natural and therefore a better candidate for a BSM theory. The flip side however, is that theories with less fine-tuning are often more complex [67].

The question is: do the couplings we establish in eq. (7.5), or in any part of our Higgs sector, constitute unnatural fine-tuning. Furthermore, if it is unnatural fine-tuning, is that a problem? We could make the argument that Yukawa couplings can be very small and differ by orders of magnitude from each other. Therefore, it would be fine for scalar masses as well.

This argument does not take away the fact that this mass fine-tuning seems very artificial. Most importantly, it does not pass the test of being stable under small changes in the parameters. Therefore, we eventually choose to find a different mass mechanism, which does not require as much fine-tuning.

7.2 Scalar Leptoquark Masses

In principle, the scalar leptoquarks identified in section 4.2.4 will obtain a mass at the Pati-Salam scale, as assumed in section 5.3.3. This in accordance with the extended survival hypothesis (section 5.4): since the leptoquarks are not necessary below the PS-scale, they obtain a mass at that scale. In this section we show how the scalar leptoquarks achieve mass, and explore whether it is possible to obtain a mass for the scalar leptoquarks that is lower than the PS-scale. In principle, the mass of the scalars is not as strictly related to the symmetry-breaking scale as the gauge boson mass. The gauge boson mass is determined only by the vacuum expectation value and the coupling constant of the associated broken symmetry. This coupling constant is determined by the running of the couplings, see section 5.4. The parameters in the Higgs sector, however, are not restricted in this way, and can therefore be tuned to achieve different masses. Excessively restricting parameters in order to get a desired outcome can be considered unnatural fine-tuning. We have briefly discussed this in section 7.1. For several reasons, including fine-tuning, we choose to provide the leptoquarks with mass at a different scale in section 7.2.1.

The scalar leptoquarks embedded in the $(15, 2, 2)$ are R_2 and $\tilde{R_2}$. We intend to calculate the masses of these particles in this section. In principle the other fields, including an SM doublet, in the $(15, 2, 2)$ should get similar masses, but this is not relevant for our purposes.

The potentials involving the 120 Higgs representation are given in section 5.3. Assuming the fields obtain a mass due to the vev of the 210, the relevant terms are:

$$V = \alpha \,\mathrm{Tr}\left[\Phi_{120}^\dagger \Phi_{120}\right] \mathrm{Tr}\left[\Phi_{210}^\dagger \Phi_{210}\right] + \beta \,\mathrm{Tr}\left[\Phi_{120}^\dagger \Phi_{210}^\dagger \Phi_{210} \Phi_{120}\right], \tag{7.1}$$

where only the (15,2,2) of the 120 is relevant. When the relevant field in the 210 obtains a vev u, this expression becomes:

$$V = 4\alpha u^2[(\tilde{R}_2)^2 + (R_2)^2] + \frac{5}{24}\beta u^2[(\tilde{R}_2)^2 + (R_2)^2], \tag{7.2}$$

where we have only kept leptoquark fields. Now it would seem that these leptoquarks obtain a mass on the order of u, assuming the couplings are of order 1. However, if we allow the couplings to be much smaller, or make them cancel out each other almost entirely, we could obtain a much lower mass than u. The mass of these particles will be as follows:

$$m_{R_2}^2 = \frac{\partial^2 V}{\partial (R_2)^2} = 8\alpha u^2 + \frac{5}{12}\beta u^2 \to m_{R_2} = u\sqrt{8\alpha + \frac{5}{24}\beta} \tag{7.3}$$

and equivalently for $\tilde{R}_2$. Since the PS-scale was constrained to lie at much higher energies in section 6.3.1, we investigate what values α and β should take in the case $u \sim 2\,\text{PeV}$, in order to obtain a leptoquark mass is $5\,\text{TeV}$. The result is:

$$\frac{m_{R_2}^2}{u^2} = 8\alpha + \frac{5}{24}\beta = \frac{1}{160000}. \tag{7.4}$$

For simplicity, assume the couplings are equal, we then obtain:

$$\alpha = \beta = 7.6 \times 10^{-7} \sim \mathcal{O}(10^{-7}), \tag{7.5}$$

which means we have to tune the parameters to 7th decimal to obtain the right mass in this case. Purely mathematically, it seems to be possible to get light scalar leptoquarks at tree level. However, we deem this not desirable, based on section 7.1.

Another thing to consider are loop-level corrections. The mass we calculated is at tree level. Diagrams at the loop level may create a higher mass. Considering how small our parameters have to be to ensure a light mass, these corrections may alter it significantly. This is akin to the hierarchy problem for the Higgs boson. The mass of the Higgs particle is pulled up to the scale of new physics by loop corrections [15, 67]. This is an unsolved issue of GUTs.

A problem of the approach in this section is that it interferes with the vev's of the doublets from the 120 established in eq. (5.60). Instead of the vev's and PS scale having a ratio of approximately 1, there is now a large hierarchy. This would cause the vev's to be much larger than desired, which will give fermions incorrect masses. To compensate for this, we would have to tune the parameters in eq. (5.60).

In conclusion, due to level of fine-tuning and the issue with the vev's, we decide to choose a different mechanism for the scalar leptoquark masses.

7.2.1 Alternative Mass Mechanism

We can attempt to give the scalar leptoquarks a mass using the vev of the 16 representation, which breaks $SU(3)_C \times SU(2)_L \times U(1)_R \times U(1)_{B-L}$ to the SM. This symmetry breaking has so far not been constrained to lie at much higher energies, so we are free to keep it at $5\,\text{TeV}$. This means that we are relaxing the extended survival hypothesis slightly, though this is not a problem, as it is merely a guiding principle. Usually, we only keep the strictly necessary Higgs multiplets at each energy scale. In this case, the leptoquarks come from the $(15, 2, 2)$ at the PS-scale. When the PS-group breaks, only the Higgs doublet contained in this representation needs to be kept massless in order to explain the fermion masses, the rest of the fields can be massive. In this section we assume that the scalar leptoquarks also stay massless along with the Higgs doublet.

The part of the potential responsible for giving the leptoquarks mass is:

$$\mathcal{V} = \alpha \Phi_{16+}^\dagger \Phi_{120}^\dagger \Phi_{120} \Phi_{16+}, \tag{7.6}$$

when the field φ_0 in the 16 acquires a vev, this term gives the following mass:

$$m_{R_2}^2 = \frac{\partial^2 V}{\partial (R_2)^2} = 2\alpha v^2, \tag{7.7}$$

and similarly for $\tilde{R}_2$. This is calculated based on the assumption that m_{120} is set to 0 in the potential at the GUT-scale. Setting $v = 5\,\text{TeV}$ and $\alpha = 1/\sqrt{2}$, we obtain the desired result:

$$m_{LQ} = 5\,\text{TeV}. \tag{7.8}$$

In fact there is no reason why we cannot make the mass even lower, as low as experimental bounds would allow for. By changing α we can feasibly get a mass of 1.5 TeV, which is about the lower limit from collider experiment, see section 7.5.2

It seems that this approach is more promising than the one in section 7.2, as we did not rely on fine-tuning. The relations determining the vev's of the doublets from the 120 in eq. (5.60) are no longer valid when using this mechanism for the mass, since the vev of the 210 and the mass of the fields in the 120 are no longer of the same order. This can be fairly easily remedied, however, as a coupling between two 16's, a 10 and a 120 can replace the terms in eq. (5.49):

$$\alpha\Phi^\dagger_{16+}\Phi^\dagger_{10}\Phi_{120}\Phi^\dagger_{16+} + h.c. \tag{7.9}$$

When the relevant fields in the 10 and 16 acquire a vev, we get the following vev's for the doublets in the 120:

$$\langle\Sigma_{1,2}\rangle \sim \alpha\frac{\langle\Phi_{16+}\rangle^2}{M^2_{120}}\langle\Phi_{10}\rangle, \tag{7.10}$$

which is in fact less complicated than the mechanism presented in section 5.4.2, since we do not need cubic terms.

The running of the couplings has changed as a result of this new mass mechanism. We will address this in section 7.4, after making some further modifications to our scalar sector in section 7.3. In conclusion, giving the scalar leptoquarks a mass through a coupling with the 16 is the approach we choose to obtain TeV-scale leptoquarks.

The findings in this section differ from [12]. In that work it was argued that all scalar leptoquarks were at the GUT-scale. Here we have shown that this is not necessarily the case.

7.3 Yukawa Couplings

In order to examine the phenomenology and assess the bounds associated with the scalar leptoquarks we need to determine their couplings with fermions. These Yukawa couplings are also responsible for making the model consistent with fermion masses. This connection allows us to create a picture of the couplings of the scalar leptoquarks. However, determining precise numerical values will prove difficult. The findings in this section will also lead us to include the 126 representation and its leptoquarks.

Several publications have attempted to reproduce fermion masses using various combinations of Higgs doublets from the 10, 120 and 126 representations [68–71]. The procedure is as follows: identify the free parameters and fit them to reproduce the fermion mass spectrum. These fits are obtained at $\mu = M_{GUT}$, so they are not valid at lower energy scales. In order to properly assess whether the couplings of the leptoquarks violate any bounds we would need to run these couplings down the SM. We will not attempt this. Furthermore, when fitting parameters to the Yukawa sector, there is a freedom to pick one Yukawa matrix to be diagonal. This freedom in determining the couplings makes this method not very suited to determining bounds on scalar leptoquarks.

At energies above the Pati-Salam scale ($\geq$ 2 PeV), the scalar leptoquarks couple to fermions in the same way as the SM doublets from the 120 and 126. Below this scale they break apart into separate representations and their couplings can deviate only a limited amount through running. For this reason we can assume that the hierarchy and order of magnitude of the couplings of the leptoquarks is similar to that of the SM Yukawa couplings, which are shown in Table 7.1.

Examining some fits to fermions masses, a problem immediately arises, as mentioned in section 5.1.1: in [71], it is clearly shown that using Higgs doublets from a complex 10 and a real 120 is not consistent with experimental data, as it leads to a 7.3σ disagreement with the τ mass. These are the same representations we are using. Therefore, we have

Yukawa coupling	y_t	y_c	y_u
Value	0.98	7.3×10^{-3}	1.4×10^{-5}
Yukawa coupling	y_b	y_s	y_d
Value	2.4×10^{-2}	6.0×10^{-4}	2.8×10^{-5}
Yukawa coupling	y_τ	y_μ	y_e
Value	0.1×10^{-2}	6.1×10^{-4}	2.9×10^{-6}

Table 7.1: Yukawa couplings of fermions, as calculated from their masses [17], according to the relation $y_f = \sqrt{2}\frac{m_f}{v}$, with $v = 246.22\,\text{GeV}$, the Higgs vev.

to conclude that the model is not viable, unless we add extra representations. In [68, 69], it is found that a Yukawa sector containing a real 10, a real 120 and a complex 126 can explain the fermion masses with minimal error. The fit performed in [70] for this setup found a significant deviation (3.5σ) for the top quark mass, however. Given that the other two publications do not have this problem, we choose to adopt the model with a real 10, a real 120 and a complex 126. Adding the 126 means the model will contain the R_2 and $\tilde{R}_2$ with symmetric couplings.

The Yukawa sector now takes the form:

$$\mathcal{L} = \Psi_L^T(Y_{10}\Phi_{10} + Y_{120}\Phi_{120} + Y_{126}\Phi_{126})\Psi_L, \tag{7.11}$$

where we have added Y_{126} and Φ_{126} to include the 126 representation. This Lagrangian will be the source of all scalar leptoquark interactions with fermions. Unfortunately, determining the Yukawa matrices (at the SM scale) in this Lagrangian is a very involved task and would rely on many assumptions. Therefore, we do not attempt to do this.

7.4 The Revised $SO(10)$ Model

In this chapter we have made several revisions to the model we treat. Firstly, in section 7.2.1 we decided to include the $(15, 2, 2)_{120}$ all the way down to M_{Z_R}, where it obtains mass. Secondly, in section 7.3 we opted to include the $(15, 2, 2)_{126}$, which like the same representation from the 120 obtains a mass at M_{Z_R}. Furthermore, we make the 10 real instead of complex. An overview of the model, listing the representations at each scale is given in Table 7.3. Another overview, showing at which scale each particle obtains mass is shown in section A.4. The revisions to the scalar sector require us to compute the running once again.

Gauge group	β-coefficients
$SU(4)_C \times SU(2)_L \times SU(2)_R \times D$	$\begin{pmatrix} 6 & \frac{31}{2} & \frac{31}{2} \end{pmatrix}$
$SU(4)_C \times SU(2)_L \times SU(2)_R$	$\begin{pmatrix} \frac{5}{3} & \frac{29}{6} & \frac{31}{2} \end{pmatrix}$
$SU(3)_C \times SU(2)_L \times U(1)_R \times U(1)_{B-L}$	$\begin{pmatrix} \frac{9}{2} & \frac{101}{12} & \frac{97}{8} & 1 \end{pmatrix}$
$SU(3)_C \times SU(2)_L \times U(1)_Y$	$\begin{pmatrix} -7 & -\frac{19}{6} & \frac{41}{10} \end{pmatrix}$

Table 7.2: β-coefficients for every gauge group in the revised model, listed in the same order as the groups they correspond to.

The change with respect to the running presented in section 5.4.2 is that the β-coefficients should be computed with the added representations, all the way down to M_{Z_R}. The new β-coefficients are listed in Table 7.2. Especially below the PS-scale there is a considerable change in these coefficients.

The result of the new running is shown in Figure 7.1. The associated coupling constant and unification energy are:

$$\alpha_U^{-1} = 3.65, \quad M_U = 1.1 \times 10^{18}\,\text{GeV}. \tag{7.12}$$

The running has been significantly altered, the unification energy is higher and the fine structure constant of the GUT is larger. The model still achieves unification below the Planck scale, as required.

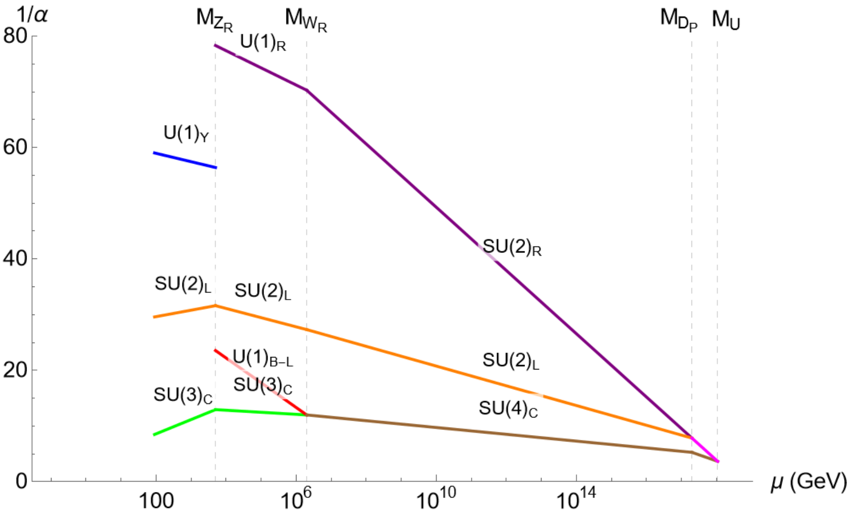

Figure 7.1: Running of the couplings including the 126 representation and scalar leptoquarks down to M_{Z_R}.

Figure 7.1 shows that for $SU(2)_L$ and $SU(3)_C$, the running is significantly altered past 5 TeV, as opposed to the running in Figure 5.3. This is an important prediction of the model and measuring these coupling constants provides another way to determine whether this model is valid.

In Figure 7.2 M_U and M_D are shown as a function of M_{W_R} and M_{Z_R}. In the graph on the left, the side on the right of the dashed lines marks the values not excluded in section 6.4. The condition that $M_U > M_D$ is clearly satisfied for the plotted regions. Therefore, both M_{W_R} and M_{Z_R} can be further increased, if experimental results demand it, without excluding the model.

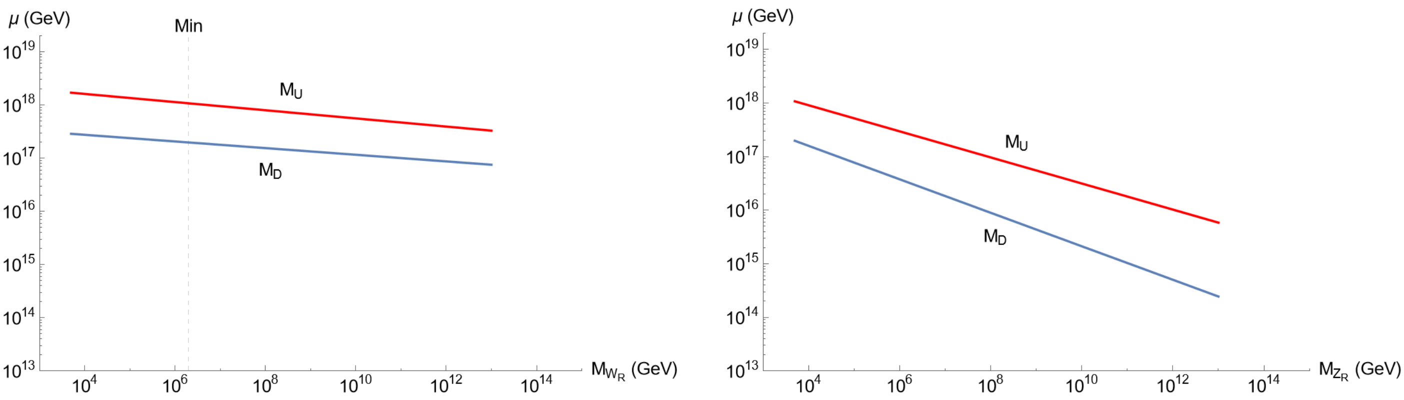

Figure 7.2: M_U and M_D as functions of M_{W_R} on the left and M_{Z_R} on the right, for the revised model. The dashed line marks the minimal value for M_{W_R}, as established in section 6.4. For the graph on the left we set $M_{Z_R} = 5$ TeV.

Symmetry Group	Energy Scale	Gauge Bosons	Fermions per generation	Scalars
$SO(10)$	$\geq M_U$ $\geq 10^{18}\,\text{GeV}$	45	16	$10, 16, 54, 120, 126, 210$
$SU(4)_C \times SU(2)_L \times SU(2)_R \times D$	$M_U - M_D$ $10^{18}\,\text{GeV} - 2 \times 10^{17}\,\text{GeV}$	$(15,1,1)$, $(1,3,1)$, $(1,1,3)$	$(4,2,1)$, $(\bar{4},1,2)$	$(1,2,2)_{10}, (1,2,2)_{120}$, $(\bar{4},1,2)_{16}, (4,2,1)_{16}$, $(15,2,2)_{120}, (15,2,2)_{126}$, $(15,1,3)_{210}, (15,3,1)_{210}$, $(1,1,1)_{210}$
$SU(4)_C \times SU(2)_L \times SU(2)_R$	$M_D - M_{W_R}$ $2 \times 10^{17}\,\text{GeV} - 2 \times 10^{6}\,\text{GeV}$	$(15,1,1)$, $(1,3,1)$, $(1,1,3)$	$(4,2,1)$, $(\bar{4},1,2)$	$(1,2,2)_{10}, (1,2,2)_{120}$, $(\bar{4},1,2)_{16}$, $(15,2,2)_{120}, (15,2,2)_{126}$, $(15,1,3)_{210}$
$SU(3)_C \times SU(2)_L \times U(1)_R \times U(1)_{B-L}$	$M_{W_R} - M_{Z_R}$ $2 \times 10^{6}\,\text{GeV} - 5 \times 10^{3}\,\text{GeV}$	$(8,1,0,0)$, $(1,3,0,0)$, $(1,1,0,0)$, $(1,1,0,0)$	$(3,2,0,1/3)$, $(\bar{3},1,1/2,1/3)$, $(\bar{3},1,-1/2,1/3)$, $(1,2,0,-1)$, $(1,1,-1/2,-1)$, $(1,1,1/2,-1)$	$(1,2,1/2,0)_{10}, (1,2,1/2,0)_{120}$, $(1,1,1/2,-1)_{16}$, $(8,2,-1/2,0)_{120}, (8,2,-1/2,0)_{126}$, $(3,2,-1/2,4/3)_{120}, (3,2,-1/2,4/3)_{126}$, $(3,2,1/2,4/3)_{120}, (3,2,1/2,4/3)_{126}$, $(1,2,-1/2,0)_{120}, (1,2,-1/2,0)_{126}$
$SU(3)_C \times SU(2)_L \times U(1)_Y$	$M_{Z_R} - M_{EW}$ $5 \times 10^{3}\,\text{GeV} - 2 \times 10^{2}\,\text{GeV}$	$(8,1,0)$, $(1,3,0)$, $(1,1,0)$	$(3,2,1/6)$, $(\bar{3},1,-2/3)$, $(\bar{3},1,1/3)$, $(1,2,-1/2)$, $(1,1,1)$	$(1,2,1/2)_{10}$
$SU(3)_C \times U(1)_Q$	$\leq M_{EW}$ $\leq 2 \times 10^{2}\,\text{GeV}$	$(8,1,0)$, $(1,1,0)$		

Table 7.3: Overview of the representations of gauge bosons, fermions and scalars, belonging to particles that are massless at the corresponding scale. For brevity the conjugate partners of the fields from the 120 and 126 are left out for $M_{W_R} - M_{Z_R}$.

Another aspect that should be checked in our revised model, is whether the 126 can achieve a vev in the same manner as the 120. In fact, using a term like the one in eq. (7.9), but replacing the 120 with the 126, provides the SM doublet from the $(15, 2, 2)_{126}$ with an appropriate vev. This should be no surprise, as the fields from the 120 and 126 are in similar representations at the associated energy scale.

In short, the adjusted model still achieves unification at an acceptable scale. The relatively low energy predictions of the model are now: an extra Z boson at or above 5 TeV, scalar leptoquarks on the TeV-scale, and a significantly adjusted running past 5 TeV.

7.5 Phenomenology

We have established that we can give the scalar leptoquarks a mass at the TeV-scale, therefore it is interesting to examine the associated phenomenology. In section 6.3.1 we touched upon the SMEFT operators associated with the new particles in the model we discuss, including those of the scalar leptoquarks. We reiterate the operators stated in Table 6.2:

Boson	Operators
R_2	$\mathcal{O}_{lu}$, $\mathcal{O}_{qe}$, $\mathcal{O}^{(1)}_{lequ}$, $\mathcal{O}^{(3)}_{lequ}$
$\tilde{R}_2$	$\mathcal{O}_{ld}$

Table 7.4: Operators generated by R_2 and $\tilde{R}_2$ scalar leptoquarks. [51]

The bounds associated with these operators can be found in Table 6.3. The largest lower bound is 8.1 TeV, however these constraints are listed assuming couplings of order 1. In section 7.3, we established that the couplings of the scalar leptoquarks are similar in hierarchy and order of magnitude to the SM Yukawa couplings. Therefore, using SMEFT bounds is not nearly as useful in this case. Other literature [72, 73] takes a different approach, and states constraints on products of the Yukawa couplings instead, assuming a mass of 1 TeV.

As established in section 7.3, the Yukawa couplings are principally responsible for reproducing the correct fermion masses, meaning there is an automatic hierarchy between the generations. The third generation will couple the most strongly to the scalar leptoquarks, the first generation will couple the least strongly. In this regard, scalar leptoquarks differ from vector leptoquarks, which couple identically to each generation, unless additional mechanisms are introduced. This has an important consequence for our case, as most stringent bounds from rare meson decays (see section 6.4) involve first and second generation fermions. On the one hand, the small Yukawa couplings needed to explain the masses of these generations help evade these bounds. On the other hand, these small couplings will suppress many interesting observables significantly, making detection difficult.

The small couplings have the risk of turning the leptoquarks into the GUT equivalent of WIMPs (weakly interacting massive particles, a candidate for dark matter). They could exist at relatively low energies, but interact so weakly that they are impossible to prove or disprove. However, detection through interactions with third generation fermions and gluons could remain a viable option. The fact that we are left with leptoquarks coupling to the third generation is not by accident. Constraints on interactions with third generations are much lower, therefore BSM theories often focus on predicting new physics in this sector. It could be the case that once experimental sensitivity catches up for third generation interactions, the room for new physics disappears.

In this section we will first look at some bounds on the couplings of the scalar leptoquarks and ultimately identify several collider observables for the R_2 and $\tilde{R}_2$ scalar leptoquarks.

7.5.1 Experimental Bounds

In section 7.3, we have established that the Yukawa couplings of the scalar leptoquarks are similar in hierarchy to the SM Yukawa couplings. However, we do not have precise values for the couplings. Therefore, constraints on these couplings will not provide a clear lower bound on the mass of the scalar leptoquarks. Nevertheless, it is important to examine some of these constraints on our parameter space. Several observables, such as atomic parity violation (APV), the electron electric dipole moment (d_e), and rare meson decays provide bounds for the couplings of scalar leptoquarks.

Bounds for scalar leptoquarks are generally set on the Yukawa couplings of a model independent Lagrangian. For the R_2 leptoquark we have the general Lagrangian [74]:

$$\begin{aligned}\mathcal{L}_Y =& z_{ij}\overline{e}^i_R d^j_L R_2^{2/3*} + (zV^\dagger_{CKM})_{ij}\overline{e}^i_R u^j_L R_2^{5/3*} \\ &+ (yV_{PMNS})_{ij}\overline{u}^i_R \nu^j_L R_2^{2/3} - y_{ij}\overline{u}^i_R e^j_L R_2^{5/3} + h.c.,\end{aligned} \tag{7.13}$$

with z_{ij} and y_{ij} Yukawa matrices. For $\tilde{R}_2$ we have:

$$\mathcal{L}_Y = -y_{ij}\overline{d}^i_R e^j_L \tilde{R}_2^{2/3*} + (yV_{PMNS})_{ij}\overline{d}^i_R \nu^j_L \tilde{R}_2^{-1/3} + h.c. \tag{7.14}$$

In Table 7.5 we have listed several bounds on scalar leptoquarks. The table list elements from the Yukawa matrices in the above Lagrangians under the leptoquark it belongs to. We use the notation $y'_{ij} = (YV^\dagger_{CKM})$.

Clearly, many of the tighter constraints are on processes involving off-diagonal couplings, or couplings with first and second generation matter.

Observable	R_2	$\tilde{R}_2$	Bound	Ref.
d_e	$\lvert\mathrm{Im}(y'_{12}z_{31})\rvert$		$< 6.2\times10^{-10}$	[73]
$\mu\to e\gamma$	$\lvert y'_{23}z_{31}\rvert^2$, $\lvert y'_{13}z_{32}\rvert^2$		$< 1.2\times10^{-15}$	[73]
$\tau\to e\gamma$	$\lvert y'_{33}z_{31}\rvert^2$, $\lvert y'_{13}z_{33}\rvert^2$		$< 1.4\times10^{-7}$	[73]
$\tau\to\mu\gamma$	$\lvert y'_{33}z_{32}\rvert^2$, $\lvert y'_{23}z_{33}\rvert^2$		$< 1.9\times10^{-7}$	[73]
$K_L^0\to\ e^\pm\mu^\mp$	$\lvert y_{21}y^*_{12}+y^*_{11}y_{22}\rvert$	$\lvert y_{21}y^*_{12}+y^*_{11}y_{22}\rvert$	$< 1.9\times10^{-5}$	[73]
$\mu - e$ conversion	$\left\lvert y'^{\dagger}_{12}z^*_{11}\right\rvert^2$	$\lvert y_{12}y^*_{11}\rvert^2$	$< 6.7\times10^{-11}, < 2.1\times10^{-11}$	[73]
$b\to s\mu^-\tau^+$	$\lvert z_{23}z^*_{32}\rvert$	$\lvert y_{22}y^*_{33}\rvert$	$< 1.28\times10^{-1}$	[72]
$b\to s\mu^+\tau^-$	$\lvert z_{33}z^*_{22}\rvert$	$\lvert y_{23}y^*_{32}\rvert$	$< 1.62\times10^{-1}$	[72]
APV	$\lvert y'_{11}\rvert$, $\lvert y_{11}\rvert$	$\lvert y'_{11}\rvert$, $\lvert y_{11}\rvert$	$\leq 0.34, \leq 0.36$	[74]

Table 7.5: Some bounds on combination of Yukawa couplings for scalar leptoquarks, with $M_{LQ} = 1\,\mathrm{TeV}$. Every bound should be multiplied by $(M_{LQ}/1\,\mathrm{TeV})^n$, with n corresponding to the order in the couplings: $\lvert y'_{23}z_{31}\rvert^2 \to (M_{LQ}/1\,\mathrm{TeV})^4$.

Kaon decay (specifically $K_L^0 \to\ e^\pm\mu^\mp$), which constrained the vector leptoquark scenario to high energies, see section 6.4, puts a fairly strong upper bound on the product of $\lvert y^*_{11}y_{22}\rvert$. We can use our estimate that $y_{11}\sim y_u$ and $y_{22}\sim y_c$, where $y_{u,c}$ are the up and charm quark Yukawa couplings. The Yukawa couplings of fermions in the SM are shown in Table 7.1. We find that the product of these couplings would be around 10^{-7}, which is well below the upper bound, though it remains a rough estimate.

Measurements of lepton flavour violating B-meson decays do not provide strong bounds on scalar leptoquarks [75], in contrast to kaon decays.

Table 7.5 constrains the parameter space for the scalar leptoquarks, but as mentioned, cannot exclude them at certain masses. At this moment there seems to be no reason to believe that the scalar leptoquarks are excluded at the TeV-scale, provided their couplings are roughly similar to the SM Yukawa couplings, for which we have given an argument.

7.5.2 Collider Processes

Considering that we have found no bounds directly excluding the existence of scalar leptoquarks with SM Higgs-like Yukawa couplings at the TeV-scale, we can examine some potential collider observables. This section focuses on processes in pp colliders such as the LHC, though some diagrams may be applicable to other colliders as well. The main reason we focus on pp colliders is their high centre of mass energy (e.g. 14 TeV for LHC, or preferably 100 TeV for FCC-hh), which is necessary for producing particles with masses on the order of several TeV. Some interesting leptoquark observables not listed here, relating to B anomalies, are discussed in [76]

One thing to note, is that the small couplings make detection of processes involving first and second generation matter highly unlikely. Assuming the couplings are similar to the SM Yukawa couplings, a process involving two vertices with strange quarks would be suppressed by 10^{-7} due to the couplings alone. Therefore, the most promising phenomenology involves third generation matter. Third generation matter would largely have to be created in processes initiated by gluons, since the associated pdf's are small, as can be seen in Figure 18.4 from [17]. Producing leptoquarks directly from gluons is also possible, though limited to pair production, due to charge conservation.

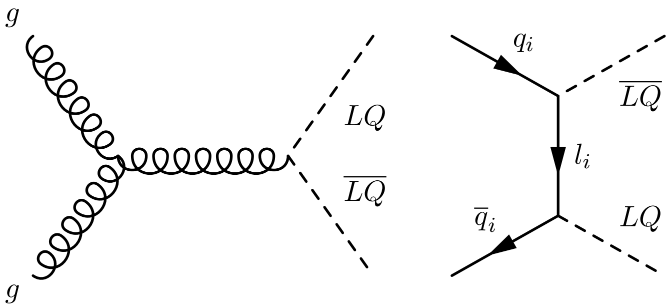

Figure 7.3: Two diagrams contributing to the potential pair production of scalar leptoquarks at LHC [77].

In Figure 7.3, two examples of scalar leptoquark pair production are shown. Generally, pair production is unfavourable, as the suppression is naturally higher when producing two heavy particles instead of one. The diagram showing $gg \to LQ\overline{LQ}$, has the advantage of involving the coupling of the strong force, which is much larger than the Yukawa couplings involved in the diagram for $q\overline{q} \to LQ\overline{LQ}$, for first or second generation fermions. The downside is, that the gluons in the proton generally have lower momenta than the quarks, as is apparent from the pdf's of the proton [49]. A search for pairs of scalar leptoquarks decaying into muons or electrons was performed at ATLAS [78]. They found that scalar leptoquarks were excluded for masses up to 1.7 TeV and 1.8 TeV in the muon and electron channels, respectively. All limits in this section are 95% C.L. (Confidence Level). Clearly, pair production observables are fairly limited in their reach. These specific results are not very relevant for us, as the scenario we discuss features small couplings to first and second generation matter. A similar search focusing on leptoquarks decaying to a bottom quark and a τ found a mass limit of 1.46 TeV [79]. Another study, focusing on $t\tau$ final states instead, excluded scalar leptoquark masses up to 1.43 TeV [80]. Both of these are relevant, as R_2 contains both leptoquarks decaying to $b\tau$ and $t\tau$. Clearly, experiments focusing on third generation final states are less sensitive than those focusing on the first and second generations.

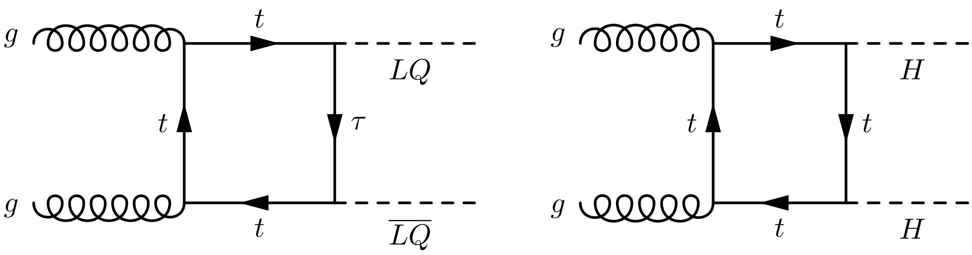

Figure 7.4: A loop diagram for leptoquark pair production, alongside the similar top quark loop diagram of Higgs pair production.

The pair production diagram from two quarks shown in Figure 7.3 suffers from the fact that there is little third generation matter in the proton. Instead, the necessary quarks could be produced from two gluons first. This is shown on the left in Figure 7.4, where it is contrasted with the pair production of the Higgs boson. Unlike single Higgs production from a top quark loop, pair production of the Higgs boson has never been observed [81]. This box diagram for leptoquark pair production should have an amplitude proportional to $g_s^2|y_{u\tau}^2|/|M_{LQ}|^4$, which is a fairly heavy suppression. Considering the ratio $|M_H|^4/|M_{LQ}|^4 \simeq 10^{-5}$, it seems practically impossible for LHC to produce a leptoquark pair in this manner, given that Higgs pair production itself has not been observed either. However, the τ instead of a top quark in one part of the loop, will approximately cause the amplitude to be bigger by a factor $(m_t/m_\tau)^2 \sim 10^4$. Therefore, these two factors could almost cancel each other, and the amplitude of the diagrams two could differ by a small amount for a unit coupling.

Pair produced leptoquarks would mostly decay to a bottom and a τ, when the leptoquark has a charge of 2/3 or a top and a τ when the charge is 5/3. Other decays involve neutrinos, but those are difficult to detect, since neutrinos are neutral. To examine pair production at collider experiments, the focus should therefore be on observing signals from $pp \to b\bar{b} + \tau\bar{\tau}$ and $pp \to t\bar{t} + \tau\bar{\tau}$ on top of an SM background.

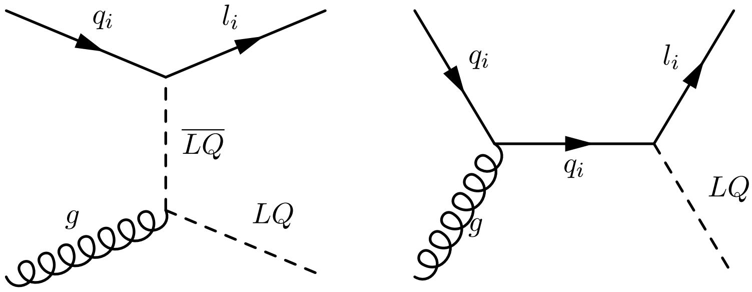

Figure 7.5: Diagrams contributing to the potential production of single scalar leptoquarks at LHC [74].

Single production of leptoquarks would require less energy, and is therefore usually favourable. However, in contrast to pair production, single production always needs interactions between leptoquarks and fermions, since gluons carry no electric charge. Figure 7.5 shows two examples of single production of scalar leptoquarks. Both of these diagrams contain one vertex with fermions and a leptoquark, and one strong interaction vertex. This means these processes suffer from heavy suppression for first and second generation interactions. Interactions with third generation matter are suppressed as well, since they require a bottom or top quark in the initial state. As stated above, these bottom and top quarks would mostly have to be produced from other particles first, causing them to have much less momentum than quarks already present in the proton. Searches for single production of leptoquarks were performed at CMS [82]. From Figure 7.6, we can see that this search obtained bounds of 800 GeV for a coupling of 1. This bound is lower than the one obtained from pair production, due to the reasons mentioned above.

An interesting process for the production of a single scalar leptoquark was presented in [48]. This process is shown in Figure 7.7. The diagram features a τ pair produced from a photon, which is present in the proton. Photon distributions generally scale with Z^2 [83], meaning it is larger in heavier nuclei such as Pb ions. Therefore, this process could be significant in colliders using Pb ions. The quark would have to be a bottom or a top to produce the leptoquarks we study. Exclusion limits from this process are relatively weak, in [48] they exclude leptoquarks coupling to $b\tau$ with a relatively large coupling constant (~ 1.9) at 600 GeV or up to 1.25 TeV with an even greater coupling constant of ~ 3.

Single production of these leptoquarks will lead to a final state of a τ pair together with either a bottom or a top quark. Therefore, collider searches would have to focus on observing $pp \to b + \tau\bar{\tau}$ and $pp \to t + \tau\bar{\tau}$ on top of an SM background in order to exclude, find or constrain these leptoquarks.

Another avenue for leptoquark detection are nonresonant processes such the Drell-Yan production of a τ pair as shown in Figure 7.8. Since this diagram only has a t-channel leptoquark, the momentum of the outgoing particles is not closely related to the mass of the leptoquark. Therefore, there would be no clear peak in the momentum distribution of the resulting pair of leptons, making this a nonresonant process. In comparison to SM Drell-Yan production of $\tau\bar{\tau}$, this t-channel could perhaps create a different angular distribution

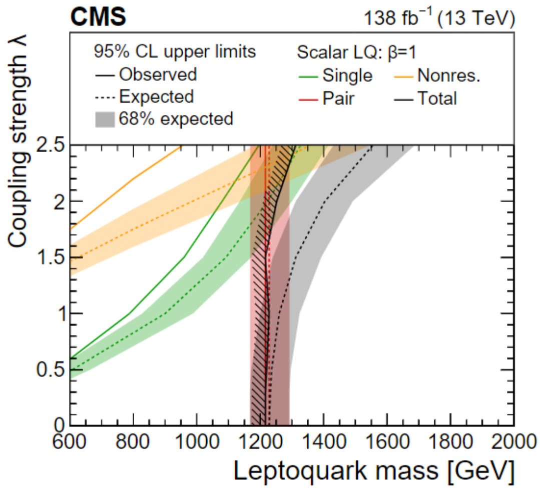

Figure 7.6: Exclusion plot for a scalar leptoquark exclusively coupling to $b\tau$, as obtained in [82]. Dotted lines represent expected 95% C.L. upper limits on the coupling strength λ of the scalar leptoquark, as a function of leptoquark mass. Solid lines represent observed limits. The lines attached to the black line, representing observed exclusion from all processes, point to the excluded region.

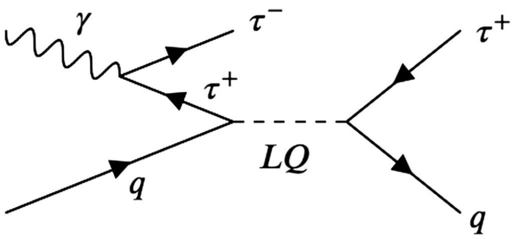

Figure 7.7: Single leptoquark production from a quark and a lepton, taken from [48].

in the resulting particles. This could provide a way to distinguish the signal from the background.

In contrast to the single and pair production processes, the Drell-Yan process corresponds directly to a dimension-6 SMEFT operator. The current lower bound on the leptoquark mass from the associated operator, $\mathcal{O}_{qe}^{[3333]}$, is 0.3 TeV, as stated in Table 6.3. Furthermore, in [82] no significant bounds on scalar leptoquarks were obtained from Drell-Yan $\tau\overline{\tau}$ production.

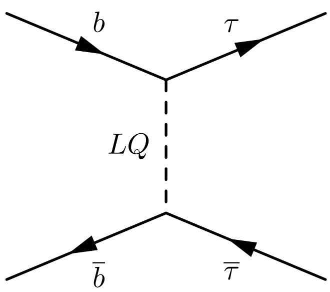

Figure 7.8: Drell-Yan production of $\tau\overline{\tau}$ mediated by a leptoquark.

In Figure 7.6 an exclusion plot for scalar leptoquarks coupling exclusively to $b\tau$ is shown, as obtained by CMS. This figure shows that the overall lower bound on a scalar leptoquark like the ones we discuss are not high at all. For leptoquarks with a mass above 1.4 GeV, the coupling does not need to be small. These bounds from CMS are somewhat smaller than those obtained by ATLAS in [79, 80].

All cited ATLAS and CMS publications in this section ([48, 78–80, 82]) establish exclusion limits on leptoquarks for certain coupling strengths. None of them find any signal that would indicate the existence of scalar leptoquarks. At current energy and integrated luminosity, it simply has not been possible to find leptoquarks. However, the exclusion limits are relatively low, leaving room for relatively light leptoquarks to exist. Collider searches focusing on $\tau\overline{\tau} + b\bar{b}$, $\tau\overline{\tau} + t\bar{t}$, $b + \tau\overline{\tau}$ and $\tau\overline{\tau}$ final states have the potential to discover or set improved bounds on the scalar leptoquarks discussed in this chapter.

7.6 Conclusions

In this chapter we have examined whether the model described in chapter 4 and chapter 5 can provide scalar leptoquarks that are potentially in range of collider experiment. To this end, we have had to make several adjustments to the model we treat. Firstly, the scale at which the scalar leptoquarks achieve mass was changed. Originally, they obtained mass at the Pati-Salam scale (M_{W_R}), in this chapter we have let them obtain a mass at M_{Z_R}, in order to make the scalar leptoquarks TeV-scale. Secondly, we have added a scalar multiplet from the 126 representation to the model, in order for the model to correctly predict fermion masses. A schematic overview of this model is given in Table 7.3.

We have established a clear model for the TeV-scale scalar leptoquarks R_2 and $\tilde{R}_2$, known by their SM representations $(3, 2, 7/6)$ and $(3, 2, 1/6)$, respectively. This model lacks precise values for the Yukawa couplings, which must be constrained by experiment. Due to the mass hierarchy of fermions and the fact that the leptoquarks are in the same representation as the SM doublets above the PS-scale, we argued that the Yukawa couplings are greatest for the third generation. Based on this, we examined collider phenomenology with third generation matter. Both pair production from two gluons, as pair production from two fermions was discussed. These pair production processes lead to $\tau\overline{\tau} + b\bar{b}$ or $\tau\overline{\tau} + t\bar{t}$ final states. Single production of leptoquarks can be caused by interactions between gluons and a bottom or top quark. The final state of such a process would be $b + \tau\overline{\tau}$ or $t + \tau\overline{\tau}$. Lastly, there is Drell-Yan production of a $\tau\overline{\tau}$ pair from a $b\bar{b}$ pair. Of these three categories of processes, the highest sensitivity has come from pair production, due to gluon fusion processes.

Based on current experimental bounds, scalar leptoquarks with $M \geq 1.5$ TeV are a possibility in the $SO(10)$ GUT we have treated. Hopefully, this motivates further experimental searches for third generation leptoquarks at LHC and potentially at the proposed FCC-hh.

Chapter 8

Conclusion

In this thesis we have discussed a model for Grand Unification based on $SO(10)$, similar to what was discussed in [12, 19], with the intent of finding TeV-scale leptoquarks and their possible collider observables. This model features three intermediate symmetry scales, including the Pati-Salam model, between the GUT-scale and the SM. An overview of the final iteration of this model can be found in section 7.4.

Firstly we discussed several GUTs originating from E_6. Based on this discussion we chose to further investigate an $SO(10)$ GUT. We identified the representations present in this model, largely based on the work of [27]. These representations contain several leptoquarks that are interesting to us. These are the vector leptoquark U_1 with SM representation $(3, 1, 2/3)$ and the scalar leptoquarks R_2 and $\tilde{R}_2$ with SM representations $(3, 2, 7/6)$ and $(3, 2, 1/6)$, respectively.

While treating this model we have had to carefully work through some challenging aspects of the theory. Among these aspects were: the splitting of the masses in the scalar representations, the correct reproduction of fermion masses and the multiple Higgs doublets which needed to obtain masses and vev's at separate scales. Furthermore, we showed that this scenario achieves unification at a scale consistent with limits from proton decay.

The Pati-Salam model contains the vector leptoquark U_1, which initially seemed like a good candidate for a TeV-scale leptoquark, as the running and unification of the couplings allowed the Pati-Salam model to be valid at energies as low as 5 TeV. However, U_1 was constrained to have a mass of around 2 PeV due to bounds from kaon decay. Flavour mixing could lower these bounds, though implementing this in a model is difficult. The U_1 leptoquark is in the same representation as the gluons, therefore it must couple diagonally to the generations, making flavour mixing impossible in the specific model we treat. Some workarounds for this problem exist in the form of nonunitary models, which often rely on different gauge groups for each generation, thereby being able to suppress leptoquark effects on the first and second generations. We did not give these more complicated models any further consideration.

The scalar leptoquarks R_2 and $\tilde{R}_2$ do not suffer from the same constraints as the vector leptoquarks. This is due to the fact that their couplings to the first and second generations can be kept small. In fact, a hierarchy between the couplings comes naturally, as these leptoquarks are in the same representations as some of the SM Higgs doublets that provide the fermions with mass. Therefore, they will couple more strongly to heavier fermions. We have identified pair production, single production and nonresonant processes that could produce leptoquarks in pp collider experiments. The relevant final states for these processes are $q\overline{q} + \tau\overline{\tau}$, $q + \tau\overline{\tau}$ and $\tau\overline{\tau}$, with q either being a top or a bottom quark. Current lower limits on the leptoquark mass from processes like these are fairly low: 1.46 TeV at 95% C.L.

From these findings, we can conclude that $SO(10)$ grand unification is one of the few GUTs from E_6 that can viably give rise to leptoquarks at the TeV-scale. Experimental research focusing on leptoquark interactions with third generation matter will have the chance to determine whether these leptoquarks exist. Discovery of these particles would be a clear hint at the existence of a GUT. Further signatures of this GUT include the Z_R boson, with a mass $\geq 5\,\text{TeV}$ and the adjusted running of the SM couplings past $5\,\text{TeV}$.

Acknowledgements

First and foremost, I would like to thank prof. dr. Daniël Boer for supervising my research and offering me a very interesting topic. Through our regular meetings I have learned a lot about the topic and particle physics in general. I certainly would not have been able to complete my research without this helpful supervision.

Furthermore, I want to thank Gefré Wortelboer for providing helpful insights in the early stages of the project and for sharing his work with me.

Appendix A

Supplementary Material

A.1 Gamma Matrices

The gamma matrices are defined as follows in the Dirac representation:

$$\gamma^0 = \begin{pmatrix} I_2 & 0 \\ 0 & I_2 \end{pmatrix}, \quad \gamma^k = \begin{pmatrix} 0 & \sigma^k \\ -\sigma^k & 0 \end{pmatrix}, \tag{A.1}$$

with σ^k the Pauli matrices:

$$\sigma^1 = \begin{pmatrix} 0 & 1 \\ 1 & 0 \end{pmatrix}, \quad \sigma^2 = \begin{pmatrix} 0 & -i \\ -i & 0 \end{pmatrix}, \quad \sigma^3 = \begin{pmatrix} 1 & 0 \\ 0 & -1 \end{pmatrix}. \tag{A.2}$$

A.2 Pati-Salam Generators in $SO(10)$ Basis

The generators corresponding to the bosons found in section 4.1.6 are listed here. We exclude the bosons that fall outside the Pati-Salam group. This appendix is entirely based on [27], where the generators of the A and Y bosons can be found as well.

The gluon generators are as follows:

$$\begin{aligned} U_{G1} = U^\dagger_{G_4} &= (\Sigma_{45} + \Sigma_{36} - i\Sigma_{53} - i\Sigma_{46})/4, \\ U_{G2} = U^\dagger_{G_5} &= (\Sigma_{52} + \Sigma_{61} - i\Sigma_{15} - i\Sigma_{62})/4, \\ U_{G3} = U^\dagger_{G_6} &= (\Sigma_{23} + \Sigma_{41} - i\Sigma_{31} - i\Sigma_{42})/4, \\ U_{G7} &= (2\Sigma_{65} + \Sigma_{43} + 2\Sigma_{21} + \Sigma_{34})/(\sqrt{2/3}), \\ U_{G8} &= (\Sigma_{43} + 2\Sigma_{21} + \Sigma_{34})/(\sqrt{2/3}). \end{aligned} \tag{A.3}$$

The U_1 leptoquark generators:

$$\begin{aligned} U_{X_1} = U^\dagger_{X_4} &= (\Sigma_{23} + \Sigma_{14} - i\Sigma_{31} + i\Sigma_{42})/4, \\ U_{X_2} = U^\dagger_{X_5} &= (\Sigma_{25} + \Sigma_{61} - i\Sigma_{51} - i\Sigma_{62})/4, \\ U_{X_3} = U^\dagger_{X_6} &= (\Sigma_{45} + \Sigma_{63} - i\Sigma_{53} - i\Sigma_{64})/4. \end{aligned} \tag{A.4}$$

The generator for the X_{B-L} boson is:

$$U_{B-L} = 2/3(\Sigma_{21} + \Sigma_{43} - \Sigma_{65}). \tag{A.5}$$

Lastly the generators for the bosons associated with $SU(2)_{L,R}$:

$$\begin{aligned} L_1 &= (\Sigma_{79} + \Sigma_{108})/2, & R_1 &= (\Sigma_{79} + \Sigma_{810})/2, \\ L_2 &= (\Sigma_{98} + \Sigma_{107})/2, & R_2 &= (\Sigma_{98} + \Sigma_{710})/2, \\ L_3 &= (\Sigma_{87} + \Sigma_{109})/2, & R_3 &= (\Sigma_{87} + \Sigma_{910})/2. \end{aligned} \tag{A.6}$$

A.3 Coefficients for Algebraic Running

The coefficients in eq. (5.79) are as follows:

$$\begin{aligned} C_1 &= b_{2L''} - b_Y, & & \\ C_2 &= b'_{2L} - \frac{3}{5}b_{1R} - \frac{2}{5}b_{B-L}, & D_1 &= b_{2L''} - b_{3C'}, \\ & & D_2 &= b_{2L'} - b_{3C}, \\ C_3 &= b_{2L} - \frac{3}{5}b_{2R} - \frac{2}{5}b'_{4c}, & D_3 &= b_{2L} - b_{4C}, \\ C_4 &= \frac{2}{5}b_{2LR} - \frac{2}{5}b_{4C}, & D_4 &= b_{2LR} - b_{4C}. \end{aligned} \tag{A.7}$$

A.4 Overview of Mass Acquisition

Symmetry Group	Energy SSB	Gauge Bosons	Fermions	Scalars	Broken By
$SO(10)$	$M_U \simeq 10^{18}\,\text{GeV}$	A, Y		All irrelevant scalars	$(1,1,1)_{54}$, parity-even
$SU(4)_C \times SU(2)_L \times SU(2)_R \times D$	$M_D \simeq 2 \times 10^{17}\,\text{GeV}$			$(4,2,1)_{16}$, $(15,3,1)_{210}$	$(1,1,1)_{210}$, parity-odd
$SU(4)_C \times SU(2)_L \times SU(2)_R$	$M_{W_R} \simeq 2 \times 10^{6}\,\text{GeV}$	U_1, W_R		$(15,1,3)_{210}$, $(\overline{3},1,-1/2,-1/3)_{16}$, $(\overline{3},1,1/2,-1/3)_{16}$, $(1,1,1/2,1)_{16}$, $(1,2,1/2,0)_{10}$, $(1,2,1/2,0)_{120}$	$(1,1,0,0) \in (15,1,3)_{210}$
$SU(3)_C \times SU(2)_L \times U(1)_R \times U(1)_{B-L}$	$M_{Z_R} \simeq 5 \times 10^{3}\,\text{GeV}$	X_{B-L}/Z_R		$(1,1,1/2,-1)_{16}$, $(1,2,-1/2,0)_{120}$, $(8,2,-1/2,0)_{120/126}$, $(3,2,-1/2,4/3)_{120/126}$, $(3,2,1/2,4/3)_{120/126}$, $(1,2,-1/2,0)_{120/126}$	$(1,1,0)_{16} \sim (1,1,1/2,-1)_{16}$
$SU(3)_C \times SU(2)_L \times U(1)_Y$	$M_{EW} \simeq 2 \times 10^{2}\,\text{GeV}$	$W^{\pm}, Z^0$	$(3,2,1/6)$, $(\overline{3},1,-2/3)$, $(\overline{3},1,1/3)$, $(1,2,-1/2)$, $(1,1,1)$	Doublets from $10, 120$ and 126 obtain vev $(1,2,1/2)_{10}$	$(1,0)_{10} \sim (1,2,1/2)_{10}$
$SU(3)_C \times U(1)_Q$					

Table A.1: Overview of the model after the modifications made in chapter 7. At each scale we show which gauge bosons, fermions and scalars obtain mass when the symmetry is broken. The field that breaks the symmetry is also shown, indicated by both their representation after and before symmetry breaking, respectively. For an overview of the fields at each scale see Table 7.3. For brevity the conjugate partners of the fields from the 120 and 126 are left out for $M_{W_R} - M_{Z_R}$. Representations that require mass splitting are shown as representation of the group below symmetry breaking.

Bibliography

[1] S. L. Glashow. Partial Symmetries of Weak Interactions. *Nucl. Phys.*, 22:579–588, 1961.

[2] Steven Weinberg. A model of leptons. *Phys. Rev. Lett.*, 19:1264–1266, Nov 1967.

[3] Abdus Salam. Weak and Electromagnetic Interactions. *Conf. Proc. C*, 680519:367–377, 1968.

[4] Georges Aad et al. Observation of a new particle in the search for the Standard Model Higgs boson with the ATLAS detector at the LHC. *Phys. Lett. B*, 716:1–29, 2012.

[5] G. 't Hooft and M. Veltman. Regularization and renormalization of gauge fields. *Nuclear Physics B*, 44(1):189–213, 1972.

[6] H. Fritzsch, M. Gell-Mann, and H. Leutwyler. Advantages of the color octet gluon picture. *Physics Letters B*, 47(4):365–368, 1973.

[7] Howard Georgi and S. L. Glashow. Unity of all elementary-particle forces. *Phys. Rev. Lett.*, 32:438–441, Feb 1974.

[8] Jogesh C. Pati and Abdus Salam. Lepton number as the fourth "color". *Phys. Rev. D*, 10:275–289, Jul 1974.

[9] Harald Fritzsch and Peter Minkowski. Unified interactions of leptons and hadrons. *Annals of Physics*, 93(1):193–266, 1975.

[10] Pran Nath and Pavel Fileviez Pérez. Proton stability in grand unified theories, in strings and in branes. *Physics Reports*, 441(5–6):191–317, apr 2007.

[11] A. Touwen. Extending Symmetries of the Standard Model towards Grand Unification . Master's thesis, Rijksuniversiteit Groningen, 2018.

[12] G. F. Wortelboer. Searching for TeV-scale leptoquarks in Grand Unified Theories. Master's thesis, Rijksuniversiteit Groningen, 2023.

[13] A. Zee. *Group Theory in a Nutshell for Physicists*. In a Nutshell. Princeton University Press, 2016.

[14] Michael E. Peskin and Daniel V. Schroeder. *An Introduction to quantum field theory*. Addison-Wesley, Reading, USA, 1995.

[15] Ruud Peeters. *Aspects of fine-tuning in theories with extended scalar sectors*. PhD thesis, University of Groningen, 2021.

[16] R.N. Mohapatra. *Unification and Supersymmetry: The Frontiers of Quark-Lepton Physics*. Graduate Texts in Contemporary Physics. Springer, 2003.

[17] R. L. Workman and Others. Review of particle physics. *PTEP*, 2022:083C01, 2022.

[18] Stefano Bertolini, Luca Di Luzio, and Michal Malinský. Intermediate mass scales in the nonsupersymmetric $so(10)$ grand unification: A reappraisal. *Phys. Rev. D*, 80:015013, Jul 2009.

[19] M Sruthilaya, Rukmani Mohanta, and Sudhanwa Patra. Neutrino mass and neutrinoless double beta decay in SO(10) GUT with Pati-Salam symmetry. *Journal of Physics G: Nuclear and Particle Physics*, 45(7):075004, jun 2018.

[20] T Van Ritbergen, AN Schellekens, and JAM Vermaseren. Group theory factors for feynman diagrams. *International Journal of Modern Physics A*, 14(01):41–96, 1999.

[21] I. Doršner, S. Fajfer, A. Greljo, J.F. Kamenik, and N. Košnik. Physics of leptoquarks in precision experiments and at particle colliders. *Physics Reports*, 641:1–68, 2016. Physics of leptoquarks in precision experiments and at particle colliders.

[22] F. Gürsey, P. Ramond, and P. Sikivie. A universal gauge theory model based on e6. *Physics Letters B*, 60(2):177–180, 1976.

[23] R. Barbieri and D.V. Nanopoulos. An exceptional model for grand unification. *Physics Letters B*, 91(3):369–375, 1980.

[24] Howard Georgi. Towards a grand unified theory of flavor. *Nuclear Physics B*, 156(1):126–134, 1979.

[25] David J. Gross and R. Jackiw. Effect of anomalies on quasi-renormalizable theories. *Phys. Rev. D*, 6:477–493, Jul 1972.

[26] Miguel Crispim Romao. The su (5) grand unification theory revisited, 2011.

[27] Alp Deniz Özer. *SO(10)-Grand Unification and Fermion Masses*. PhD thesis, Ludwig-Maximilians-Universität München, December 2005.

[28] D. Chang, R. N. Mohapatra, J. M. Gipson, R. E. Marshak, and M. K. Parida. Experimental tests of new so(10) grand unification. *Phys. Rev. D*, 31:1718–1732, Apr 1985.

[29] R. N. Mohapatra and B. Sakita. SO($2n$) grand unification in an SU(n) basis. *Phys. Rev. D*, 21:1062–1066, Feb 1980.

[30] S. Rajpoot. Symmetry breaking and intermediate mass scales in the so(10) grand unified theory. *Phys. Rev. D*, 22:2244–2254, Nov 1980.

[31] R. Slansky. Group theory for unified model building. *Physics Reports*, 79(1):1–128, 1981.

[32] F. Del Aguila and L.E. Ibáñez. Higgs bosons in so(10) and partial unification. *Nuclear Physics B*, 177(1):60–86, 1981.

[33] Marcus Pernow. *Phenomenology of SO(10) Grand Unified Theories*. PhD thesis, Royal Inst. Tech., Stockholm, 2019.

[34] J. Maalampi and J. Pulido. Prospects for supersymmetric so(10) models with an intermediate mass scale. *Nuclear Physics B*, 228(2):242–258, 1983.

[35] Borut Bajc and Goran Senjanović. Radiative seesaw mechanism and degenerate neutrinos. *Phys. Rev. Lett.*, 95:261804, Dec 2005.

[36] D. Chang, R. N. Mohapatra, and M. K. Parida. Decoupling of parity- and SU(2)$_R$-breaking scales: A new approach to left-right symmetric models. *Phys. Rev. Lett.*, 52:1072–1075, Mar 1984.

[37] Jeffrey Alan Harvey. *Baryon number generation and mass relations in SO (10) unified models.* PhD thesis, California Institute of Technology, 1981.

[38] Masaki Yasuè. Symmetry breaking of so(10) and constraints on the higgs potential: Adjoint 45 and spinorial 16 representations. *Phys. Rev. D*, 24:1005–1013, Aug 1981.

[39] Stefano Bertolini, Luca Di Luzio, and Michal Malinsky. On the vacuum of the minimal nonsupersymmetric SO(10) unification. *Phys. Rev. D*, 81:035015, 2010.

[40] K. S. Babu and Ernest Ma. Symmetry breaking in so(10): Higgs-boson structure. *Phys. Rev. D*, 31:2316–2322, May 1985.

[41] K. S. Babu and R. N. Mohapatra. Predictive neutrino spectrum in minimal SO(10) grand unification. *Phys. Rev. Lett.*, 70:2845–2848, 1993.

[42] S. Dimopoulos and H.M. Georgi. Extended survival hypothesis and fermion masses. *Physics Letters B*, 140(1):67–70, 1984.

[43] Rabindra N. Mohapatra and Goran Senjanović. Higgs-boson effects in grand unified theories. *Phys. Rev. D*, 27:1601–1612, Apr 1983.

[44] K. Abe and Others. Search for proton decay via $p \to e^+\pi^0$ and $p \to \mu^+\pi^0$ in 0.31 megaton·years exposure of the super-kamiokande water cherenkov detector. *Phys. Rev. D*, 95:012004, Jan 2017.

[45] Stephen F. King, Silvia Pascoli, Jessica Turner, and Ye-Ling Zhou. Confronting SO(10) GUTs with proton decay and gravitational waves. *Journal of High Energy Physics*, 2021(10), oct 2021.

[46] Armen Tumasyan et al. Search for a right-handed W boson and a heavy neutrino in proton-proton collisions at $\sqrt{s} = 13$ TeV. *JHEP*, 04:047, 2022.

[47] Debasish Borah, Arnab Dasgupta, Chayan Majumdar, and Dibyendu Nanda. Observing left-right symmetry in the cosmic microwave background. *Physical Review D*, 102(3), aug 2020.

[48] Aram Hayrapetyan et al. Search for Scalar Leptoquarks Produced via τ-Lepton–Quark Scattering in pp Collisions at s=13 TeV. *Phys. Rev. Lett.*, 132(6):061801, 2024.

[49] Tie-Jiun Hou, Jun Gao, T. J. Hobbs, Keping Xie, Sayipjamal Dulat, Marco Guzzi, Joey Huston, Pavel Nadolsky, Jon Pumplin, Carl Schmidt, Ibrahim Sitiwaldi, Daniel Stump, and C.-P. Yuan. New cteq global analysis of quantum chromodynamics with high-precision data from the lhc. *Phys. Rev. D*, 103:014013, Jan 2021.

[50] D.J. Griffiths. *Weak Interactions*, chapter 10, pages 301–341. John Wiley & Sons, Ltd, 1987.

[51] J. de Blas, J. C. Criado, M. Pérez-Victoria, and J. Santiago. Effective description of general extensions of the standard model: the complete tree-level dictionary. *Journal of High Energy Physics*, 2018(3), mar 2018.

[52] Adam Falkowski. Lectures on SMEFT. *Eur. Phys. J. C*, 83(7):656, 2023.

[53] Aneesh V. Manohar. Introduction to effective field theories, 2018.

[54] Georges Aad et al. Search for new non-resonant phenomena in high-mass dilepton final states with the ATLAS detector. *JHEP*, 11:005, 2020. [Erratum: JHEP 04, 142 (2021)].

[55] Jorge de Blas, Mikael Chala, and Jose Santiago. Global constraints on lepton-quark contact interactions. *Physical Review D*, 88(9):095011, 2013.

[56] Michael Carpentier and Sacha Davidson. Constraints on two-lepton two-quark operators. *The European Physical Journal C*, 70(4):1071–1090, nov 2010.

[57] Ingolf Bischer, Werner Rodejohann, PS Bhupal Dev, Xun-Jie Xu, and Yongchao Zhang. Searching for new physics from smeft and leptoquarks at the p2 experiment. *Physical Review D*, 105(9):095016, 2022.

[58] Lukas Allwicher, Claudia Cornella, Gino Isidori, and Ben A. Stefanek. New physics in the third generation: A comprehensive smeft analysis and future prospects, 2023.

[59] G. Valencia and S. Willenbrock. Quark-lepton unification and rare meson decays. *Phys. Rev. D*, 50:6843–6848, Dec 1994.

[60] O. Shanker. $\pi\ell 2, K\ell 3$ and $K_0 - \overline{K_0}$ constraints on leptoquarks and supersymmetric particles. *Nuclear Physics B*, 204(3):375–386, 1982.

[61] Hedvika Gedeonová and Mat ěj Hudec. All possible first signals of gauge leptoquark in quark-lepton unification and beyond. *Phys. Rev. D*, 107:095029, May 2023.

[62] A. D. Smirnov. Vector leptoquark mass limits and branching ratios of $K_L^0, B^0, B_s \to l_i^+ l_j^-$ decays with account of fermion mixing in leptoquark currents. *Mod. Phys. Lett. A*, 33:1850019, 2018.

[63] Joe Davighi, Gino Isidori, and Marko Pesut. Electroweak-flavour and quark-lepton unification: a family non-universal path. *Journal of High Energy Physics*, 2023(4), April 2023.

[64] Marzia Bordone, Claudia Cornella, Javier Fuentes-Martín, and Gino Isidori. A three-site gauge model for flavor hierarchies and flavor anomalies. *Physics Letters B*, 779:317–323, 2018.

[65] Mario Fernández Navarro and Stephen F. King. B-anomalies in a twin pati-salam theory of flavour including the 2022 lhcb $R_{K^{(*)}}$ analysis. *Journal of High Energy Physics*, 2023(2), February 2023.

[66] C. Hati, J. Kriewald, J. Orloff, and A.M. Teixeira. A nonunitary interpretation for a single vector leptoquark combined explanation to the b-decay anomalies. *Journal of High Energy Physics*, 2019(12), December 2019.

[67] Alexei Grinbaum. Which fine-tuning arguments are fine? *Foundations of Physics*, 42(5):615–631, February 2012.

[68] Anjan S. Joshipura and Ketan M. Patel. Fermion masses in $so(10)$ models. *Phys. Rev. D*, 83:095002, May 2011.

[69] KS Babu, Borut Bajc, and Shaikh Saad. Yukawa sector of minimal so (10) unification. *Journal of High Energy Physics*, 2017(2):1–25, 2017.

[70] Alexander Dueck and Werner Rodejohann. Fits to so(10) grand unified models. *Journal of High Energy Physics*, 2013(9), September 2013.

[71] Takeshi Fukuyama, Nobuchika Okada, and Hieu Minh Tran. Alternative renormalizable so(10) guts and data fitting. *Nuclear Physics B*, 954:114992, 2020.

[72] Jin-Huan Sheng, Ru-Min Wang, and Ya-Dong Yang. Scalar leptoquark effects in the lepton flavor violating exclusive $b \to s\ell i - \ell j + b \to s\ell_i^- \ell_j^+$ decays. *International Journal of Theoretical Physics*, 58(2):480–492, November 2018.

[73] Rusa Mandal and Antonio Pich. Constraints on scalar leptoquarks from lepton and kaon physics. *Journal of High Energy Physics*, 2019(12):1–40, 2019.

[74] Ilja Doršner, Svjetlana Fajfer, and Admir Greljo. Cornering scalar leptoquarks at lhc. *Journal of High Energy Physics*, 2014(10), October 2014.

[75] Suchismita Sahoo and Rukmani Mohanta. Scalar leptoquarks and the rare b meson decays. *Phys. Rev. D*, 91:094019, May 2015.

[76] Jakub Kwaśniak. Beyond the standard model: Leptoquark explanations for $R(D)$ and $R(D^*)$ flavour anomalies. Bachelor's thesis, Rijksuniversiteit Groningen, 2024.

[77] Bastian Diaz, Martin Schmaltz, and Yi-Ming Zhong. The leptoquark hunter's guide: pair production. *Journal of High Energy Physics*, 2017(10), October 2017.

[78] Georges Aad et al. Search for pairs of scalar leptoquarks decaying into quarks and electrons or muons in $\sqrt{s} = 13$ TeV pp collisions with the ATLAS detector. *JHEP*, 2010:112, 2020.

[79] Georges Aad et al. Search for pair production of third-generation leptoquarks decaying into a bottom quark and a τ-lepton with the ATLAS detector. *Eur. Phys. J. C*, 83(11):1075, 2023.

[80] Georges Aad et al. Search for pair production of third-generation scalar leptoquarks decaying into a top quark and a τ-lepton in pp collisions at $\sqrt{s} = 13$ TeV with the ATLAS detector. *JHEP*, 06:179, 2021.

[81] The CMS Collaboration. A portrait of the higgs boson by the cms experiment ten years after the discovery. *Nature*, 607(7917):60–68, 2022.

[82] Aram Hayrapetyan et al. Search for a third-generation leptoquark coupled to a τ lepton and a b quark through single, pair, and nonresonant production in proton-proton collisions at $\sqrt{s} = 13$ TeV. arXiv:2308.07826, August 2023.

[83] L. Frankfurt and M. Strikman. Photon parton distributions in nuclei and the emc effect. *Physical Review C*, 82(6), December 2010.